UNIVERSITY OF CALIFORNIA, SAN DIEGO

G-Protein Mediated Trafficking of Inwardly Rectifying Potassium Channels

A dissertation submitted in partial satisfaction of the requirements for the degree

Doctor of Philosophy

in

Neurosciences

by

Stephanie B. Boyer

Committee in charge:

Professor Paul A. Slesinger, Chair
Professor Joan Heller Brown
Professor Jeffry Isaacson
Professor Ardem Patapoutian
Professor Mauricio Montal

2008

The dissertation of Stephanie B. Boyer is approved, and it is acceptable in quality and form for publication on microfilm:

_____

_____

_____

_____

_____

Chair

University of California, San Diego

2008

TABLE OF CONTENTS

LIST OF FIGURES AND TABLES

ACKNOWLEDGEMENTS

I AM SINCERELY GRATEFUL TO:

Paul Slesinger, for taking me in when I was an orphaned grad student, and for the help and encouragement he has provided.

All of the members of the Slesinger lab, who have been both fantastic colleagues and great friends.

My family, whose positive support has been unfailing.

Austin Nelson, for many back massages and a lot of patience.

Chapter 1 has been submitted for publication of the material as it may appear in the Journal of Cellular Physiology, 2008, Boyer SB, Slesinger PA, and Jones SVP. The dissertation author was the primary investigator and author of this paper.

A portion of Chapter 2 has been published in Clancy SM, Boyer SB, and Slesinger PA (2007) Coregulation of natively expressed pertussis toxin-sensitive muscarinic receptors with G-protein-activated potassium channels. JNeurosci 27:6388-99. The data presented in Chapter 2 represent work for which the thesis author was primarily responsible and are used by permission of the co-authors. Other parts of Chapter 2 are in preparation for publication of the material as it may appear in the Journal of Neuroscience, 2008, Boyer SB, Clancy SM, Thomas SM, and PA Slesinger. The dissertation author was the primary investigator and author of this paper.

VITA

2002	Bachelor of Science, University of Oklahoma, Norman, OK
2003-2006	Graduate Student Researcher, UCSD, Dr. S.V. Penelope Jones
2006-2008	Graduate Student Researcher, UCSD, Dr Paul A. Slesinger
2008	Doctor of Philosophy, University of California, San Diego

PUBLICATIONS

Boyer SB, Clancy SM, Thomas SM, & PA Slesinger (2008) $GABA_B$ receptors rescue surface expression of m2 muscarinic receptors during chronic agonist exposure. *Submitted to Journal of Neuroscience.*

Boyer SB, Slesinger PA, & SVP Jones (2008). Kir2 channel trafficking is differentially regulated by the Rho GTPase, Rac1. *Submitted to Journal of Cell Physiology.*

Labouebe G, Lomazzi M, Cruz HG, Creton C, Lujan R, Li M, Yanagawa Y, Obata K, Watanabe M, Wickman K, **Boyer SB**, Slesinger PA, & C Luscher (2007). RGS2 modulates coupling between GABA(B) receptors and GIRK channels in dopamine neurons of the ventral tegmental area. *Nat Neurosci* 10(12):1559-68.

Clancy SM, **Boyer SB** & PA Slesinger (2007). Coregulation of natively expressed pertussis toxin-sensitive muscarinic receptors with G-protein-activated potassium channels. *J Neurosci* 27(24): 6388-99.

ABSTRACT OF THE DISSERTATION

G-Protein Mediated Trafficking

of Inwardly Rectifying Potassium Channels

by

Stephanie B. Boyer

Doctor of Philosophy in Neurosciences

University of California, San Diego, 2008

Professor Paul A. Slesinger, Chair

Understanding the mechanisms which regulate trafficking and surface expression of membrane-associated proteins is crucial to understanding their function in a physiological context. We have used a combination of electrophysiological, biochemical and imaging techniques to address G-protein mediated trafficking of inwardly rectifying potassium channels.

Inwardly rectifying potassium channels play an important role in both cardiac and neuronal cells by stabilizing the resting membrane potential and shaping the action potential. Kir2 channels underlie the cardiac inwardly rectifying potassium

conductance termed I_{k1} and alterations in Kir2 expression have significant consequences for cardiac function, leading to potentially fatal arrhythmias. We show that surface expression of Kir2 channels is regulated by another class of proteins important for cardiac functioning, RhoGTPases. These proteins act as molecular switches for a variety of signaling cascades. We show specifically that Kir2.1, but not Kir2.2 or 2.3, subunits are regulated by Rac1. This suggests that Kir2 surface expression may be more actively regulated than previously thought, and that formation of native heteromeric channels may contribute to the diversity of Kir2 function.

G-protein coupled inwardly rectifying potassium channels of the Kir3 family associate with heterotrimeric G-proteins of the Gαi/o class. In neuronal cells, signaling to Kir3 channels mediates slow post-synaptic inhibition. Evidence for signaling complexes consisting of Kir3 channels, G-proteins and G-protein coupled receptors (GPCRs) has been shown recently. We show here that Kir3 channels can be trafficked as a complex with certain GPCRs, including muscarinic m2 and $GABA_B$ receptors. Furthermore, m2 and $GABA_B$ receptors are capable of direct interactions which alter the trafficking of both the receptors and associated Kir3 channels. This represents a novel mechanism for regulation of m2 receptor trafficking, and suggests that macromolecular complex formation may have important consequences for Kir3 signaling in neuronal cells.

This work provides evidence for novel mechanisms of regulating surface expression of inwardly rectifying potassium channels. We propose that trafficking of these channels is a complex process that depends upon co-localization with effector proteins and formation of macromolecular complexes. This work will aid us in understanding the role of inwardly rectifying potassium channels in both cardiac and neuronal function.

INTRODUCTION

Trafficking, in the parlance of cell biology, defines a complex, dynamic process of protein movement within a cell. In the case of plasma membrane-associated proteins, this most often refers to insertion into and removal from the cell surface. As transmembrane signaling molecules depend on proper surface expression for function, the factors that regulate trafficking are necessarily of interest. These factors are widely varied depending on the protein of interest, and can take the form of extracellular signals such as agonist exposure or intracellular effectors such as chaperone proteins, anchoring/scaffolding proteins, kinases/phosphatases, GTPases and more. Figure I-1 summarizes a few of the pathways and proteins relevant to this work. This dissertation aims to address two specific questions in the field of trafficking. First, how is the trafficking of the constitutively cardiac inward rectifier I_{k1} regulated? Second, how does the formation of macromolecular complexes, including G-protein coupled receptors (GPCRs), G-proteins and ion channels, affect trafficking? Answering these questions will aid our understanding of the complex processes that regulate proper surface expression.

THE CARDIAC INWARDLY RECTIFYING POTASSIUM CONDUCTANCE I_{K1}

Ion channels act as gates protecting the cell from the extracellular environment. By allowing only specific ions to flow across the lipid bi-layer, they directly affect the electrical excitability of a cell and/or ignite intracellular signaling cascades. One of the most important and broadest classes of ion channels is potassium channels. The cardiac inwardly rectifying potassium conductance, termed I_{k1}, was originally discovered in the mid-20th century and has since been shown to be present in both ventricular and atrial myocytes. Because of its property of inward rectification (allowing greater current flow into the cell and than out; see Figure I-2), I_{k1} plays an important role in shaping the cardiac action potential. I_{k1} is particularly important for the

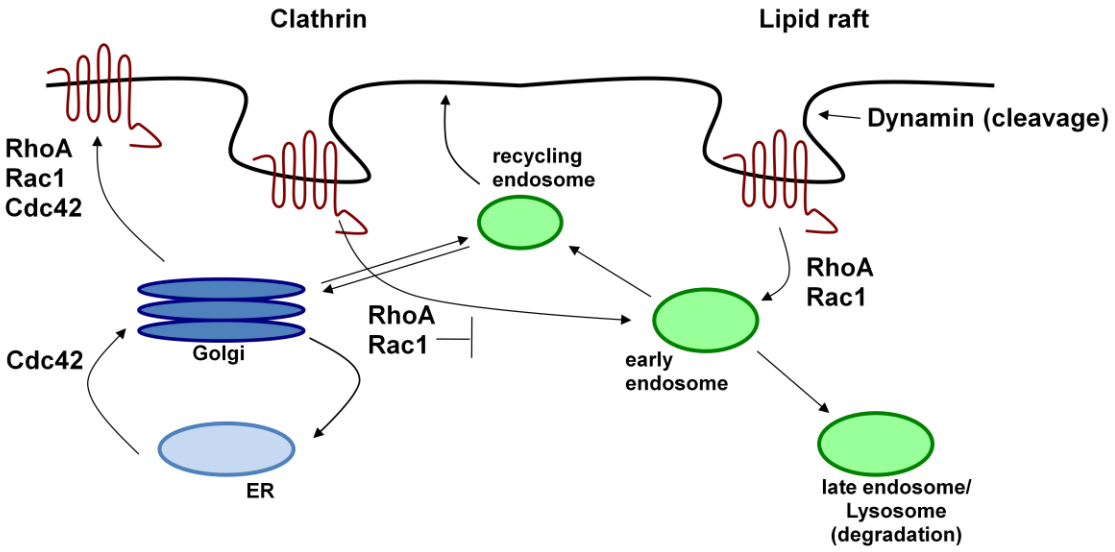

FIGURE I-1: OVERVIEW OF TRAFFICKING PATHWAYS AND THE ROLE OF RHOGTPASES IN TRAFFICKING

Plasma membrane proteins are born in the endoplasmic reticulum (ER) where quality control checkpoints ensure that only properly folded and complexed proteins continue on. From there, proteins are trafficked to the Golgi apparatus for sorting, then on to the plasma membrane. Once at the surface, proteins can be internalized to early endosomes, recycled back to the plasma membrane via recycling endosomes or targeted for degradation to late endosomes/lysosomes. A large number of intracellular proteins assist in regulating this process, and only a handful of proteins relevant to this work have been included here. Dynamin is a small GTPase known to be involved in cleaving nascent vesicles as they internalize from the plasma membrane in both clathrin-dependent and lipid raft mediated endocytosis. Rho family GTPases, including Rho, Rac and Cdc42, can act at various points in the trafficking pathway, and these roles differ among clathrin and non-clathrin mediated routes. For instance, in clathrin-mediated endocytosis activation of RhoA and Rac1 are inhibitory, while they are necessary for lipid raft mediated endocytosis.

plateau phase and repolarization phase of the action potential as well as stabilization and maintenance of the resting membrane potential (see Fig I-1; for reviews see Lopatin & Nichols, 2001; Dhamoon & Jalife, 2005). With the advent of cloning and genetic manipulation, the molecular identity of I_{k1} was determined to be the Kir2 family of inward rectifiers.

The molecular basis of I_{k1}: Kir2 Channels

Kir2 (also known as IRK1) channels are one of six families of inwardly rectifying potassium channels that includes G-protein and ATP-gated inward rectifiers among others (for review, see Nichols & Lopatin, 1997). While these families share a conserved two transmembrane-spanning domain structure and potassium selectivity, members of the Kir2 family differ by being constitutively active. Rather than being gated by ligand binding, conductance of Kir2 channels depends on the balance of extracellular potassium to intracellular potassium. There are four family members, Kir2.1 through Kir2.4, that are capable of forming either homo- or hetero-tetramers. Although they vary slightly in their distribution, Kir2.1-2.3 are broadly expressed throughout the brain and in the heart, while Kir2.4 is found mainly in the spinal cord (Stanfield et al, 2002). This work will focus on Kir2.1-2.3.

A combination of genetic approaches has been used to probe the role of Kir2 channels in cardiac function. Kir2.1 appears to be the predominant subunit underlying I_{k1}. Silencing Kir2.1 through knockout or transgenic dominant-negatives reveals a 50 to 95% reduction of I_{k1} current (McLerie & Lopatin, 2003; Nakamura et al, 1998; Zaritsky et al, 2001; Zobel et al, 2003). Kir2.2 knockout mice, in contrast, show only a partial reduction in I_{k1} (Zaritsky et al, 2001). Furthermore, while some studies report that Kir2.3 is not expressed in cardiac myocytes (Zobel et al, 2003), other studies suggest that the distinct properties of Kir2.1, 2.2 and 2.3 may explain anatomical and species-specific differences in I_{k1} (Dhamoon et al, 2004). This suggests that while Kir2.1 subunits predominantly underlie I_{k1}, native conductances may be mediated by heterotetramers of the Kir2 family.

The importance of Kir2 channels in the heart can be seen in the consequences of Kir2 channelopathies. In the heart, Kir2 channels directly influence repolarization of the cardiac action potential during the QT interval; overexpression of Kir2 leads to a shorter QT interval while decreases in Kir2 expression lead to a prolonged QT interval, either of which can lead to potentially fatal arrhythmias. Mutations in Kir2.1 leading to increased activity have been associated with Short QT Syndrome (Priori et al, 2005) as well as familial atrial fibrillation (Xia et al, 2005). Dominant-negative mutations in Kir2.1 are associated with Andersen's Syndrome (or Andersen-Tawil Syndrome), an autosomal dominant disorder characterized by periodic paralysis, facial dysmorphisms and cardiac arrhythmias (Plaster et al, 2001). Over 20 mutations in Kir2.1 have been associated with Andersen's Syndrome to date, at least four of which lead to changes in channel trafficking (Bendahhou et al, 2003; Ballester et al, 2006).

Kir2 channels have long been ignored in neurons owing to their lack of conventional gating mechanisms, yet they likely a play a crucial role in regulating neuronal excitability. Similar to their role in cardiac cells, Kir2 channels affect the resting membrane potential and the shape of the action potential in neurons. Increased activity of Kir2 channels acts to dampen the excitability of neurons due to the negative nature of the potassium reversal potential (E_k), while inhibition of Kir2 channels increases neuronal excitability. For instance, in striatopallidal neurons, Kir2 currents are potently reduced by activation of the m1 muscarinic receptor, leading to enhanced dendritic excitability and increased temporal summation (Carr & Surmeier, 2007). These channels also modulate the function of other channels by altering the membrane potential, leading to even greater changes in cellular excitability. Studies in mouse prefrontal pyramidal neurons, for example, reveal interplay between Kir2 channels and hyperpolarization/cyclic nucleotide gated (HCN) channels. Inhibition of Kir2 channels leads to depolarization and deactivation of HCN channels, leading to enhanced temporal summation (Day et al, 2005). This suggests that Kir2 channels are necessary to allow HCN channels to contribute to normal sublinear summation in

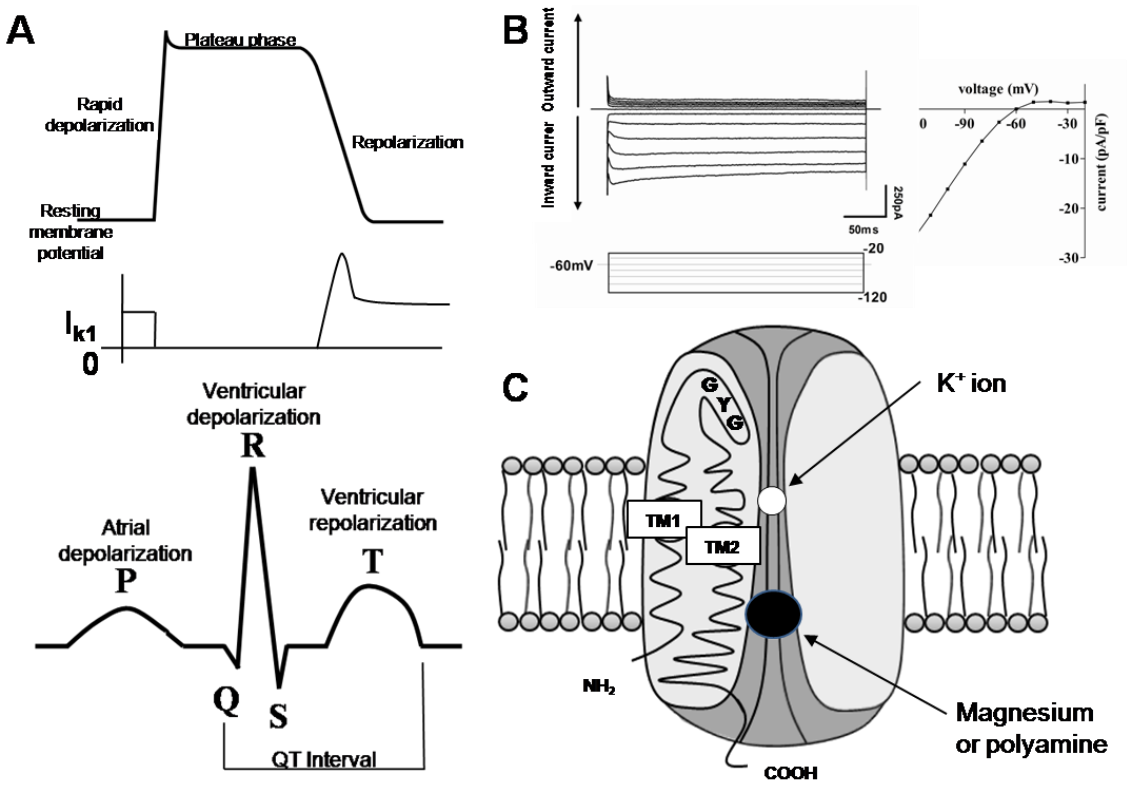

FIGURE I-2: THE CARDIAC INWARDLY RECTIFYING CONDUCTANCE, I_{K1}, AND ITS MOLECULAR BASIS, KIR2 CHANNELS

A) (top) Schematic of the cardiac action potential showing resting, rapid depolarization, plateau & repolarizing phases.
(middle) I_{k1} is open and plays a role in setting the resting membrane potential. I_{k1} is rapidly shut off at the start of the cardiac action potential due to rectification at depolarized potentials, but opens again as the cell repolarizes. I_{k1} also accelerates the return to the resting membrane potential.
(bottom) Schematic of an electrocardiogram (EKG). Because of its role in repolarization, I_{k1} helps to determine the length of the QT interval.

B) Example whole-cell current traces from a cell expressing Kir2 during a series of hyperpolarizing and depolarizing voltage steps. Kir2 channels pass inward current at voltages hyperpolarized to the potassium equilibrium potential, and are closed rapidly at depolarized potentials, passing little current. (bottom) Voltage protocol used. (right) Current-voltage (I-V) plot from recording. Traditionally, inward current is represented as negative while outward current is represented as positive.

C) Cartoon of a cross-section through a Kir2 channel, showing the transmembrane domain and intracellular amino- and carboxyl-terminals. A GYG motif in the pore forming regions forms the potassium selectivity filter. At depolarized potentials, the pore is blocked by positively charged magnesium and polyamines, preventing the flow of potassium ions.

these cells. Furthermore, Kir2 channels are expressed in glial cells and likely contribute to neuronal function through a mechanism known as spatial buffering. Action potential firing changes the extracellular concentration of potassium, which would in turn influence the extracellular environment and driving force on a neuron if not dispersed. Kir2 channels in glia are thought to absorb and redistribute this excess potassium, such as in Müller cells of the retina where Kir2.1 channels are positioned near the soma and axons of retinal neurons (Kofuji et al, 2002). Thus, Kir2 channels play important roles in both cardiac and neuronal cells.

Trafficking of Kir2 Channels

Members of the Kir2 family share a number of conserved features governing trafficking. For instance, all share an F_CYENE ER export motif in the carboxyl terminus, as well as a series of basic, positively charged residues in the amino terminus necessary for Golgi export (Ma et al, 2001; Stockklausner et al, 2001; Stockklausner & Klocker, 2003). Furthermore, all share a conserved tyrosine residue implicated in channel endocytosis (Tong et al, 2001). Kir2 channels have also been shown to complex with scaffolding proteins such as PSD-95, SAP97 and CASK that may alter their trafficking or localization (Leonoudakis et al, 2004). Trafficking of these channels is of particular interest as several mutations implicated in Andersen's syndrome result in channels that lose their ability to traffic to the surface. Nonetheless, it is not yet known what, if any, signals actively regulate Kir2 plasma membrane expression. This work aims, in part, to address whether other key proteins in cardiac singaling, namely RhoGTPases, might be involved in Kir2 trafficking.

RhoGTPases in Cardiac Function and Trafficking

RhoGTPases are a family of small monomeric G-proteins that act as molecular switches for a variety of signal transduction cascades by cycling between an active GTP-bound state and

an inactive GDP-bound state. There are several family members but the most well characterized to date are RhoA, Rac1 and Cdc42. Their cycling is highly regulated by three classes of proteins. Guanine nucleotide exchange factors (GEFs) stimulate the exchange of GDP for GTP to activate RhoGTPases. GTPase activating proteins (GAPs) accelerate the endogenous GTPase activity to deactivate RhoGTPases. Finally, guanine nucleotide dissociation inhibitors (GDIs) are able to bind RhoGTPases in their inactive form and prevent activation (for review, see Ridley AJ, 2006).

RhoGTPases are well studied in cardiac signaling, mainly in the context of cardiac hypertrophy and cardiac failure. Transgenic mice overexpressing wild-type or constitutively active RhoA develop heart failure, and in many cases atrial fibrillation and atrioventricular block, reducing the heart rate (Sah et al, 1999). Transgenic mice expressing constitutively active Rac1 develop cardiac myopathy (Sussman et al, 2000). Furthermore, RhoA has been shown to affect cardiac ion channels including Kv1.2 and L-type calcium channels. In the case of Kv1.2 channels, RhoA can directly interact with the channel, and disrupting RhoA signaling reduces the m1 muscarinic-mediated, tyrosine-kinase dependent suppression of Kv1.2 current (Cachero et al, 1998). Furthermore, inhibition of RhoA reduces L-type calcium currents in transgenic cardiac myocytes without reducing overall protein expression of the channel (Yatani et al, 2005).

While RhoGTPases may directly affect ion channel phosphorylation or interact with signaling cascades, all Rho family members have also been shown to act at different points in the trafficking pathway (summarized in Figure I-1; for reviews see Ridley, AJ, 2006; Symons & Rusk, 2003; Qualmann & Mellor, 2003). Chapter 1 aims to determine if RhoGTPases affect the cardiac inwardly rectifying potassium channels, Kir2, and if so, if this might be through changes in trafficking.

MACROMOLECULAR SIGNALING COMPLEXES AT THE PLASMA MEMBRANE

GPCR Dimerization

GPCRs comprise the largest class of transmembrane signaling proteins in biology. All share a seven transmembrane domain structure with extracellular amino and intracellular carboxyl termini, and are divided into three classes based on structural similarity. Although once thought to exist as monomers, it has been recently shown that many GPCRs function as dimers or even higher order oligomers (Franco et al, 2007). GPCR oligomerization appears to occur in one of three ways; 1) The formation of disulfide bonds in the extracellular, amino terminus, as in the case of class C calcium receptors (Ray et al, 1999) and metabotropic glutamate receptors (Kunishima et al, 2000); 2) Interactions between transmembrane domains, including i) contact dimers such as β2-adrenergic (Hebert et al, 1996) and dopamine D2 receptor (Guo et al, 2005) homodimers, and ii) domain swapping, such as in the case of m3 muscarinic and α2c adrenergic receptor heterodimers (Maggio et al, 1993); and 3) Interactions between intracellular, carboxyl terminal domains as with δ opioid receptor homodimers (Cvejic & Devi, 1997) and δ and μ opioid receptor heterodimers (Fan et al, 2005).

Oligomerization of GPCRs can have a variety of consequences depending on the receptors involved. In some cases, heterodimerization can lead to cross-talk between receptors. For instance, μ opioid receptors and α2 adrenergic receptors have recently been shown to interact. When co-expressed, morphine activates μ receptors and initiates a conformational change in the α2 receptors that inhibits G-protein activation by the α2 receptor ligand (Vilardaga et al, 2008). Also, serotonin 5-HT_{2A} receptors and metabotropic glutamate receptor 2 (mGluR2) dimerize. While 5-HT_{2A} receptors normally show very weak activation of Gαi, this activation is markedly enhanced by co-expression of mGluR2 (Gonzalez-Maeso et al, 2008). In other cases heterodimerization can lead to novel signaling properties of the receptors. μ and δ opioid receptors expressed individually both signal to pertussis toxin (PTX) sensitive Gαi/o proteins; upon co-expression, however, signaling continues despite the presence of PTX, suggesting a

shift in G-protein coupling (George et al, 2000). Finally, heterodimerization can lead to changes in trafficking of the receptor complex. Dopamine D1 receptors show agonist-induced internalization while D3 receptors do not. Upon dimerization, D1 internalization is markedly reduced in response to D1 agonist stimulation. Co-application of D1 and D3 specific ligands, however, results in internalization of the D1/D3 receptor complex (Fiorentini et al, 2008). Similarly, β2-adrenergic receptors normally undergo agonist-induced internalization but when complexed with κ opioid receptors, which do not, they fail to be downregulated by adrenergic agonists (Jordan et al, 2001).

$GABA_B$ Receptors

The gamma-aminobutyric acid type B ($GABA_B$) receptor is especially interesting as the first receptor to exhibit a functional requirement for heterodimerization (see Figure I-3). Although first discovered in the early 1980s for their ability to bind GABA with properties distinct from the classical ionotropic $GABA_A$ receptor, the first $GABA_B$ subunit was not cloned until 1997 (Hill & Bowery, 1981; Kaupmann et al, 1997). This subunit, termed R1, showed ligand binding, but was non-functional when individually expressed and in fact retained in intracellular compartments (Couve et al, 1998). Shortly after cloning of the R1 came cloning of the R2 subunit, and the discovery that heterodimerization of the two could rescue surface expression and receptor function (Jones et al, 1998; Kaupmann et al, 1998; Kuner et al, 1999; White et al, 1999).

Intracellular retention of the R1 subunit has since been shown to be due to an RXRR type ER retention motif in the R1 C-terminus (Margeta-Mitrovic et al, 2000; Pagano et al, 2001). This motif is hidden by dimerization with R2, allowing surface expression of the heterodimer. Interestingly, the R1 and R2 subunits contain parallel coiled-coil domains in their C-terminals, and this region is thought to be mainly responsible for dimerization. Indeed, the coiled-coil domain of the R1 subunit can pull down the full-length R2 in coprecipitation experiments (Kuner et al, 1999) and peptides of the coiled-coil domains can interact *in vitro* (Kammerer et al, 1999). Recent work

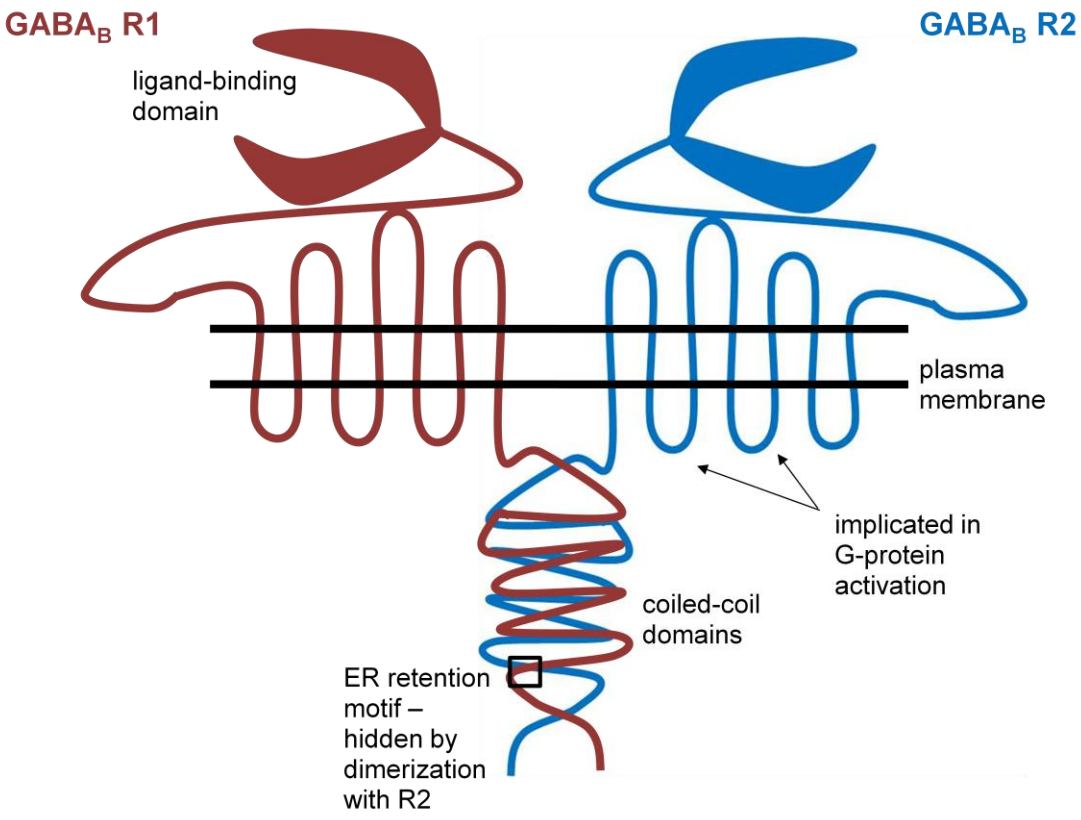

FIGURE I-3: GABA$_B$ RECEPTORS

suggests that other regions may also contribute to dimerization. C-terminally truncated R1 subunits can also precipitate R2 (Calver et al, 2001), and a splice variant of R1, known as R1e and consisting solely of the extracellular domain, can dimerize with R2 and in fact disrupt full-length R1/R2 interactions (Schwarz et al, 2000).

Beyond simply acting as a chaperone for R1 trafficking, the R2 subunit has also been shown to be responsible for G-protein signaling of the heterodimer (Galvez et al, 2001; Margeta-Mitrovic et al, 2001). Specifically, residues in the second and third intracellular loops of the R2 subunit have been implicated in G-protein activation (Robbins et al, 2001; Duthey et al, 2002). Recently, single amino acid substitutions at the border of the third transmembrane domain and second intracellular loop were shown to abolish signaling. These substitutions are at positions analogous to the (D/E)RY motif in class A GPCRS, also thought to mediate G-protein activation (Binet et al, 2007). This suggests some degree of conservation among different classes of GPCRs.

Recently, $GABA_B$ receptors have been shown to be more promiscuous than previously thought. The R1 subunit can complex with the γ2S subunit of the ionotropic $GABA_A$ receptor, which promotes surface expression of the R1 subunit although it remains functionally inactive. Furthermore, association of $GABA_A$ with the R1/R2 heterodimer enhances agonist-induced internalization (Balasubramanian et al, 2004). Also, both the R1 and R2 subunits can independently dimerize with an extracellular calcium sensing receptor (ECaR) of the same class of GPCRs. Co-expressing R1 reduces surface expression of ECaR, while R2 co-expression promotes it; the R1 or R2 subunit both show increased surface expression when the ECaR is present. Contrary to the association with $GABA_A$, this interaction appears to be competitive, such that binding of R1 to ECaR reduces the interaction of R1 with R2, and vice versa (Chang et al, 2007).

Macromolecular Signaling Complexes

Several studies indicate that GPCRs, G-proteins and channels exist in a signaling complex at the cell surface. For instance, Kir3 (also known as GIRK) channels share current profile and structural similarities with Kir2 channels (see Figure I-2), but have little constitutive activity and are instead activated by the membrane-delimited actions of pertussis toxin (PTX) sensitive G-proteins. There is now evidence that both Gαi (Ivanina *et al*, 2004) and Gαo, but not PTX-insensitive Gαq and Gαs (Clancy et al, 2005), G-proteins directly interact with Kir3 channels. Furthermore, some studies suggest that G-proteins may undergo structural rearrangements rather than fully dissociating (Bunemann *et al,* 2003), and that the G-protein heterotrimer remains associated with GPCRs following activation (Lachance *et al,* 1999). Kir3 channels have also been shown to form stable complexes with dopamine (Lavine *et* al, 2002) and $GABA_B$ (David *et al,* 2006; Fowler *et al,* 2007) receptors. Furthermore, accessory proteins like regulators of G-protein signaling (RGS) proteins have been shown to interact with Kir3 channels and may also comprise members of this complex (Fig. 1-4C-E; Labouebe et al, 2007). The existence of macromolecular complexes consisting of GPCRs, Kir3 channels and heterotrimeric G-proteins anchored by the Gα subunit helps explain the membrane-delimited action of Gβγ activation. There is still debate, however, as to whether these signaling complexes exist only at the plasma membrane or comprise preassembled complexes that traffic together through the cell.

Studies of natively expressed receptors and channels in PC12 cells suggest that receptor trafficking can in fact influence channel trafficking as well. PC12 cells are a rat adrenal-derived cell line. When treated with nerve growth factor (NGF), they extend neurites as well as synthesize and secrete neurotransmitters, including dopamine, norepinephrine and acetylcholine. Thus PC12 cells are a good cell culture model for neuronal behavior. Work from our lab has shown that upon 7 day NGF treatment PC12s cells upregulate transcripts for a PTX-sensitive signaling pathway, including m2 muscarinic receptors, GIRK2c channels and Gαi G-proteins. Despite this increase, the receptor and channel are functionally silent, showing neither

FIGURE I-4: M2 MUSCARINIC RECEPTORS AND KIR3 CHANNELS ARE TRAFFICKED AS A COMPLEX IN PC12 CELLS

A) (left) 7 day Nerve growth factor (NGF) treated PC12 cells lack functional muscarinic-induced (oxo) or basal (Ba+) Kir3 currents.
(right) Lack of surface expression of HA-tagged Kir3.2c channels receptors, as seen with immunocytochemistry.

B) (left) 2 hour treatment with the muscarinic antagonist atropine rescues basal and muscarinic-mediated Kir3 currents.
(right) Atropine treatment rescues Kir3.2c surface expression.

Adapted from Clancy, Boyer & Slesinger, 2007.

C) Representative images from cells expressing RGS2-YFP and Kir3.3-CFP, Kir3.2-WT (top) or Kir3.2-CFP (bottom) before and after acceptor photobleaching.

D) Histograms showing %FRET (100*(CFPpost-CFPpre)/CFPpre) by bin count for the cells shown in (*C)*.

E) Bar graph showing %FRET by transfection condition. Note that RGS2 shows a specific association with Kir3, but not Ki2, subunits.

Adapted from Labouebe G, Lomazzi M, Cruz HG, Creton C, Lujan R, Li M, Yanagawa Y, Obata K, Watanabe M, Wickman K, Boyer SB, Slesinger PA & Luscher C (2007).

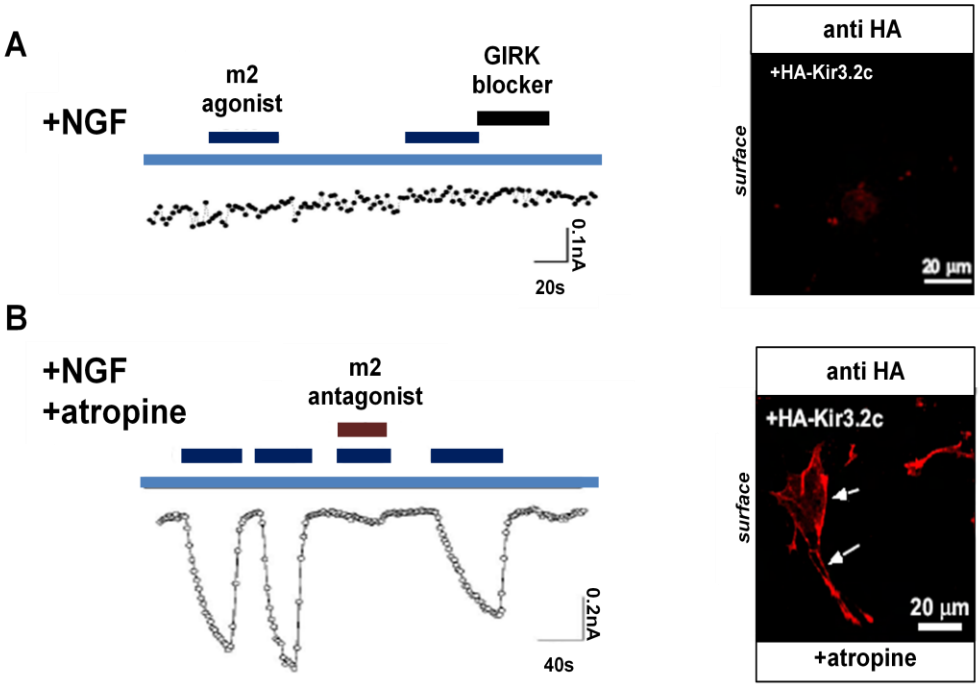
A
+NGF
m2
agonist
GIRK
blocker
0.1nA
20s
anti HA
+HA-Kir3.2c
surface
20 µm
B
+NGF
+atropine
m2
antagonist
0.2nA
40s
anti HA
+HA-Kir3.2c
surface
20 µm
+atropine

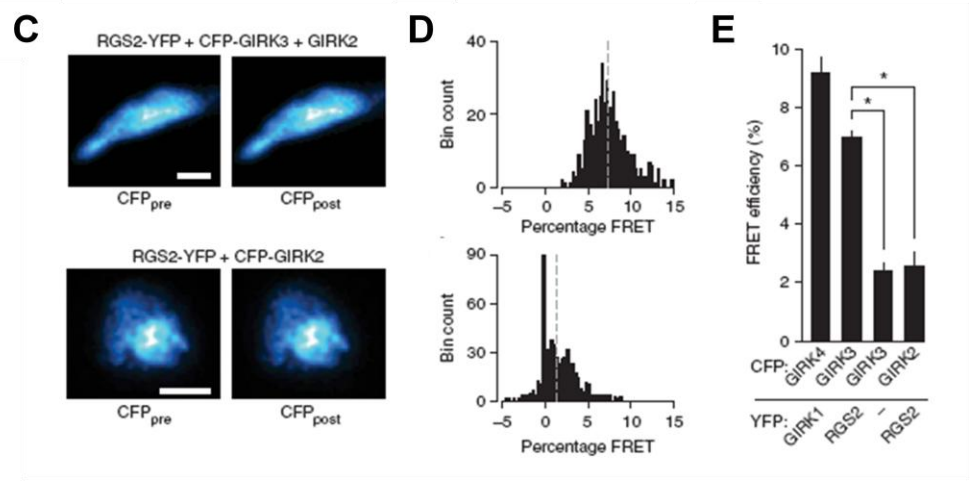
C
RGS2-YFP + CFP-GIRK3 + GIRK2
CFPpre
CFPpost
RGS2-YFP + CFP-GIRK2
CFPpre
CFPpost
D
Bin count
Percentage FRET
Bin count
Percentage FRET
E
FRET efficiency (%)
CFP:
GIRK4
GIRK3
GIRK3
GIRK2
YFP:
GIRK1
RGS2
–
RGS2

muscarinic-mediated nor basal Kir3 currents in whole-cell electrophysiological recordings. This functional silence is due to the fact that the receptor is not expressed on the cell surface, as assayed by immunocytochemistry (Figure I-4A). Treatment of cells for two hours with a competitive muscarinic antagonist is sufficient to rescue channel surface expression and function (Figure I-4B; Clancy et al, 2007). This suggests that downregulation of m2 muscarinic receptors may influence Kir3 channel trafficking through complex formation.

Chapter 2 aims to follow up on these findings by looking at surface expression of m2 receptors directly as well as to determine whether other GPCRs such as $GABA_B$ receptors are able to traffic Kir3 channels.

OVERVIEW OF METHODOLOGY

Detailed procedures for methodology will be described within each chapter. This section aims to provide background and general theory behind certain microscopic techniques used throughout this work.

Total Internal Reflection Fluorescence Microscopy (TIRF)

Through-the-objective TIRF microscopy occurs when collimated laser light is offset to illuminate the back focal plane of the objective, which causes the laser light to arrive at the coverslip at an angle (see Figure I-5A). When this angle is greater than the critical angle (θ), an evanescent wave of excitation light is produced at the interface between two media having different refractive indices, i.e. the glass coverslip and media/cell membrane (Axelrod et al., 1983). The intensity of this evanescent wave falls off exponentially with distance above the interface, allowing selective imaging within ~100nm of the glass/medium interface (i.e. plasma membrane and sub-membrane regions).

Fluorescence Resonance Energy Transfer (FRET)

FRET is a technique for determining inter- and intra-molecular interactions within a distance of 10nm (100Å). Molecules are labeled with fluorescent probes, known as the donor and the acceptor, where the absorption spectrum of the acceptor overlaps with the emission spectrum of the donor (see Figure 1-5B). When the donor fluorophore is excited, some energy is transferred to the acceptor fluorophore, and the efficiency of this energy transfer is inversely proportional to the sixth power of the distance between the two fluorophores. Because of these properties, and because fluorophores can be engineered onto proteins in living cells, FRET is a useful tool to determine molecular interactions. Although many techniques can be used to quantify FRET efficiency, this work uses the acceptor photobleaching technique, also known as donor de-quenching. In this technique, the acceptor fluorophore is destroyed by direct photobleaching such that any energy transfer that may have been occurring between the donor and acceptor is no longer possible (Figure I-5C). Thus FRET, expressed as %FRET, can be measured as an increase in donor emission before and after photobleaching using the simple equation:

$$\text{Eq. 1} \quad \%FRET = 100 \times (D_{post} - D_{pre})/D_{pre}$$

where D_{pre} is the donor emission before photobleaching and D_{post} is the donor emission after photobleaching (for review, see Takanishi et al, 2006).

FIGURE I-5: OVERVIEW OF TIRF MICROSCOPY & FRET

A) (top) Schematic of epifluorescent (epi) and TIRF fluorescent microscopy. In epi, the laser light shines vertically into the cell and illuminates all the fluorophores within the cell. In TIRF, the angle of the laser light is adjusted to the critical angle (θ) such that the light reflects off the coverslip, creating an evanescent wave that only illuminates fluorophores ~100nm into the cell, i.e. on or near the plasma membrane.
(bottom) Representative cell with a cyan fluorescent protein (CFP) tag imaged under epi (left) and TIRF (right).

B) Graph showing overlap of donor and acceptor excitation and emission spectra. The dashed region represents the overlap in donor emission/acceptor excitation and is where FRET occurs.

C) Schematic showing overview of FRET by acceptor photobleaching. If the fluorescently tagged proteins are within 100Å, energy from the donor (cyan fluorescent protein: CFP) will be lost to the acceptor (yellow fluorescent protein: YFP). After direct photobleaching of the acceptor, an increase can be seen in donor intensity. If the fluorescently tagged proteins are greater than 100Å apart, the donor intensity will remain the same after acceptor photobleaching.

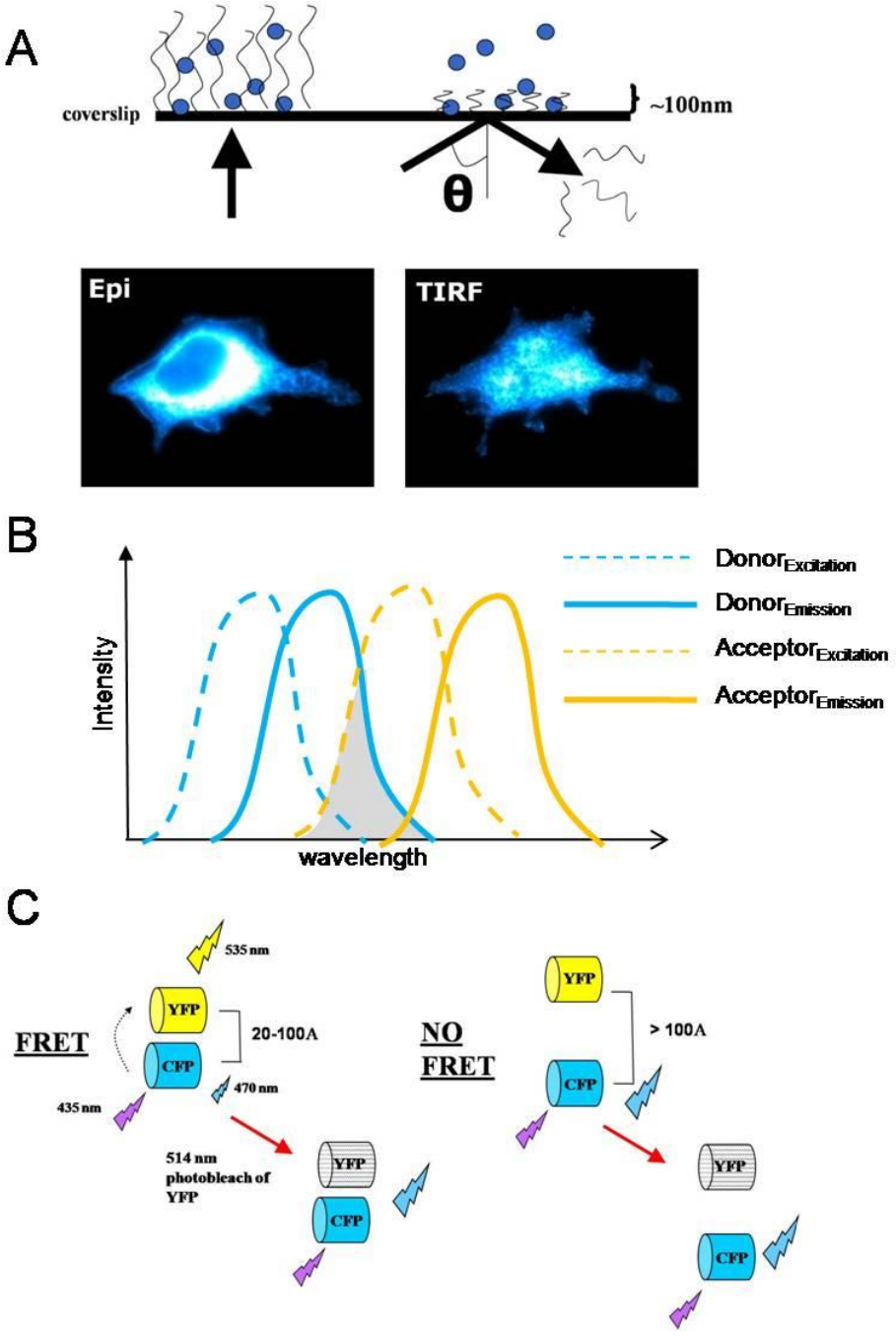
A
coverslip
~100nm
θ
Epi
TIRF
B
Intensity
wavelength
Donor Excitation
Donor Emission
Acceptor Excitation
Acceptor Emission
C
535 nm
YFP
CFP
20-100A
FRET
435 nm
470 nm
514 nm
photobleach of
YFP
NO
FRET
> 100A

LITERATURE CITED

Axelrod D, Thompson NL, Burghardt TP (1983) Total internal inflection fluorescent microscopy. J Microsc 129:19-28.

Balasubramanian S, Teissere JA, Raju DV, Hall RA (2004) Hetero-oligomerization between GABAA and GABAB receptors regulates GABAB receptor trafficking. J Biol Chem 279:18840-18850.

Ballester Ly BDWWBLIHMKDVCGGAL, Jr. (2006) Trafficking-competent and trafficking-defective KCNJ2 mutations in Andersen syndrome. Human Mutation 27:388-388.

Bendahhou S DMRPNMT-FMFYHPLJ (2003) Defective potassium channel Kir2.1 trafficking underlies Andersen-Tawil syndrome. Journal of Biological Chemistry 278:51779-51785.

Bernard V, Brana C, Liste I, Lockridge O, Bloch B (2003) Dramatic depletion of cell surface m2 muscarinic receptor due to limited delivery from intracytoplasmic stores in neurons of acetylcholinesterase-deficient mice. Mol Cell Neurosci 23:121-133.

Binet V, Duthey B, Lecaillon J, Vol C, Quoyer J, Labesse G, Pin JP, Prezeau L (2007) Common structural requirements for heptahelical domain function in class A and class C G protein-coupled receptors. J Biol Chem 282:12154-12163.

Bunemann M, Frank M, Lohse MJ (2003) Gi protein activation in intact cells involves subunit rearrangement rather than dissociation. Proc Natl Acad Sci U S A 100:16077-16082.

Cachero TG, Morielli AD, Peralta EG (1998) The small GTP-binding protein RhoA regulates a delayed rectifier potassium channel. Cell 93:1077-1085.

Calver AR, Robbins MJ, Cosio C, Rice SQ, Babbs AJ, Hirst WD, Boyfield I, Wood MD, Russell RB, Price GW, Couve A, Moss SJ, Pangalos MN (2001) The C-terminal domains of the GABA(b) receptor subunits mediate intracellular trafficking but are not required for receptor signaling. J Neurosci 21:1203-1210.

Carr Db SDJ (2007) M1 muscarinic receptor modulation of Kir2 channels enhances temporal summation of excitatory synaptic potentials in prefrontal cortex pyramidal neurons. Journal of Neurophysiology 97:3432-3438.

Chang W, Tu C, Cheng Z, Rodriguez L, Chen TH, Gassmann M, Bettler B, Margeta M, Jan LY, Shoback D (2007) Complex formation with the Type B gamma-aminobutyric acid receptor affects the expression and signal transduction of the extracellular calcium-sensing receptor. Studies with HEK-293 cells and neurons. J Biol Chem 282:25030-25040.

Clancy SM, Boyer SB, Slesinger PA (2007) Coregulation of natively expressed pertussis toxin-sensitive muscarinic receptors with G-protein-activated potassium channels. J Neurosci 27:6388-6399.

Clancy SM, Fowler CE, Finley M, Suen KF, Arrabit C, Berton F, Kosaza T, Casey PJ, Slesinger PA (2005) Pertussis-toxin-sensitive Galpha subunits selectively bind to C-terminal domain of neuronal GIRK channels: evidence for a heterotrimeric G-protein-channel complex. Mol Cell Neurosci 28:375-389.

Couve A, Filippov AK, Connolly CN, Bettler B, Brown DA, Moss SJ (1998) Intracellular retention of recombinant GABAB receptors. J Biol Chem 273:26361-26367.

Cvejic S, Devi LA (1997) Dimerization of the delta opioid receptor: implication for a role in receptor internalization. J Biol Chem 272:26959-26964.

David M, Richer M, Mamarbachi AM, Villeneuve LR, Dupre DJ, Hebert TE (2006) Interactions between GABA-B1 receptors and Kir 3 inwardly rectifying potassium channels. Cell Signal 18:2172-2181.

Day M, Carr DB, Ulrich S, Ilijic E, Tkatch T, Surmeier DJ (2005) Dendritic excitability of mouse frontal cortex pyramidal neurons is shaped by the interaction among HCN, Kir2, and Kleak channels. J Neurosci 25:8776-8787.

Dhamoon AS, Jalife J (2005) The inward rectifier current (IK1) controls cardiac excitability and is involved in arrhythmogenesis. Heart Rhythm 2:316-324.

Dhamoon AS, Pandit SV, Sarmast F, Parisian KR, Guha P, Li Y, Bagwe S, Taffet SM, Anumonwo JM (2004) Unique Kir2.x properties determine regional and species differences in the cardiac inward rectifier K+ current. Circ Res 94:1332-1339.

Duthey B, Caudron S, Perroy J, Bettler B, Fagni L, Pin JP, Prezeau L (2002) A single subunit (GB2) is required for G-protein activation by the heterodimeric GABA(B) receptor. J Biol Chem 277:3236-3241.

Fan T, Varghese G, Nguyen T, Tse R, O'Dowd BF, George SR (2005) A role for the distal carboxyl tails in generating the novel pharmacology and G protein activation profile of mu and delta opioid receptor hetero-oligomers. J Biol Chem 280:38478-38488.

Fiorentini C, Busi C, Gorruso E, Gotti C, Spano P, Missale C (2008) Reciprocal regulation of dopamine D1 and D3 receptor function and trafficking by heterodimerization. Mol Pharmacol.

Fowler CE, Aryal P, Suen KF, Slesinger PA (2007) Evidence for association of GABA(B) receptors with Kir3 channels and regulators of G protein signalling (RGS4) proteins. J Physiol 580:51-65.

Franco R, Casado V, Cortes A, Ferrada C, Mallol J, Woods A, Lluis C, Canela EI, Ferre S (2007) Basic concepts in G-protein-coupled receptor homo- and heterodimerization. ScientificWorldJournal 7:48-57.

Galvez T, Duthey B, Kniazeff J, Blahos J, Rovelli G, Bettler B, Prezeau L, Pin JP (2001) Allosteric interactions between GB1 and GB2 subunits are required for optimal GABA(B) receptor function. Embo J 20:2152-2159.

George SR, Fan T, Xie Z, Tse R, Tam V, Varghese G, O'Dowd BF (2000) Oligomerization of mu- and delta-opioid receptors. Generation of novel functional properties. J Biol Chem 275:26128-26135.

Gonzalez-Maeso J, Ang RL, Yuen T, Chan P, Weisstaub NV, Lopez-Gimenez JF, Zhou M, Okawa Y, Callado LF, Milligan G, Gingrich JA, Filizola M, Meana JJ, Sealfon SC (2008) Identification of a serotonin/glutamate receptor complex implicated in psychosis. Nature 452:93-97.

Guo W, Shi L, Filizola M, Weinstein H, Javitch JA (2005) Crosstalk in G protein-coupled receptors: changes at the transmembrane homodimer interface determine activation. Proc Natl Acad Sci U S A 102:17495-17500.

Hebert TE, Moffett S, Morello JP, Loisel TP, Bichet DG, Barret C, Bouvier M (1996) A peptide derived from a beta2-adrenergic receptor transmembrane domain inhibits both receptor dimerization and activation. J Biol Chem 271:16384-16392.

Hill DR, Bowery NG (1981) 3H-baclofen and 3H-GABA bind to bicuculline-insensitive GABA B sites in rat brain. Nature 290:149-152.

Ivanina T, Varon D, Peleg S, Rishal I, Porozov Y, Dessauer CW, Keren-Raifman T, Dascal N (2004) Galphai1 and Galphai3 differentially interact with, and regulate, the G protein-activated K+ channel. J Biol Chem 279:17260-17268.

Jones KA, Borowsky B, Tamm JA, Craig DA, Durkin MM, Dai M, Yao WJ, Johnson M, Gunwaldsen C, Huang LY, Tang C, Shen Q, Salon JA, Morse K, Laz T, Smith KE, Nagarathnam D, Noble SA, Branchek TA, Gerald C (1998) GABA(B) receptors function as a heteromeric assembly of the subunits GABA(B)R1 and GABA(B)R2. Nature 396:674-679.

Jordan BA, Trapaidze N, Gomes I, Nivarthi R, Devi LA (2001) Oligomerization of opioid receptors with beta 2-adrenergic receptors: a role in trafficking and mitogen-activated protein kinase activation. Proc Natl Acad Sci U S A 98:343-348.

Kammerer RA, Frank S, Schulthess T, Landwehr R, Lustig A, Engel J (1999) Heterodimerization of a functional GABAB receptor is mediated by parallel coiled-coil alpha-helices. Biochemistry 38:13263-13269.

Kaupmann K, Huggel K, Heid J, Flor PJ, Bischoff S, Mickel SJ, McMaster G, Angst C, Bittiger H, Froestl W, Bettler B (1997) Expression cloning of GABA(B) receptors uncovers similarity to metabotropic glutamate receptors. Nature 386:239-246.

Kaupmann K, Schuler V, Mosbacher J, Bischoff S, Bittiger H, Heid J, Froestl W, Leonhard S, Pfaff T, Karschin A, Bettler B (1998) Human gamma-aminobutyric acid type B receptors are differentially expressed and regulate inwardly rectifying K+ channels. Proc Natl Acad Sci U S A 95:14991-14996.

Kofuji P, Biedermann B, Siddharthan V, Raap M, Iandiev I, Milenkovic I, Thomzig A, Veh RW, Bringmann A, Reichenbach A (2002) Kir potassium channel subunit expression in retinal glial cells: implications for spatial potassium buffering. Glia 39:292-303.

Kuner R, Kohr G, Grunewald S, Eisenhardt G, Bach A, Kornau HC (1999) Role of heteromer formation in GABAB receptor function. Science 283:74-77.

Kunishima N, Shimada Y, Tsuji Y, Sato T, Yamamoto M, Kumasaka T, Nakanishi S, Jingami H, Morikawa K (2000) Structural basis of glutamate recognition by a dimeric metabotropic glutamate receptor. Nature 407:971-977.

Labouebe G, Lomazzi M, Cruz HG, Creton C, Lujan R, Li M, Yanagawa Y, Obata K, Watanabe M, Wickman K, Boyer SB, Slesinger PA, Luscher C (2007) RGS2 modulates coupling

between GABAB receptors and GIRK channels in dopamine neurons of the ventral tegmental area. Nat Neurosci 10:1559-1568.

Lachance M, Ethier N, Wolbring G, Schnetkamp PP, Hebert TE (1999) Stable association of G proteins with beta 2AR is independent of the state of receptor activation. Cell Signal 11:523-533.

Lavine N, Ethier N, Oak JN, Pei L, Liu F, Trieu P, Rebois RV, Bouvier M, Hebert TE, Van Tol HH (2002) G protein-coupled receptors form stable complexes with inwardly rectifying potassium channels and adenylyl cyclase. J Biol Chem 277:46010-46019.

Leonoudakis D CLRRCMMLMVCA (2004) A multiprotein trafficking complex composed of SAP97, CASK, Veli, and Mint1 is associated with inward rectifier Kir2 potassium channels. Journal of Biological Chemistry 729:19051-19063.

Lopatin AN, Nichols CG (2001) Inward rectifiers in the heart: an update on I(K1). J Mol Cell Cardiol 33:625-638.

Ma D ZNLYFCAYMJYNJLY (2001) Role of ER export signals in controlling surface potassium channel numbers. Science 291:316-319.

Maggio R, Vogel Z, Wess J (1993) Coexpression studies with mutant muscarinic/adrenergic receptors provide evidence for intermolecular "cross-talk" between G-protein-linked receptors. Proc Natl Acad Sci U S A 90:3103-3107.

Margeta-Mitrovic M, Jan YN, Jan LY (2000) A trafficking checkpoint controls GABA(B) receptor heterodimerization. Neuron 27:97-106.

Margeta-Mitrovic M, Jan YN, Jan LY (2001) Function of GB1 and GB2 subunits in G protein coupling of GABA(B) receptors. Proc Natl Acad Sci U S A 98:14649-14654.

McLerie M, Lopatin AN (2003) Dominant-negative suppression of I(K1) in the mouse heart leads to altered cardiac excitability. J Mol Cell Cardiol 35:367-378.

Nakamura Ty AMRBCWA (1998) Inhibition of rat ventricular IK1 with antisense oligonucleotides targeted to Kir2.1 mRNA. Am J Physiol 274:H892-H900.

Pagano A, Rovelli G, Mosbacher J, Lohmann T, Duthey B, Stauffer D, Ristig D, Schuler V, Meigel I, Lampert C, Stein T, Prezeau L, Blahos J, Pin J, Froestl W, Kuhn R, Heid J, Kaupmann K, Bettler B (2001) C-terminal interaction is essential for surface trafficking but not for heteromeric assembly of GABA(b) receptors. J Neurosci 21:1189-1202.

Plaster Nm TRT-FMCSBSTADMRISTBEBRCJ (2001) Mutations in Kir2.1 cause the developmental and episodic electrical phenotypes of Andersen's syndrome. Cell 105:511-519.

Priori Sg PSVRIBOREDANCAJdBMRGSBG (2005) A novel form of short QT syndrome (SQT3) is caused by a mutation in the KCNJ2 gene. Circulation Research 97:800-807.

Qualmann B, Mellor H (2003) Regulation of endocytic traffic by Rho GTPases. Biochem J 371:233-241.

Ray K, Hauschild BC, Steinbach PJ, Goldsmith PK, Hauache O, Spiegel AM (1999) Identification of the cysteine residues in the amino-terminal extracellular domain of the human Ca(2+) receptor critical for dimerization. Implications for function of monomeric Ca(2+) receptor. J Biol Chem 274:27642-27650.

Ridley AJ (2006) Rho GTPases and actin dynamics in membrane protrusions and vesicle trafficking. Trends Cell Biol 16:522-529.

Robbins MJ, Calver AR, Filippov AK, Hirst WD, Russell RB, Wood MD, Nasir S, Couve A, Brown DA, Moss SJ, Pangalos MN (2001) GABA(B2) is essential for g-protein coupling of the GABA(B) receptor heterodimer. J Neurosci 21:8043-8052.

Sah VP, Minamisawa S, Tam SP, Wu TH, Dorn GW, 2nd, Ross J, Jr., Chien KR, Brown JH (1999) Cardiac-specific overexpression of RhoA results in sinus and atrioventricular nodal dysfunction and contractile failure. J Clin Invest 103:1627-1634.

Schwarz DA, Barry G, Eliasof SD, Petroski RE, Conlon PJ, Maki RA (2000) Characterization of gamma-aminobutyric acid receptor GABAB(1e), a GABAB(1) splice variant encoding a truncated receptor. J Biol Chem 275:32174-32181.

Stanfield PR, Nakajima S, Nakajima Y (2002) Constitutively active and G-protein coupled inward rectifier K+ channels: Kir2.0 and Kir3.0. Rev Physiol Biochem Pharmacol 145:47-179.

Stockklausner C KN (2003) Surface expression of inward rectifier potassium channels is controlled by selective Golgi export. Journal of Biological Chemistry 278:17000-17005.

Stockklausner C LJRJPKN (2001) A sequence motif responsible for ER export and surface expression of Kir2.0 inward rectifier K(+) channels. FEBS Letters 493:129-133.

Sussman MA, Welch S, Walker A, Klevitsky R, Hewett TE, Price RL, Schaefer E, Yager K (2000) Altered focal adhesion regulation correlates with cardiomyopathy in mice expressing constitutively active rac1. J Clin Invest 105:875-886.

Symons M RN (2003) Control of vesicular trafficking by Rho GTPases. Current Biology 13:R409-R418.

Takanishi CL, Bykova EA, Cheng W, Zheng J (2006) GFP-based FRET analysis in live cells. Brain Res 1091:132-139.

Tong Y BGSLMSGSEKADDALHA (2001) Tyrosine decaging leads to substantial membrane trafficking during modulation of an inward rectifier potassium channel. Journal of General Physiology 117:103-118.

Vilardaga JP, Nikolaev VO, Lorenz K, Ferrandon S, Zhuang Z, Lohse MJ (2008) Conformational cross-talk between alpha2A-adrenergic and mu-opioid receptors controls cell signaling. Nat Chem Biol 4:126-131.

White JH, Wise A, Main MJ, Green A, Fraser NJ, Disney GH, Barnes AA, Emson P, Foord SM, Marshall FH (1998) Heterodimerization is required for the formation of a functional GABA(B) receptor. Nature 396:679-682.

Xia M, Jin Q, Bendahhou S, He Y, Larroque MM, Chen Y, Zhou Q, Yang Y, Liu Y, Liu B, Zhu Q, Zhou Y, Lin J, Liang B, Li L, Dong X, Pan Z, Wang R, Wan H, Qiu W, Xu W, Eurlings P, Barhanin J, Chen Y (2005) A Kir2.1 gain-of-function mutation underlies familial atrial fibrillation. Biochem Biophys Res Commun 332:1012-1019.

Yatani A, Irie K, Otani T, Abdellatif M, Wei L (2005) RhoA GTPase regulates L-type Ca2+ currents in cardiac myocytes. Am J Physiol Heart Circ Physiol 288:H650-659.

Zaritsky JJ, Redell JB, Tempel BL, Schwarz TL (2001) The consequences of disrupting cardiac inwardly rectifying K(+) current (I(K1)) as revealed by the targeted deletion of the murine Kir2.1 and Kir2.2 genes. J Physiol 533:697-710.

Zobel C CHCNTTPRDRJWGJBPH (2003) Molecular dissection of the inward rectifier potassium current (IK1) in rabbit cardiomyocytes: evidence for heteromeric co-assembly of Kir2.1 and Kir2.2. J Physiol 550:365-372.

CHAPTER 1 – KIR2 CHANNEL TRAFFICKING IS DIFFERENTIALLY REGULATED BY THE RHOGTPASE RAC1

ABSTRACT

Kir2 potassium channels help control the resting membrane potential and shape the action potential in cardiac cells. Changes in Kir2 trafficking have been linked to Andersen's Syndrome, a disorder characterized by cardiac arrhythmias. Here, we investigated the role of Rac1, a small GTPase, on Kir2.1 channels expressed in mammalian tsA201 cells. Expression of the dominant-negative form of Rac1 ($Rac1_{DN}$) led to a 2-fold increase in Kir2.1 current density. Similarly, treatment of cells with *C. difficile* toxin B, an inhibitor of the famly of Rho GTPases, also potentiated Kir2.1 currents. The dominant-negative forms of Rho or Cdc42 did not alter Kir2.1 currents, suggesting a selective effect of Rac1 on Kir2.1 channels. Single-channel properties of Kir2.1 (γ, τo, τc) were unchanged with coexpression of $Rac1_{DN}$. Examination of channel surface expression using total internal reflectance fluorescence microscopy and CFP-tagged Kir2.1 channels revealed increased surface expression of CFP-Kir2.1 in cells coexpressing $Rac1_{DN}$. Taken together, these results suggest that $Rac1_{DN}$ expression led to an increase in the number of channels on the plasma membrane. To investigate whether $Rac1_{DN}$ interfered with internalization of Kir2.1, we compared the effect of dominant-negative form of dynamin, Dyn_{DN}, which interferes with endocytosis, with that of $Rac1_{DN}$. Expression of Dyn_{DN} alone increased Kir2.1 current density and, importantly, occluded the potentiation effect of $Rac1_{DN}$. Interestingly, $Rac1_{DN}$ did not alter the current density in cells expressing Kir2.2 or Kir2.3 channels, indicating a selective effect of Rac on Kir2.1. Studies with Kir2.1/2.2 chimeric channels implicated the C-terminal domain of Kir2.1 in the potentiating effect of $Rac1_{DN}$. These results indicate that Rac regulates surface expression of Kir2.1 channels and are discussed in terms of a novel mechanism for regulating Kir2 channels in the heart.

INTRODUCTION

Inwardly rectifying potassium channels, and Kir2 channels in particular, are crucial for setting a sharp threshold for excitation in excitable cells, as well as stabilizing the resting membrane potential in both excitable and non-excitable cells. Because of these properties, Kir2 channels regulate a variety of physiological processes, including heart rate, neuronal firing patterns, vascular smooth muscle tone, hormone secretion and activation of immune responses. They are particularly important in cardiac cells where they underlie I_{K1}, the cardiac inward rectifying potassium conductance, and play a crucial role in shaping the action potential. Kir2.1 knockout mice die shortly after birth; however, studies in neonates reveal a lack of I_{K1} current, broadened action potentials and ineffective clamping of the resting membrane potential leading to spontaneous action potentials (Zaritsky *et al*, 2001). Furthermore Kir2.2 knockout mice show a 50% reduction in I_{K1}, supporting the idea that heteromers of Kir2 channels comprise I_{K1} (Zaritsky *et al*, 2001).

Changes in Kir2 function have been implicated in a number of cardiac diseases. Reductions in Kir2.1 have been linked to hypertrophy (McIntosh *et al*, 1998), while gain-of-function mutations are associated with atrial fibrillation (Xia *et al.,* 2005) and short QT Syndrome (Priori *et al., 2005)*. Andersen's syndrome is an autosomal dominant disorder caused by mutations in the gene encoding Kir2.1 that leads to periodic paralysis, dysmorphic features and cardiac arrhythmias (Plaster *et al.,* 2001). Studies in heterologous cells have shown that such mutations act by exerting a dominant-negative effect on mutated Kir2.1-containing heteromers (Plaster *et* al, 2001; Preisig-Muller *et al*, 2002), and recent work suggests that this may be due in part to defects in Kir2.1 trafficking (Bendahhou *et al*, 2003) and changes in PIP_2 affinity (Lopes *et al*, 2002).

The Kir2 family consists of four subunits, the first three of which (Kir2.1-2.3) share a high degree of homology and can form functional homo- or hetero-meric tetramers. Kir2.1-2.3 subunits also share several trafficking motifs. For instance, all three subunits share an ER-export motif (Ma *et al.,* 2001), as well as conserved residues involved in Golgi export (Stockklausner and

Klocker, 2003). In addition, a conserved tyrosine residue at position 242 in Kir2.1 may play a role in endocytosis (Tong *et al.,* 2001). Finally, Kir2 channels contain PDZ binding motifs, and interact with a number of PDZ domain-containing scaffolding proteins that affect trafficking and channel stabilization in the plasma membrane (Leonoudakis *et al*, 2004). However, the cytoplasmic proteins that regulate Kir2 trafficking remain largely unknown.

One candidate family of proteins that might regulate Kir2 trafficking are the small G proteins, the Rho family GTPases. Rho GTPases act as signal transducers for a variety of cellular processes and have been well studied in cardiac cells as players in hypertrophy and heart failure (reviewed by Brown *et al*, 2006). Of the Rho family, Rho, Rac and Cdc42 are the most fully characterized. They have recently been implicated in channel trafficking. Bezzerides *et al.* (2004) revealed that Rac1 is required for rapid vesicular insertion of the TRPC5 cation channel into the plasma membrane, while other evidence points to a role for Rac in internalization (Lamaze *et al.,* 2001). Furthermore, Kv1.2, a delayed rectifier potassium current, is inhibited by tyrosine kinase phosphorylation in a Rho-dependent manner (Cachero *et al.,* 1998). Stimulation of m1-muscarinic receptors leads to inhibition of Kir2.1 via RhoA (Jones, 2003), although the exact mechanism remains unresolved. Here, we examined whether RhoGTPases could regulate trafficking of I_{K1} channels (Kir2).

MATERIALS AND METHODS

Cell culture and transfection procedures

tsA 201 cells were grown in Dulbecco's modified Eagle's medium supplemented with 10% fetal calf serum, and incubated at 37 ^{o}C in 5% CO2. Cells were transiently transfected with two or more cDNAs using Lipofectamine 2000 (Invitrogen, Carlsbad, CA). Control cells were co-transfected with Kir2 cDNA and either β-galactosidase (β-gal) or empty pcDNA3 vector, while test cells were co-transfected with the Kir2 and small G-protein cDNAs, at a ratio of 1:1. For occlusion experiments, cells were transfected with Kir2.1 and each of two small G-protein cDNAs at a ratio of 1:1:1; control cells were transfected with Kir2.1 and the control plasmid at 1:2 to obtain the

same total amount of cDNA transfected. Cells were recorded from 2 days following transfection. Several separate transfections were performed for each set of conditions. Control and test transfections were performed in pairs and the experiments were interleaved. For experiments using *C. difficile* toxin B (Calbiochem, San Diego, CA), 100 pg/mL toxin B was diluted in DMSO (vehicle: VEH) and added to cells transfected with Kir2.1 and β-gal for 3 or 6 hours at 37^{o}C prior to electrophysiological recording.

DNA Constructs

Kir2.1, kindly provided by Dr. L.Y. Jan (Kubo *et al.,* 1993), has been inserted into the vector pcDNA3 (Invitrogen, Carlsbad, CA) as reported previously (Jones, 1996). Kir2.2 and Kir2.3 were kind gifts from Dr. Kurachi (Morishige *et al.,* 1994; Takahashi *et al.*, 1994) and were inserted into pcDNA3 as described previously (Rossignol and Jones, 2005). Dr. S. Schmid generously donated the dominant negative dynamin-1 mutant (DynK44A, Dyn_{DN}) (Hinshaw and Schmid, 1995). The mutant forms of the RhoGTPases were generous gifts from Dr. J.S. Gutkind (Coso *et al.,* 1995). The constitutively active mutants were generated by replacing glutamine for leucine by PCR-directed mutagenesis in a position analogous to that of codon 61 of Ras, generating $Rac1_{QL}$ at codon 61 as described by Coso *et al.* (1995). Such a mutation has been shown to inhibit the GTPase activity of these proteins resulting in a constitutively active protein. The dominant negative mutants of the small G-proteins were synthesized by replacement of the amino acid threonine for asparagine in a position analogous to codon 17 of Ras, generating Rac1N17 ($Rac1_{DN}$), Cdc42N17 ($Cdc42_{DN}$) and RhoAN19 ($RhoA_{DN}$). These inhibitory mutants act as antagonists by competitively inhibiting the interaction of endogenous G-proteins with their respective guanine nucleotide exchange factors (GEFs) and blocking transduction of the signal. GFP-Kir2.1 was created in pcDNA3 by fusing GFP directly to the C-terminus of a Kir2.1 construct containing a GYG to AAA mutation in the selectivity filter and was kindly provided by Dr. A. Lopatin (McLerie and Lopatin, 2003). Chimeric channels were generously donated by Dr. A. Collins (Collins *et al.,* 2005) and Dr. L.Y. Jan (Tinker *et al.,* 1996), and were subcloned into

pcDNA3.1. For total internal reflection fluorescence (TIRF) experiments, cells were plated on 35mm glass bottom culture dishes (MatTek) coated with rat tail collagen and poly-D-lysine.

Electrophysiological recordings

Kir2.1 whole-cell currents were recorded using a List EPC-7 patch clamp amplifier, as described previously (Jones, 1996). All experiments were carried out at room temperature. Electrodes were pulled on a three stage horizontal puller (Mecanex, Basel, Switzerland) to yield resistances of 4-8 MΩs. Currents were low-pass filtered at 1 kHz with an 8-pole Bessel filter, digitized through an ITC-16 analog-digital converter (Instrutech, Port Washington, NY) and sampled at 2 kHz with a Macintosh Quadra 800 computer. Currents were acquired with Axodata (Axon Instruments, Union City, CA). Cellular capacitance was determined by integration of the capacitative transient elicited by a 2 mV step. Control capacitance was 27 ± 2 pF (n=35) and remained constant throughout the study with the exception of Dyn_{DN}-transfected cells which displayed an average capacitance of 20 ± 1 pF (n=21). Series resistance was generally low (around 12 mOhm) and no series resistance compensation was applied; however, voltage errors were calculated in each cell with the known Rs values and cells with errors greater than 10 mV were excluded from further analysis.

Currents were elicited by holding the cells in whole-cell voltage-clamp at a potential of -60 mV and stepping the membrane to potentials ranging from -160 to 10 mV for 200 ms in 10 mV increments as described previously (Jones, 1996; 2003). This protocol was repeated every 2 minutes for the duration of the experiment. After initial breakthrough into the whole cell mode, a 10-minute period was allowed for stabilization of the current amplitude prior to final current measurements. Transfection was assayed by the presence of an inwardly rectifying current with reversal at E_k. Previous experiments have indicated a high degree of co-transfection with the methods used here.

Single-channel recordings were performed using the cell-attached patch configuration. Electrodes were coated with Sylgard™ and fire polished. Recordings were performed in high potassium solution to force the resting membrane potential toward 0 mV. Spontaneous channel

activity was monitored at potentials ranging from 0 to -120 mV, for 30 s to several minutes. Currents were sampled at 5 kHz and subsequently low-pass filtered offline at 500 Hz using a Bessel 8-pole filter.

Data analysis

Currents were analyzed off-line, using Axograph software and P-Clamp 9.0 (Axon Instruments). For whole-cell currents, measurements were determined by averaging the last 10 data points of the 200 ms step. Current amplitudes were divided by cellular capacitance to account for differences in cell size and are reported as current density (pA/pF). Single-channel characteristics such as single channel amplitude, probability of opening and open and closed dwell times were analyzed using P-Clamp. Linear fits were made to I-V plots using at least three data points per cell to calculate slope conductance. Statistical significance was determined using non-parametric statistical methods. Data are presented as the mean ± the standard error.

Recording solutions

The extracellular recording solution was composed of (in mM): 150 NaCl, 5 KCl, 2 CaCl2, 1 MgCl2, 5 HEPES, 20 glucose. The pH was adjusted to 7.4 and the osmolarity was adjusted to 325-330 mmol/kg. The intracellular patch pipette solution contained (in mM): 150 K-gluconate, 2 MgCl2, 1.1 EGTA, 0.1 CaCl2, 5 HEPES, 5 Mg-ATP, 0.1 Li-GTP. The pH was adjusted to 7.2 and the osmolarity to 315-320 mmol/kg. Single-channel recordings were performed in symmetrical, high potassium solution consisting of (in mM): 150 KCl, 2 CaCl2, 1 MgCl2, 5 HEPES, 25 glucose. The pH was adjusted to 7.4 and the osmolarity to 320-330 mmol/kg.

Total Internal Reflection Fluorescence (TIRF) Microscopy

TIRF microscopy was used to analyze surface expression of CFP-tagged IRK1. Through-the-objective TIRF microscopy occurs when collimated laser light is offset to illuminate the back focal plane of the objective, which causes the laser light to arrive at the coverslip at an angle. When this angle is greater than the critical angle (θ), an evanescent wave of excitation light is

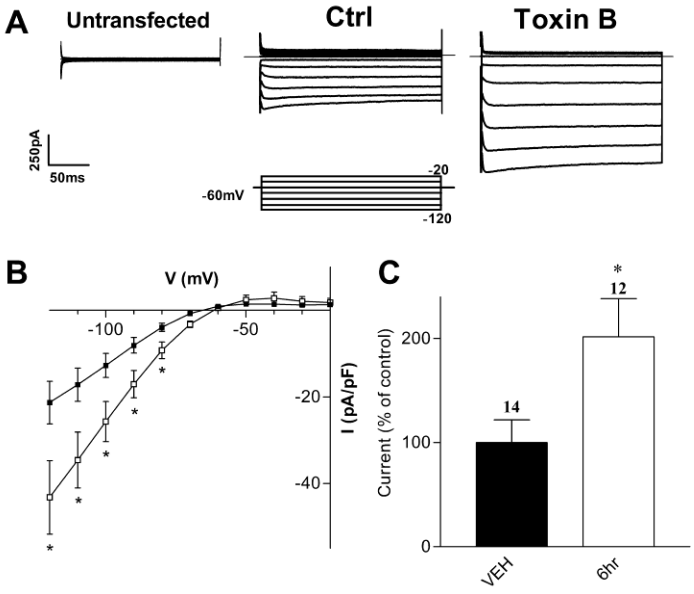

FIGURE 1-1. INHIBITING RHO FAMILY GTPASES INCREASES KIR2.1 CURRENT DENSITY.

A) Representative current traces from tsA201 cells co-transfected with Kir2.1 and β-gal under control conditions or after pre-incubation with 100 pg/mL *C. difficile* toxin B. Superimposed current traces are shown for 200 ms voltage steps from -120 to -20 mV in 10 mV increments from a holding potential of -60 mV. Inset shows the voltage protocol used. *B)* Current-voltage (I-V) relationship of control cells (vehicle, filled squares) and cells incubated with toxin B for 6 hours (open squares). The currents are presented as pA/pF to compensate for potential cell size differences. *C)* Normalized current densities at –100 mV, presented as percent of control currents. Currents were normalized to the mean of control cells by day of recording. Numbers above columns indicate number of cells in each condition. Asterisks denote statistically significantly different from control cells, using non-parametric t-test, at *, $p<0.05$.

produced at the interface between two media having different refractive indices, the glass coverslip and media/cell membrane (Axelrod et al., 1983). The intensity of this evanescent wave falls off exponentially with distance above the interface, allowing selective imaging within ~100nm of the glass/medium interface (i.e. plasma membrane and sub-membrane regions). A Nikon TE2000 microscope was equipped with a 60x oil-immersion TIRF objective (Nikon; 1.45 NA) and a solid state DPSS 442nm laser (Melles Griot – model: 85 BTL 010), which could be adjusted manually for epifluorescence and TIRF. The Nikon filter cube contained a polychroic mirror with reflection bands at 440nm and 510nm, and band-passes at 475/30nm and 560/60nm (z442/514rpc; Chroma technologies). No excitation filter was used. A CFP emission filter (470/30) was placed in a filter wheel (Sutter Instruments) and controlled by a Lambda 10-2 controller (Sutter Instruments). Images (16 bit) were acquired with a 12.5 MHz Imago CCD camera (Till Photonics). The camera, laser shutters and filter wheel were electronically controlled by TILLvisION software. Transfected cells were imaged first using epifluorescence (100 ms exposure time) and, after adjusting the laser, using TIRF (500 ms exposure) microscopy. Fluorescent intensity was analyzed using NIH ImageJ software. Background was first subtracted, then a region of interest (ROI) was drawn around the entire cell (epi) or the footprint (TIRF), and the average fluorescent intensity (in arbitrary units) was measured.

RESULTS

Involvement of Rho-family GTPase Rac1 in regulating Kir2.1 channels

To investigate the putative involvement of the Rho-family of small GTPases (including Rho, Rac and Cdc42) in the regulation of Kir2.1 channels we first utilized the bacterial cytotoxin *C. difficile* toxin B, which inhibits members of the Rho family (Just *et al.,* 1995). tsA201 cells transfected with Kir2.1 cDNA displayed strong, inwardly rectifying currents (Figs. 1-1A and 1-1B). Kir2.1-transfected cells incubated with 100 pg/mL *C. difficile* toxin B (for ≥ 6 h) displayed a significant increase in Kir2.1 current density (Figs. 1-1A and 1-1B). At -100 mV, the current density increased to 202 ± 18% of control, from -13 ± 3 pA/pF (n=14) to -26 ± 5 pA/pF (n=12) in

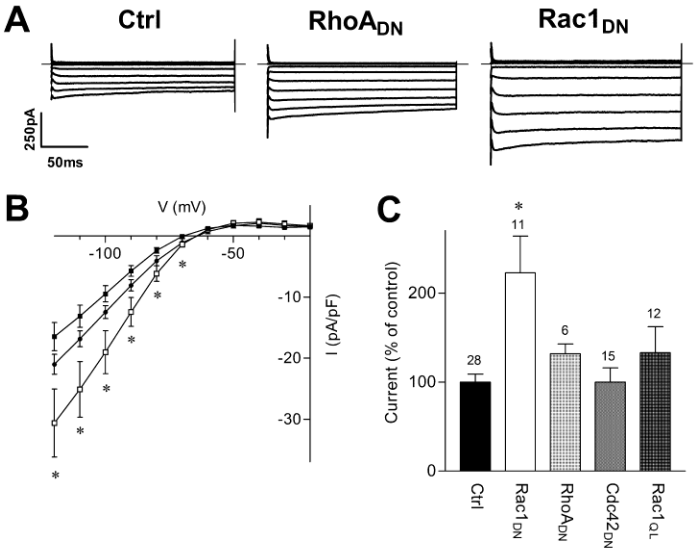

FIGURE 1-2. EFFECTS OF RHO FAMILY MUTANTS ON KIR2.1 WHOLE-CELL CURRENTS.

A) Representative current traces from tsA201 cells co-transfected with Kir2.1 and a control plasmid (Ctrl), dominant-negative RhoA ($RhoA_{DN}$) or dominant-negative Rac1 ($Rac1_{DN}$). Superimposed current traces are shown for 200 ms voltage steps from -120 to +10 mV in 10 mV increments from a holding potential of -60 mV. Scale bars: 50 ms and 250 pA. *B*) Current-voltage (I-V) relationship of control (filled squares), $Rac1_{DN}$ (open squares) and $RhoA_{DN}$ transfected cells (filled circles). *C*) Normalized current densities at –100 mV from control and mutant-GTPase transfected cells. $Cdc42_{DN}$ represents the dominant-negative mutant of Cdc42, and $Rac1_{QL}$ represents the activated mutant of Rac1. Numbers above columns indicate number of cells in each condition. Asterisks denote statistically significantly different from control cells, using Kruskal-Wallis nonparametric ANOVA followed by Dunn's multiple comparison procedure, at *, $p<0.01$.

cells pretreated with Toxin B. The increase in Kir2.1 current density with *C. difficile* toxin B suggests that the Rho-family of GTPases regulate Kir2.1 channels.

To investigate which Rho-family GTPase could be involved in regulating Kir2.1 channels, we took advantage of dominant-negative forms of Rho, Rac and Cdc42 (Coso *et al.,* 1995). Dominant negative versions of these GTPases act as antagonists by competitively inhibiting the interaction of endogenous G-proteins with their respective guanine nucleotide exchange factors (GEFs) and blocking transduction of the signal. In Kir2.1-transfected cells, co-transfection of the dominant-negative mutant of Rac1 ($Rac1_{DN}$) significantly increased Kir2.1 current density to 223 ± 18% of control cells (Fig. 1-2B), from –9 ± 1 pA/pF (n=28) in control cells to -19 ± 4 pA/pF (n=11) at -100 mV in cells transfected with $Rac1_{DN}$. Activation of RhoA has been shown previously to inhibit Kir2.1 channels, while dominant-negative RhoA had no effect (Jones, 2003). Similarly, here co-expression of the dominant-negative forms of RhoA ($RhoA_{DN}$) or Cdc42 ($Cdc42_{DN}$) did not significantly alter Kir2.1 current density, suggesting a specific role for Rac1 (Fig. 1-2C). Interestingly, the constitutively active mutant of Rac ($Rac1_{QL}$) did not significantly alter Kir2.1 current density (-11 ± 2 pA/pF (n=12)).

Analysis of single-channel properties of Kir2.1 channels in cells coexpressing $Rac1_{DN}$

An increase in Kir2.1 current density could be caused by an increase in the number of channels in the membrane, or by a change in the single-channel properties, such as unitary conductance (*i*), open probability (P_o) or open dwell time. To investigate the latter, we used the cell-attached patch-clamp technique to compare Kir2.1 single-channels in the absence or presence of co-expressed $Rac1_{DN}$. Unitary events for Kir2.1 channels could be recorded in cell attached patches from both cell types. To determine the single-channel conductance, we measured the unitary current between -40 and -120 mV (using equimolar K^+ to zero the cell's resting membrane potential). Single-channel conductance was calculated by determining the slope of the linear fit to the single-channel current-voltage relationship (Figure 1-3B). Coexpression of $Rac1_{DN}$ had little effect on Kir2.1 single channel properties, with a conductance of 15 ± 1 pS (n=4) in control cells and 15 ± 3 pS (n=6) in cells expressing $Rac1_{DN}$ (Fig. 1-3B). We

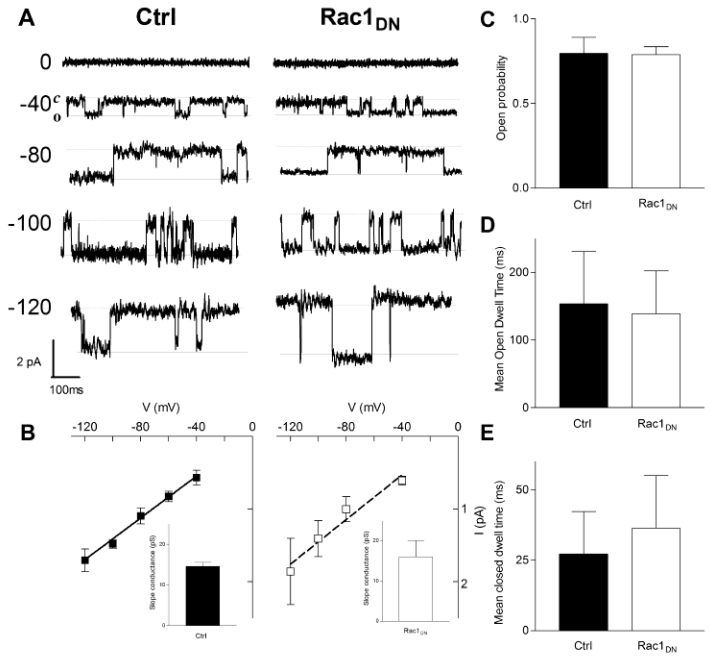

FIGURE 1-3. RAC1 HAS NO EFFECT ON KIR2.1 SINGLE-CHANNEL PROPERTIES.

A) Representative single-channel traces from control (Ctrl) and $Rac1_{DN}$ transfected cells in cell-attached patch clamp recordings at various voltages. The dashed line represents the closed state of the channel and the solid line represents the open state. *B*) Current-voltage relationship of single-channel currents from control (filled squares) and $Rac1_{DN}$ transfected cells (open squares). Lines represent linear fits to the data points; the solid line is the fit to control cells, the dashed line is the fit to $Rac1_{DN}$ transfected cells. Insets: Slope conductance calculated from linear fit to current amplitudes of individual cells using three or more data points. *C)* Open probability of Kir2.1 in control and $Rac1_{DN}$ transfected cells at –40 mV. *D)* Mean open and *E)* closed dwell times of control and $Rac1_{DN}$ transfected cells at –40 mV. Significance was tested using non-parametric t-tests. Data was obtained from 5-6 cells per condition.

also examined the kinetics of single-channel opening and closings by measuring the open and closed dwell times at -40 mV (comparable to -100 mV in whole-cell recordings) in 30 s traces. The mean open times at -40 mV were 154 ± 77 ms in control cells and 139 ± 63 ms in $Rac1_{DN}$ transfected cells (NS; p>0.05 Fig. 1-3D). The mean closed times were 27 ± 15 ms in control cells and 36 ± 17 ms in $Rac1_{DN}$ transfected cells (NS; p>0.05 Fig. 1-3E). Similarly, the open probability of the channel was also not significantly different (Fig. 1-3C), with Po = 0.8 ± 0.1 in control, 0.8 ± 0.05 in $Rac1_{DN}$ transfected cells at -40 mV (n=5-6, NS; p>0.05). Macroscopic current (I) is determined by the number of channels (N), P_o and *i* ($I = NP_o i$), therefore, these experiments suggest that $Rac1_{DN}$ instead alters the number (N) of channels on the plasma membrane.

Inhibiting endocytosis with Dyn_{DN} occludes potentiation effect of $Rac1_{DN}$

A change in the number of Kir2.1 channels could be caused by an insertion of new Kir2.1 channel protein into the membrane, a reduction in endocytosis or a combination of the two. To test the effect of reduced endocytosis on Kir2.1 current density, we utilized a dominant negative form of dynamin (Dyn_1K44A or Dyn_{DN}), which blocks the endocytic process (Hinshaw and Schmid, 1995). Co-expression of Dyn_{DN} significantly increased Kir2.1 current density (Figure 1-4). As with $Rac1_{DN}$, the current density for both inward and outward currents increased (Fig. 1-4B). Expression of Dyn_{DN} increased Kir2.1 current density to 191 ± 12% of control (-9 ± 2 pA/pF for control (n=16) vs. -18 ± 2 pA/pF in Dyn_{DN} transfected cells (n=15)' p<0.01, Fig. 1-4C). Thus, inhibiting endocytosis increases Kir2.1 current density.

We then examined the effect of expressing $Rac1_{DN}$ with Dyn_{DN}. If $Rac1_{DN}$ promotes exocytosis while Dyn_{DN} inhibits endocytosis, we would expect to see an additive effect and an increase in Kir2.1 current. The Kir2.1 current density increased to 202 ± 13% (n=12) of control, which was not significantly different from that caused by Dyn_{DN} or $Rac1_{DN}$ alone (Fig. 1-2C, Fig. 1-4C). Thus, inhibiting endocytosis appears to occlude the effect of $Rac1_{DN}$, suggesting that Rac1DN interferes with endocytosis.

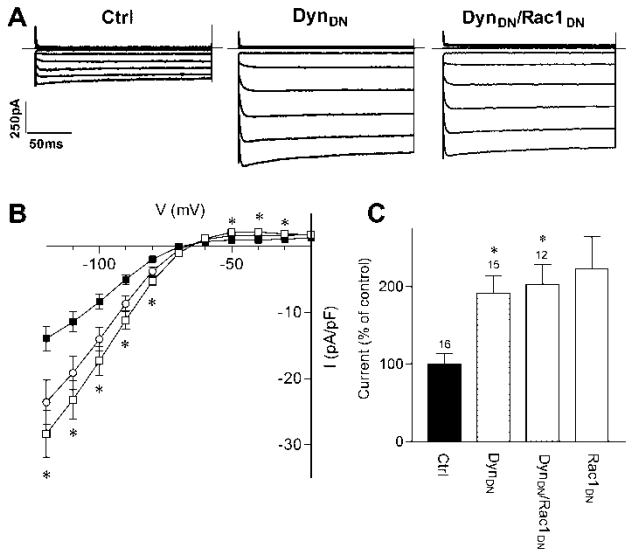

FIGURE 1-4. DOMINANT-NEGATIVE DYNAMIN MIMICS/OCCLUDES THE EFFECT OF RAC1$_{DN}$ ON KIR2.1 CURRENTS.

A) Representative current traces from cells transfected with Kir2.1 and a control plasmid (Ctrl), dominant-negative dynamin (Dyn$_{DN}$) or dominant-negative dynamin and dominant negative Rac1 together (Dyn$_{DN}$/ Rac1$_{DN}$). Superimposed current traces are shown for 200 ms voltage steps from -120 to -20 mV in 10 mV increments from a holding potential of -60 mV. Scale bars: 50 ms and 250 pA. *B*) Current-voltage relationship of control (filled squares), Dyn$_{DN}$ (open squares) and Dyn$_{DN}$/ Rac1$_{DN}$ (open circles) transfected cells. *C*) Normalized current densities measured in control, Dyn$_{DN}$, and Dyn$_{DN}$/ Rac1$_{DN}$ transfected cells at –100 mV. Rac1$_{DN}$ transfected cells from Fig. 2 are also included for comparison. Numbers above columns indicate number of cells in each condition. Asterisks denote statistically significantly different from control cells, using a non-parametric Kruskil-Wallis ANOVA, followed by Dunn's multiple comparison procedure, at *, $p<0.05$.

$Rac1_{DN}$ increases surface expression of Kir2.1

To independently assess whether changes in Kir2.1 current density could be attributed to changes in surface expression, we used TIRF microscopy to study the surface expression of CFP-tagged Kir2.1 channels in the absence or presence of coexpressed $Rac1_{DN}$. TIRF microscopy allows visualization of channel proteins expressed in the plasma membrane and sub-membrane regions (Axelrod *et al.*, 1983; Fowler *et al*., 2007). To visualize Kir2.1 channels, we fused cyan fluorescent protein (CFP) to the N-terminus Kir2.1 and imaged under both wide-field epifluorescence and TIRF. CFP-Kir2.1 was detected using both wide-field and TIRF illumination. The intensity of CFP-Kir2.1 fluorescence under TIRF increased to 213 ± 18% of control in cells coexpressing $Rac1_{DN}$, (Fig. 1-5A). Similarly, inhibition of endocytosis with Dyn_{DN} increased surface fluorescence of CFP-Kir2.1 (189 ±22% of control). By contrast, coexpression of $Rac1_{QL}$ or Rho_{DN} did not significantly alter CFP-Kir2.1 fluorescence on the plasma membrane (Fig. 1-5B). These changes in surface expression of CFP-Kir2.1 channels measured with TIRF are similar to the changes in current density measured with patch-clamp electrophysiology. Taken together, these results suggest that Rac1 modulates surface levels of Kir2.1 channel expression.

Rac1 regulates surface expression of Kir2.1 but not Kir2.2 or Kir2.3

Kir2.1, Kir2.2 and Kir2.3 share 60% or greater identity in amino acid sequence. We investigated whether Kir2.2 or Kir2.3 channels were sensitive to regulation by Rac1. Expression of Kir2.2 or Kir2.3 cDNA yielded inwardly rectifying K^+ currents that were similar to Kir2.1 channels (Figs. 1-6A and 1-6C). Co-expression of $Rac1_{DN}$ did not significantly alter the current density (Figs. 6B and 6D), suggesting that the effect of Rac1 on channel trafficking is specific to Kir2.1 subunits. Thus, the effect of Rac1 modulation appears to be specific for the Kir2.1 channel subtype .

To localize the region of Kir2.1 channels that could mediate reglation by Rac, we utilized Kir2.1/2.2 chimeric channels (Collins *et al.,* 2005; Tinker *et al.,* 1996), in which the N-and C-terminal domains were exchanged (Fig. 1-7A) . Chimera 2.1_N-2.2 contains the N-terminal domain

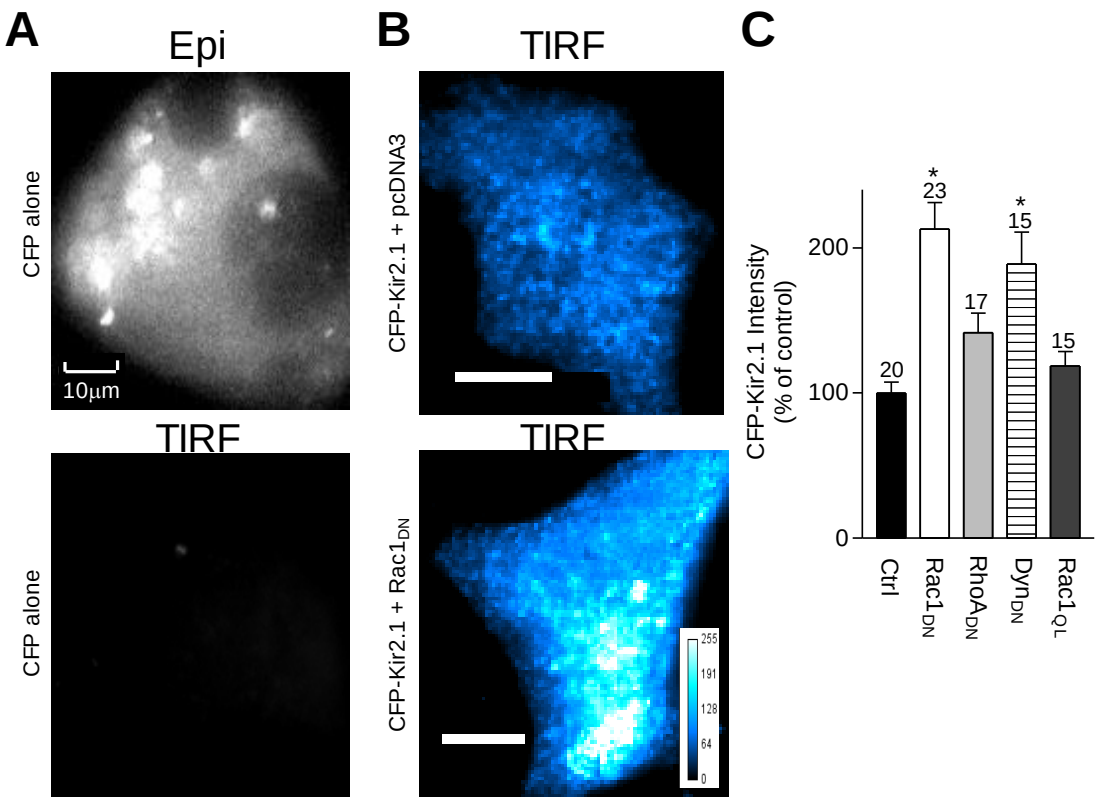

FIGURE 1-5. $RAC1_{DN}$ INCREASES SURFACE EXPRESSION OF CFP-KIR2.1.

TIRF microscopy was used to monitor plasma membrane expression of CFP-Kir2.1 in transfected tsA201 cells. *A)* Representative images from cells transfected with CFP cDNA viewed with epifluorescence (top: Epi) or TIRF (bottom) microscopy. Images have been scaled to the same intensity. *B)* Representative images from cells transfected with CFP-Kir2.1 cDNA and either empty vector pcDNA3 (top panel) or $Rac1_{DN}$ pcDNA3 (bottom panel) cDNA, viewed with TIRF microscopy. Images have been scaled to the same intensity. Inset shows scale bar used to calibrate intensity. *C)* Quantitative analysis of CFP-Kir2.1 intensity under TIRF. Images were background-subtracted and analyzed using ImageJ software. Asterisks denote significance determined by non-parametric ANOVA and Dunn's post-hoc test, at *, $p < 0.01$ and **, $p < 0.001$.

of Kir2.1 fused to Kir2.2 at amino acid 78 (Collins *et al.,* 2005) and chimera 2.2_N-2.1 contains the N-terminal and first transmembrane domain of Kir2.2 fused to Kir2.1 at amino acid 121(Tinker *et al,* 1996). Transfection of cDNA for 2.1_N-2.2 and 2.2_N-2.1 yielded inwardly rectifying K currents, having current densities of -36.3 ± 8.3 pA/pF and -8.2 ± 2.3 pA/pF for 2.1_N-2.2 and 2.2_N-2.1, respectively.

Similar to Kir2.2, co-expression of $Rac1_{DN}$ did not change the current-voltage relationship or current density for 2.1_N-2.2 channels (Figs. 1-7B and 1-7C). By contrast, $Rac1_{DN}$ coexpression increased 2.2_N-2.1current density to 178 ± 29% (n=9) of control (Fig. 1-7E, $p<0.05$), without altering the current kinetics or current-voltage relationship. Taken together, these experiments suggest that the selective effects of Rac1 involve the C-terminal domain of Kir2.1.

DISCUSSION

In this study, we investigated whether the Rho-family of small GTPases regulates the Kir2 family of inwardly rectifying potassium channels. Selective inhibition of the endogenous GTPase Rac with $Rac1_{DN}$ led to a nearly two-fold increase in Kir2.1 current density, while the dominant-negative mutants of Cdc42 or RhoA did not significantly alter the current density. $Rac1_{DN}$ did not alter the single-channel kinetics or conductance, suggesting that the number of Kir2.1 channels expressed in the plasma membrane was changed by $Rac1_{DN}$. Consistent with this interpretation, the intensity of CFP-tagged Kir2.1 channels increased in the plasma membrane in the presence of $Rac1_{DN}$. Finally, we found that a dominant-negative mutant of dynamin, known to be involved in endocytosis, mimics and occludes the effect of $Rac1_{DN}$, suggesting Rac1 is involved in regulating the rate of internalization of Kir2.1 channels from the plasma membrane. The lack of effect with the constitutively active Rac1 suggests that levels of endogenous activated Rac are sufficient to maximally regulate Kir2.1 expression. These results suggest that regulation of Kir2.1 channels on the plasma membrane is controlled, in part, by Rac1.

An increase in current density due to Rac-induced changes in membrane PIP2 levels is possible. This explanation seems unlikely since Kir2.1 channels bind PIP_2 with high affinity and

would show little change with increased levels of PIP_2 (Huang et al, 1998). An increase in current density could also arise from an increase in functional Kir2.1 channels that are already expressed on the plasma membrane. Indeed, Sun et al. (2004) reported that a fraction of Kir2.1 channels on the plasma membrane appear electrically silent. This possibility also seems unlikely because a similar magnitude increase in surface expression was measured with CFP-Kir2.1 using TIRF microscopy. Using CFP-Kir2.1 enabled us to study both electrically active and possibly silent channels in the plasma membrane. Previous reports suggest that Kir2.1 shows a high degree of constitutive internatlization (Leyland & Dart, 2004). Given the classical role for RhoGTPases in membrane trafficking, the most parsimonious explanation for the potentiation of Kir2.1 current is that the rate of Kir2.1 endocytosis is altered by interfering with endogenous Rac1. Consistent with this interpretation, we did not observe an additive effect of $Rac1_{DN}$ with Dyn_{DN}, suggesting Rac1DN acts predominantly on the internalization of Kir2.1.

Interestingly, Rac1DN altered the current density for Kir2.1 channels but not for Kir2.2 or Kir2.3 channels. Kir2.1-2.3 are highly homologous (60% or greater homology), including several conserved regions implicated previously in trafficking (Ma *et al*, 2001; Stockklausner & Klocker, 2003; Tong *et al,* 2001). One possibility is that Kir2.2/2.3 internalize via a mechanism fundamentally different from that for Kir2.1. Alternatively, Kir2.2/2.3 channels may lack an internalization signal required for Rac1 modulation. For example, Kir2.1 contains a dileucine motif at amino acids 231-232, which could account for the differential effects of Rac on Kir2 trafficking. Consistent with this, the chimeric channel containing the C-terminal domain and part of the pore is sensitive to regulation by Rac1. Because Kir2 channels form heteromeric channels, the balance of different internalization motifs will likely dictate how native, heteromeric channel complexes are regulated by Rho GTPases.

The activated mutant of Rac1 did not alter Kir2.1 current density. We had anticipated that constitutively active Rac1 would reduce the levels of Kir2.1 channels, similar to constitutively active RhoA (Jones, 2003). Studies with interleukin 2 (IL2) receptors also found that the dominant negative mutant of Rac suppressed receptor internalization, while the activated mutant has no

FIGURE 1-6. KIR2.2 AND KIR2.3 ARE NOT REGULATED BY RAC.

A&C) Representative current traces from cells transfected with *(A)* Kir2.2 or *(C)* Kir2.3 and a control plasmid (Ctrl) or dominant-negative Rac1 ($Rac1_{DN}$). Superimposed current traces are shown for 200 ms voltage steps from -120 to -20 mV in 10 mV increments from a holding potential of -60 mV. Scale bars: 50 ms and 250 pA. *B&D) Left:* Current-voltage relationship of Kir2.2 (B) or Kir2.3 (D) in control (filled squares) and $Rac1_{DN}$ (open squares) transfected cells. Right: Normalized current densities measured in control and $Rac1_{DN}$ transfected cells at –100 mV. Numbers above columns indicate number of cells in each condition. No significance was detected with non-parametric t-tests at <0.05.

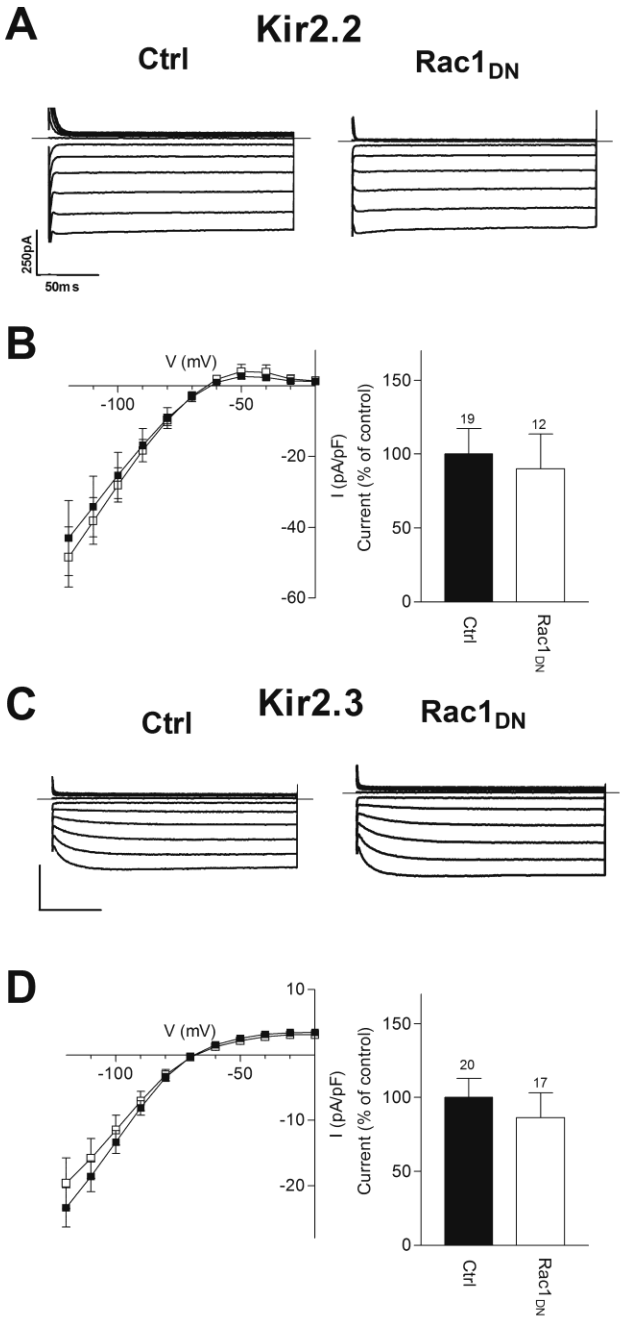
A
Kir2.2
Ctrl
Rac1DN
250pA
50ms
B
V (mV)
-100
-50
-20
-40
-60
I (pA/pF)
Current (% of control)
150
100
50
0
19
12
Ctrl
Rac1DN
C
Kir2.3
Ctrl
Rac1DN
D
10
V (mV)
-100
-50
-10
-20
I (pA/pF)
Current (% of control)
150
100
50
0
20
17
Ctrl
Rac1DN

effect (Lamaze *et al.,* 2001). One possible explanation is that endogenous levels of Rac1 mask the effect of ectopically expressed Rac1 or that ectopically expressed Rac1 levels are too low. Alternatively, the dominant negative Rac1 may suppress the activity of all subtypes of Rac (Rac1-3) in the cell, while activating only Rac1 is insufficient to alter trafficking. Of note, IL2 receptors have been shown to localize to detergent resistant membrane fractions, or lipid rafts, as have Kir2 family members (Romanenko *et al.,* 2004). This may reflect a more general role for Rac in lipid raft endocytosis.

The mechanism by which Rac affects Kir2.1 endocytosis remains to be determined. Rho GTPases are key players in cardiac signaling, having been well studied in the context of cardiac hypertrophy. Hypertrophic agonists such as phenylephrine and endothelin-1, as well as angiotensin-II have been shown to activate Rac1, while statins block the isoprenylation and thus membrane targeting and functional activation of Rac1 in cardiac cells (Brown et al, 2006). Rac activates a number of downstream effectors that have been implicated in endocytosis. Rac activates p21-activated kinase (PAK) , for instance, which plays a role in cardiomyocyte contractility, and silencing PAK1 leads to a reduction in endocytosis (Pelkmans et al, 2005). Alternatively, Rac could alter Kir2.1 endocytosis through its effects on the actin cytoskeleton. Filamin A is an actin binding protein and missense mutations in filmain A lead to cardiac malformations (Hart et al, 2006). Filamin A also binds Rac and has been shown to increase surface expression of Kir2.1 (Sampson et al, 2003). The specificity of the effect of Rac1 for Kir2.1 in cardiac signaling likely arises from the involvement of Rac-specific GEFs and/or subcellular localization.

The cardiac inwardly rectifying potassium conductance I_{k1} plays a crucial role in shaping the cardiac action potential, particularly during the plateau and repolarization phases. Studies in knockout mice suggest while I_{k1} is composed of both Kir2.1 and 2.2, Kir2.1 is the dominant subunit; Kir2.1 knockout mice completely lack I_{k1}, while Kir2.2 knockout mice show approximately 50% reduction in I_{k1}(Zaritsky et al, 2001). Regulation of Kir2.1 currents by Rac could have important consequences for cardiac function. Upregulation of Kir2.1 currents leads to

multiple abnormalities of cardiac excitability, including atrioventricular (AV) block and atrial fibrillation (AF) (Li *et al*, 2004). Interestingly, transgenic mice expressing a cardiac-targeted guanine nucleotide dissociation inhibitor (GDI) that binds Rho family members (including Rho, Rac and Cdc42) in their inactive, GDP-bound forms resulted in normal ventricular conductance, but several atrial arrhythmias, including AV block in all animals and atrial fibrillation in a small percentage of animals (Wei *et al*, 2004). While the exact mechanism through which Rac regulates Kir2 trafficking remains to be determined, we speculate that Rac1 plays an important role in preventing overexpression of Kir2.1 in the heart.

FIGURE 1-7. THE C-TERMINUS OF KIR2.1 MEDIATES EFFECTS OF RAC.

A) Schematic of construction of chimeric subunits. 2.1_N-2.2, the N terminus of Kir2.1fused to Kir2.2 at position 78. 2.2_N-2.1, Kir2.1 fused to Kir2.2 at position 121. *B)* Representative current traces from 2.1_N-2.2 transfected cells under control conditions or co-transfected with $Rac1_{DN}$. Superimposed current traces are shown for 200 ms voltage steps from -120 to -20 mV in 10 mV increments from a holding potential of -60 mV. *C) Left* Current-voltage traces of 2.1_N-2.2 under control conditions (filled squares) or co-transfected with $Rac1_{DN}$ (open squares). *Right:* Normalized current densities measured in 2.1_N-2.2 transfected cells under control conditions and co-transfected with $Rac1_{DN}$, at –100 mV. *D)* Representative current traces from 2.2_N-2.1 transfected cells under control conditions or co-transfected with $Rac1_{DN}$. Scale bars: 50 ms and 250 pA. *E) Left:* Current-voltage traces of 2.2_N-2.1 under control condtions (filled squares) or co-transfected with $Rac1_{DN}$ (open squares). *Right:* Normalized current densities measured in 2.2_N-2.1 transfected cells under control conditions and co-transfected with $Rac1_{DN}$, at -100 mV. Numbers above columns indicate number of cells in each condition. Asterisks denote significance with non-parametric t-tests, at *, $p<0.05$.

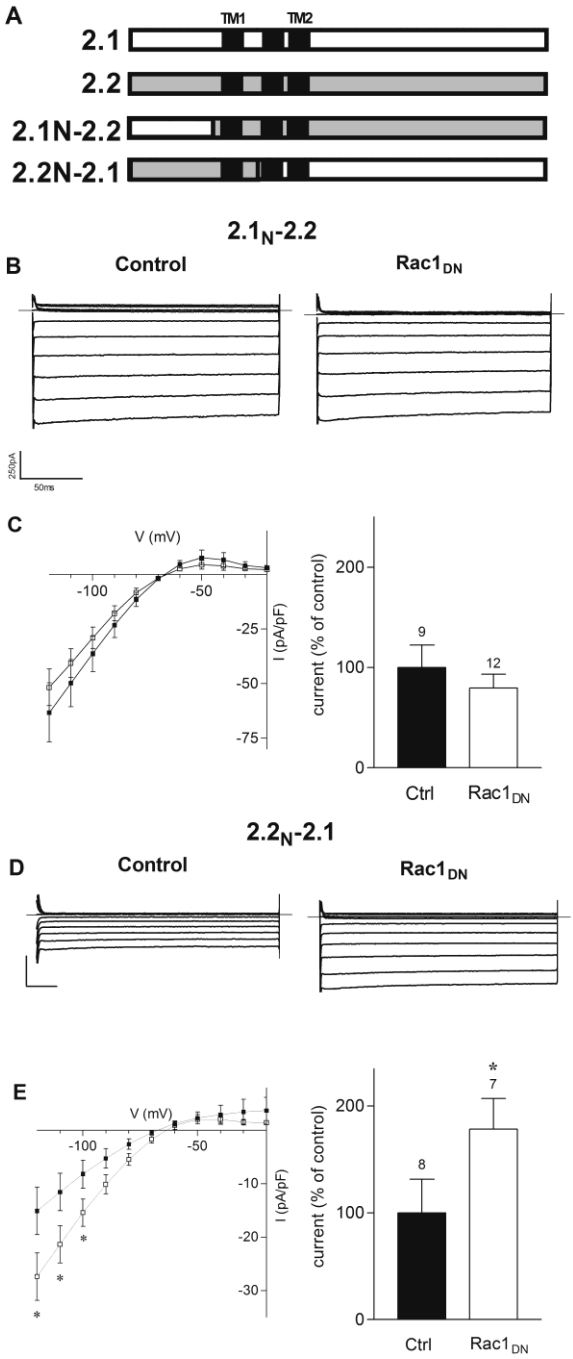
A
TM1
TM2
2.1
2.2
2.1N-2.2
2.2N-2.1
2.1N-2.2
B
Control
Rac1DN
250pA
50ms
C
V (mV)
-100
-50
-25
-50
-75
I (pA/pF)
current (% of control)
200
100
0
9
12
Ctrl
Rac1DN
2.2N-2.1
D
Control
Rac1DN
E
V (mV)
-100
-50
-10
-20
-30
I (pA/pF)
current (% of control)
200
100
0
8
7
*
Ctrl
Rac1DN

LITERATURE CITED

Axelrod D, Thompson NL, Burghardt TP (1983) Total internal inflection fluorescent microscopy. J Microsc 129:19-28.

Bendahhou S DMRPNMT-FMFYHPLJ (2003) Defective potassium channel Kir2.1 trafficking underlies Andersen-Tawil syndrome. Journal of Biological Chemistry 278:51779-51785.

Bezzerides Vj RISKSGACDE (2004) Rapid vesicular translocation and insertion of TRP channels. Nature Cell Biology 6:709-720.

Brown Jh DRDPSMA (2006) The Rac and Rho hall of fame: a decade of hypertrophic signaling hits. Circulation Research 98:730-742.

Cachero TG, Morielli AD, Peralta EG (1998) The small GTP-binding protein RhoA regulates a delayed rectifier potassium channel. Cell 93:1077-1085.

Collins A, Wang H, Larson MK (2005) Differential sensitivity of Kir2 inward-rectifier potassium channels to a mitochondrial uncoupler: identification of a regulatory site. Mol Pharmacol 67:1214-1220.

Coso OA, Chiariello M, Yu JC, Teramoto H, Crespo P, Xu N, Miki T, Gutkind JS (1995) The small GTP-binding proteins Rac1 and Cdc42 regulate the activity of the JNK/SAPK signaling pathway. Cell 81:1137-1146.

del Pozo MA, Alderson NB, Kiosses WB, Chiang HH, Anderson RG, Schwartz MA (2004) Integrins regulate Rac targeting by internalization of membrane domains. Science 303:839-842.

Fowler CE, Aryal P, Suen KF, Slesinger PA (2007) Evidence for association of GABA(B) receptors with Kir3 channels and regulators of G protein signalling (RGS4) proteins. J Physiol 580:51-65.

Hart AW, Morgan JE, Schneider J, West K, McKie L, Bhattacharya S, Jackson IJ, Cross SH (2006) Cardiac malformations and midline skeletal defects in mice lacking filamin A. Hum Mol Genet 15:2457-2467.

Hinshaw JE, Schmid SL (1995) Dynamin self-assembles into rings suggesting a mechanism for coated vesicle budding. Nature 374:190-192.

Huang CL, Feng S, Hilgemann DW (1998) Direct activation of inward rectifier potassium channels by PIP2 and its stabilization by Gbetagamma. Nature 391:803-806.

Jones SV (1996) Modulation of the inwardly rectifying potassium channel IRK1 by the m1 muscarinic receptor. Mol Pharmacol 49:662-667.

Jones SV (2003) Role of the small GTPase Rho in modulation of the inwardly rectifying potassium channel Kir2.1. Mol Pharmacol 64:987-993.

Just I GR (2004) Large clostridial cytotoxins. Reviews of Physiology, Biochemistry and Pharmacology 152:23-47.

Kubo Y, Baldwin TJ, Jan YN, Jan LY (1993) Primary structure and functional expression of a mouse inward rectifier potassium channel. Nature 362:127-133.

Lamaze C DABTLCGBAD-VA (2001) Interleukin 2 receptors and detergent-resistant membrane domains define a clathrin-independent endocytic pathway. Molecular Cell 7:661-671.

Leonoudakis D CLRRCMMLMVCA (2004) A multiprotein trafficking complex composed of SAP97, CASK, Veli, and Mint1 is associated with inward rectifier Kir2 potassium channels. Journal of Biological Chemistry 729:19051-19063.

Leyland ML, Dart C (2004) An alternatively spliced isoform of PSD-93/chapsyn 110 binds to the inwardly rectifying potassium channel, Kir2.1. J Biol Chem 279:43427-43436.

Li J MMLAN (2004) Transgenic upregulation of IK1 in the mouse heart leads to multiple abnormalities of cardiac excitability. American Journal of Physiology Heart Circulation Physiology 287:H2790-H2802.

Lopes Cm ZHRTJTYJLDE (2002) Alterations in conserved Kir channel-PIP2 interactions underlie channelopathies. Neuron 34:933-944.

Ma D ZNLYFCAYMJYNJLY (2001) Role of ER export signals in controlling surface potassium channel numbers. Science 291:316-319.

McIntosh MA, Cobbe SM, Kane KA, Rankin AC (1998) Action potential prolongation and potassium currents in left-ventricular myocytes isolated from hypertrophied rabbit hearts. J Mol Cell Cardiol 30:43-53.

McLerie M, Lopatin AN (2003) Dominant-negative suppression of I(K1) in the mouse heart leads to altered cardiac excitability. J Mol Cell Cardiol 35:367-378.

Morishige K, Takahashi N, Jahangir A, Yamada M, Koyama H, Zanelli JS, Kurachi Y (1994) Molecular cloning and functional expression of a novel brain-specific inward rectifier potassium channel. FEBS Lett 346:251-256.

Pelkmans L, Fava E, Grabner H, Hannus M, Habermann B, Krausz E, Zerial M (2005) Genome-wide analysis of human kinases in clathrin- and caveolae/raft-mediated endocytosis. Nature 436:78-86.

Plaster Nm TRT-FMCSBSTADMRISTBEBRCJ (2001) Mutations in Kir2.1 cause the developmental and episodic electrical phenotypes of Andersen's syndrome. Cell 105:511-519.

Preisig-Muller R, Schlichthorl G, Goerge T, Heinen S, Bruggemann A, Rajan S, Derst C, Veh RW, Daut J (2002) Heteromerization of Kir2.x potassium channels contributes to the phenotype of Andersen's syndrome. Proc Natl Acad Sci U S A 99:7774-7779.

Priori Sg PSVRIBOREDANCAJdBMRGSBG (2005) A novel form of short QT syndrome (SQT3) is caused by a mutation in the KCNJ2 gene. Circulation Research 97:800-807.

Romanenko Vg FYBFTAJVCARGHLI (2004) Cholesterol sensitivity and lipid raft targeting of Kir2.1 channels. Biophysics Journal 87:3850-3861.

Rossignol Tm JSV (2006) Regulation of a family of inwardly rectifying potassium channels (Kir2) by the m1 muscarinic receptor and the small GTPase Rho. Pflugers Archive 452:164-174.

Sampson LJ, Leyland ML, Dart C (2003) Direct interaction between the actin-binding protein filamin-A and the inwardly rectifying potassium channel, Kir2.1. J Biol Chem 278:41988-41997.

Stockklausner C KN (2003) Surface expression of inward rectifier potassium channels is controlled by selective Golgi export. Journal of Biological Chemistry 278:17000-17005.

Storey NM, O'Bryan JP, Armstrong DL (2002) Rac and Rho mediate opposing hormonal regulation of the ether-a-go-go-related potassium channel. Curr Biol 12:27-33.

Sun H, Shikano S, Xiong Q, Li M (2004) Function recovery after chemobleaching (FRAC): evidence for activity silent membrane receptors on cell surface. Proc Natl Acad Sci U S A 101:16964-16969.

Sussman MA, Welch S, Walker A, Klevitsky R, Hewett TE, Price RL, Schaefer E, Yager K (2000) Altered focal adhesion regulation correlates with cardiomyopathy in mice expressing constitutively active rac1. J Clin Invest 105:875-886.

Takahashi N, Morishige K, Jahangir A, Yamada M, Findlay I, Koyama H, Kurachi Y (1994) Molecular cloning and functional expression of cDNA encoding a second class of inward rectifier potassium channels in the mouse brain. J Biol Chem 269:23274-23279.

Tinker A, Jan YN, Jan LY (1996) Regions responsible for the assembly of inwardly rectifying potassium channels. Cell 87:857-868.

Tong Y BGSLMSGSEKADDALHA (2001) Tyrosine decaging leads to substantial membrane trafficking during modulation of an inward rectifier potassium channel. Journal of General Physiology 117:103-118.

Wei L, Taffet GE, Khoury DS, Bo J, Li Y, Yatani A, Delaughter MC, Klevitsky R, Hewett TE, Robbins J, Michael LH, Schneider MD, Entman ML, Schwartz RJ (2004) Disruption of Rho signaling results in progressive atrioventricular conduction defects while ventricular function remains preserved. Faseb J 18:857-859.

Xia M JQBSHYLMMCYZQYYLYLBZQZY (2005) A Kir2.1 gain-of-function mutation underlies familial atrial fibrillation. Biochemical Biophysical Research Communications 332:1012-1019.

Zaritsky JJ, Redell JB, Tempel BL, Schwarz TL (2001) The consequences of disrupting cardiac inwardly rectifying K(+) current (I(K1)) as revealed by the targeted deletion of the murine Kir2.1 and Kir2.2 genes. J Physiol 533:697-710.

Chapter 2, in part, has been submitted for publication of the material as it may appear in the Journal of Cellular Physiology, 2008, Boyer SB, Slesinger PA, and Jones SVP. The dissertation author was the primary investigator and author of this paper.

CHAPTER 2: DIRECT INTERACTION OF $GABA_B$ RECEPTORS WITH M2 MUSCARINIC RECEPTORS RESCUES MUSCARINIC SIGNALING

ABSTRACT

An emerging theme among G protein-coupled receptors (GPCR) is that the GPCR, G proteins and effectors exist in a macromolecular signaling complex. In neuronal PC12 cells, m2 muscarinic receptors and G protein-activated inwardly rectifying potassium (GIRK) channels both undergo internalization in response to chronic muscarinic stimulation. Here, we showed that expression of $GABA_B$ R1/R2 subunits rescues GIRK expression in NGF-differentiated PC12 cells. Surprisingly, expression of $GABA_B$ R1/R2 or even R2 alone rescued muscarinic receptor-activated GIRK channels. In fact, co-expression of the R2 subunit appeared to promote muscarinic m2 (m2R) expression at the plasma membrane, as detected using total internal reflection fluorescence (TIRF) microscopy. Furthermore, fluorescence resonance energy transfer (FRET) measurements using TIRF suggested a close (<100 Å) association between $GABA_B$ R2 and m2R. $GABA_B$ R2 did not FRET with m1 or m4 muscarinic receptors or with μ opioid receptors, suggesting a selective interaction between m2R and $GABA_B$ receptors. Consistent with this, the C-terminal domain of the $GABA_B$ R2 bound directly to m2R but did not require the coiled-coiled domain of R2. Similarly, deletion of the coiled-coiled domain did not disrupt FRET between the m2R and $GABA_B$ R2. Taken together, these results suggest the $GABA_B$ R2 subunit associates directly with m2R and traffics the complex to the plasma membrane, thereby compensating for acetylcholine-induced down-regulation of m2R and GIRK channels. This novel form of cholinergic regulation provides a unique role for $GABA_B$ receptors in neurons.

INTRODUCTION

Ligand binding to G protein coupled receptors (GPCRs) leads to diverse effects in the central nervous system. Viewed initially as monomers, there is accumulating evidence for GPCR signaling as dimers (Franco et al, 2007). For example, the $GABA_B$ receptor has been shown to function as an obligatory heterodimer of two subunits, R1 and R2 (White et al, 1998). An ER retention motif on $GABA_B$ R1 is shielded by association with R2, allowing receptor trafficking to the plasma membrane. (Margeta-Mitrovic et al, 2000). Additionally, studies have shown that the $GABA_B$ R1 subunit contains the agonist binding site while the R2 subunit signals to G proteins (Robbins et al, 2001). Recently, the $GABA_B$ receptor has been shown to be more promiscuous than previously thought. The γ2 subunit of the ionotropic $GABA_A$ receptor can complex with the $GABA_B$ R1 subunit (Balasubramanian et al, 2004). This interaction promotes surface expression of $GABA_B$ R1, in the absence of the R2 subunit, and also affects internalization of the $GABA_B$ R1/R2 heterodimer. Also, Chang et al (2007) provided evidence that both $GABA_B$ R1 and R2 subunits can affect surface expression of the extracellular calcium sensing receptor through direct interaction. These studies raise the possibility of $GABA_B$ receptors interacting with other integral membrane protein.

m2 muscarinic receptors play diverse roles in the central nervous system. They signal to G protein-coupled inwardly rectifying potassium (GIRK or Kir3) channels postsynaptically to mediate inhibition, while presynaptically they act as auto- or hetero-receptors to modulate transmitter release. Physiologically, they are involved in processes from cognition to neuropathic pain (Youdim et al, 2005; Pan et al, 2008). Furthermore, cross-talk between m2R and other neurotransmitter systems likely expands the diversity of m2R function. For instance, a $GABA_B$ antagonist attenuates the muscarinic-mediated reduction in nociception (Li et al, 2002). This raises the possibility of cross-talk between these transmitter systems, although no direct interaction between m2R and $GABA_B$ has been shown.

We have recently shown that endogenous m2 muscarinic receptors couple to GIRK channels in the neuronal PC12 cell line (Clancy et al, 2007). PC12 cells develop a neuronal-like

phenotype in the presence of nerve growth factor (NGF), extending neurites and secreting neurotransmitters including dopamine, norepinephrine and acetylcholine (Dichter et al, 1977). Although mRNA and protein for m2R and the GIRK2c subunit were upregulated in NGF-differentiated PC12s, the channel was located cytoplasmically unless cells were exposed to a muscarinic antagonist. We proposed that endogenously released acetylcholine chronically stimulates m2R, leading to internalization of a signaling complex containing m2R and GIRK channels (Clancy et al, 2007). Because $GABA_B$ receptors are known to couple with GIRK channels (David et al, 2006; Fowler et al, 2007), we investigated whether expression of $GABA_B$ receptors would rescue GIRK signaling in NGF-differentiated PC12 cells. Surprisingly, we found that $GABA_B$ receptors not only coupled to endogenously expressed GIRK channels but also rescued m2R signaling. Furthermore, we provide evidence that rescue is mediated by a direct interaction between the C-terminal domains of the $GABA_B$ R2 and m2 muscarinic receptors.

MATERIALS & METHODS

Cell Culture & Transfection

HEK293 cells were maintained in 10% fetal bovine serum (FBS) in DMEM in a humidified 37°C incubator with 95% air/5% CO2. PC12 cells were kindly provided by Dr M. Montminy, Salk Institute for Biological Studies, La Jolla, CA, and were maintained in DMEM supplemented with FBS (5%) and horse serum (10%) (Invitrogen Corp., Carlsbad, CA) in a humidified 37°C incubator with 95% air/5% CO2. Nerve growth factor (NGF) (50ng/ml, Sigma-Aldrich, Inc., St. Louis, MO or Promega, Madison, WI) differentiated PC12 cells were maintained in serum-free DMEM supplemented with NGF for 7-8 days, with regular medium changes every 24 hours. For electrophysiological recordings, cells were plated onto 12-mm glass cover slips (Warner Instruments, Hamden, CT) coated with poly-D-lysine (20mg/ml; Sigma-Aldrich, Inc., St. Louis, MO) and collagen (100mg/ml; BD Biosciences, Franklin lakes, NJ) in 24-well plates. For total internal reflection fluorescence (TIRF) and fluorescence resonance energy transfer (FRET) experiments, cells were plated on 35mm glass bottom culture dishes (MatTek Corporation:

Ashland, MA) and coated as described above. 5-day NGF-differentiated PC12 cells were transfected with cDNA using Lipofectamine 2000 (Invitrogen Corp, Carlsbad, CA), and cultured for at an additional 48-hours before analysis. HEK cells were transfected with the calcium phosphate method as described (Fowler et al, 2007) and cultured for an additional 48 hours before analysis. Previous experiments suggest a high degree of variability in endogenous expression; however, exogenously expressed receptors and channels appear to be regulated in the same manner as those endogenously expressed (Clancy et al, 2007). Therefore, to reduce variability, recordings in PC12 cells were performed in the background of transfection of the muscarinic m2 receptor as well as the GIRK2c subunit. PC12 cells were also treated with 1mM carbachol (Sigma-Adrich) for 24 hours prior to recordings to account for any variability in endogenous acetylcholine release.

Constructs

The m2 muscarinic receptor was fused to CFP (m2-CFP) by engineering a XhoI site and Kozak sequence (GCCACC) 5' to the start codon of m2R and a HindIII site prior to the stop codon using PCR, and then subcloned into pECFP-N1 (Clontech, Mountain View, CA). For $GABA_B$ R1/R2–YFP and R1/R2–CFP, $GABA_B$ R1 and R2 cDNAs were subcloned by PCR into EcoR1/Age1 sites of pEYFP-N1/pECFP-N1. $GABA_B$ R2Δ748-YFP was created by engineering a SacII site into $GABA_B$R2 after R748 and subcloning to peYFP-N1 using HindIII/SacII. $GABA_B$ R2Δ776 and Δ820 were created by engineering an AgeI site at amino acids 776 and 820 and subcloning into peYFP-N1 using EcoRI/AgeI. $GABA_B$ R1R2C-YFP was created by engineering a KpnI site into a conserved region of $GABA_B$ R1 and R2, substituting a phenylalanine for a lysine (R1F883L/R2F739L) and subcloning the C-terminus of $GABA_B$ R2 into $GABA_B$ R1-YFP using KpnI/AgeI. These substitutions resulted in receptors that functioned similar to wild-type. $GABA_B$ $R2_{R575D}$-YFP and all other single amino acid substitutions were created using the QuikChange XL kit from Stratagene. Chimeras swapping the C-terminal domains between m1 and m2 muscarinic receptors were created by overlap PCR. GST fusion constructs were created by fusing the

region of interest to the 3' end of GST using pGEX-2T. H8 fusion constructs were created using pHis8.3. Fusion constructs were expressed in BL21 (DE3) *E.Coli* and affinity purified as previously described (Lunn et al, 2007)

TIRF Microscopy & FRET Measurements

A Nikon TE2000 microscope was equipped with a 60x oil-immersion TIRF objective (Nikon; 1.45 NA) and a solid state DPSS 442nm laser (Melles Griot – model: 85 BTL 010) YFP laser, which could be adjusted manually for epifluorescence and TIRF. The TIRF angle was adjusted using a fixed point on the back focal plane. The Nikon filter cube contained a polychroic mirror with reflection bands at 440nm and 510nm, and band-passes at 475/30nm and 560/60nm (z442/514rpc; Chroma technologies). No excitation filter was used. CFP and YFP emission filters (470/30 and 535/50, respectively) were placed in a filter wheel (Sutter Instruments, Novato, CA) and controlled by a Lambda 10-2 controller (Sutter Instruments, Novato, CA). Images (12bit) were acquired with a 12.5 MHz Imago CCD camera (Till Photonics). The camera, laser shutters and filter wheel were electronically controlled by TILLvisION software. Transfected cells were imaged first using epifluorescence (100 ms exposure time) and, after adjusting the laser, using TIRF (500 ms exposure) microscopy. Fluorescent intensity was analyzed using NIH ImageJ software. Background was first subtracted, then a region of interest (ROI) was drawn around the entire cell (epi) or the footprint (TIRF), and the average fluorescent intensity (in arbitrary units) was measured.

For FRET measurements, cells were fixed in ice-cold methanol on the day of the experiment to avoid movement of fluorophores during bleaching. FRET efficiency (%FRET) was measured using the acceptor photobleaching (APB) method. The 442 nm laser was used to locate transfected cells and to focus the image. After 60 second photobleaching, images were acquired for CFP fluorescence (100ms exposure, 2 x 2 binning – 442nm laser, CFPEm filter) and YFP fluorescence (30ms exposure, 2 x 2 binning – 514nm laser, YFPEm filter) before and after photobleaching with the 514nm laser. FRET efficiency (%FRET) was calculated as the percentage increase in CFP emission after photobleaching YFP, where %FRET =100* (CFPEm-

post – CFPEm-pre)/CFPEm-pre. CFPEm-post is CFP emission after photobleaching YFP, CFPEm-pre is CFP before photobleaching YFP. We measured the %FRET pixel-by-pixel with two CFP images (CFPEm-post and CFPEm-pre) and two YFP images (YFPEm-post and YFPEm-pre) using NIH ImageJ plugin *FRETcalc* software. 12-bit images were converted to 8-bit, background subtracted and smoothed twice prior to FRET analysis. We used the following parameters for *FRETcalcv1*: -50% %FRET threshold; 1- sub-ROI size. Donor and acceptor thresholds were determined cell by cell to maximize colocalization between the CFP image, the YFP image and the calculated FRET image. CFP images were scaled to the same intensity range for each pair of pre- and post-bleaching images.

Electrophysiology

Whole-cell patch clamp technique was used to record macroscopic currents from NGF-differentiated treated PC12 cells. Borosilicate glass electrodes (#P6165T: Warner Instruments, Hamden, CT) were pulled on a Narashige puller, and used without Sylgard or fire polishing. Electrodes had resistances of 5-7 Mohms. Membrane currents were recorded with an Axon Axopatch 200B (Molecular Devices Corp., Sunnyvale, CA) amplifier at room temperature, filtered at 2 kHz, digitized at 5 kHz with a Axon Digidata 1320 interface (Molecular Devices Corp., Sunnyvale, CA). The intracellular pipette solution contained (in mM) 130 KCl, 20 NaCl, 5 EGTA, 2.56 K2ATP, 5.46 MgCl2 and 10 HEPES (pH7.2 with KOH). Li2GTP (300 mM, Sigma-Aldrich, Inc., St. Louis, MO) was added fresh to the intracellular pipette solution. The external bath solution (20K) contained in mM 140 NaCl, 20 KCl, 0.5 CaCl2, 2MgCl2, and 10 HEPES (pH 7.2 with NaOH). BaCl2 (1 mM; Sigma-Aldrich, Inc., St. Louis, MO) was added directly to the 20K solution. Oxotremorine (Sigma-Aldrich, Inc., St. Louis, MO) was made up as a 1mM stock and diluted on the day of experiment. A ramp voltage protocol (-120 to +50 mV) was used to study GIRK currents. Mean ± SEM are shown.

In Vitro Binding Assay

Far western *in vitro* binding assays were performed as previously described (Lunn et al, 2007). Briefly, fusion proteins were expressed and purified in BL21(*DE3*) *E. coli* as described above. GST-fused proteins (2 ug) were separated by SDS-PAGE, transferred to nitrocellulose, and then stained with Ponceau S to visualize transferred proteins. Blots were placed in blocking buffer containing 2.5% BSA in TBST (25 mM Tris pH 7.4, 150 mM NaCl, 2 mM KCl, 0.05% Tween-20) and incubated overnight at 4 °C. Fusion protein probes (100 nM) were added to blocking buffer with 5 uM b-mercaptoethanol and incubated for 1 hr on a shaker at 22–25 °C. Western immunoblotting was carried out with anti-HisProbe HRP-conjugated (Pierce; 1:2,500 dilution) antibodies in TBST (0.05–0.1% Tween-20). Blots were washed, incubated with SuperSignal ECL reagents (Pierce) and exposed to BioMax XAR film (Eastman Kodak) for a range of times.

RESULTS

Muscarinic Antagonist Treatment or Inhibition of Endocytosis Rescues m2 Surface Expression in PC12 cells

We have shown previously that NGF-treated PC12 cells endogenously express m2 receptors and GIRK channels, but lack functional signaling due to lack of surface expression of the channel. Two hours of atropine treatment was sufficient to rescue GIRK surface expression and muscarinic-mediated GIRK singaling (Clancy et al, 2007). To provide additional evidence that m2 muscarinic receptors were also expressed at low levels on the plasma membrane before atropine treatment, we investigated the surface expression of the m2 receptor using total internal reflectance fluorescence microscopy (TIRF). TIRF allows visualization of proteins in the plasma membrane and sub-membrane regions of a depth of approximately 100 nm only (Axelrod et al., 1983). In NGF-differentiated PC12 cells transfected with m2 receptor fused to CFP, m2-CFP could be visualized by epifluorescence but not by TIRF (Figure 2-1A). Treating the cells for 2hrs in atropine, however, led to dramatically increased levels of fluorescence using TIRF microscopy (Figure 2-1A). Quantitation of the levels of fluorescence on the plasma membrane revealed a

significant increase in surface expression of m2 muscarinic receptors following atropine treatment (Figure 2-1B). Interestingly, co-expression of both Kir3.2c channel and m2-CFP receptor did not lead to surface expression of m2 muscarinic receptors in the absence of atropine (Figure 2-1B).

One possible mechanism to explain the lack of both the m2 muscarinic receptors and Kir3.2c channels is that chronic stimulation of muscarinic receptors causes endocytosis of the m2 receptor/channel complex. To explore this further, we examined the effect of pharmacologically disrupting endocytosis with wortmannin, an inhibitor of PI3/PI4-kinases and endocytosis. NGFdifferentiated PC12 cells were transfected with cDNA for the m2-CFP receptor, and exposed to wortmannin (10 □ M) for 2 hours at 37°C. Using TIRF microscopy, the levels of m2-CFP receptor expressed on the plasma membrane were significantly increased above control cells and similar to atropine-treated cells (Figure 2-1C&D). Although GPCRs are well known for their ability to undergo endocytosis during chronic stimulation, the concomitant loss of the effector, GIRK channels, on the plasma membrane surface was unexpected.

$GABA_B$ Expression Rescues Muscarinic/GIRK Signaling in PC12 cells

Although both GIRK2c and m2R transcripts were upregulated in NGF-differentiated PC12 cells, neither protein expressed on the plasma membrane (Clancy et al., 2007; Fig. 2-1). Surface and functional expression of GIRK/m2R complex was rescued by inhibiting endocytosis or treating with a muscarinic antagonist, suggesting endogenous release of acetylcholine down-regulates the GIRK/m2R complex (Clancy et al, 2007). To investigate whether another GPCR was capable of forming a complex with GIRK channels and rescuing functional expression, we transiently expressed the $GABA_B$ receptor in PC12s. Expression of both subunits of the $GABA_B$ receptor or the R2 subunit alone was able to rescue basal GIRK currents compared to untransfected PC12 cells (Fig. 2-2B-C, Table 2-1, R1/R2, -5.3 ± 1.1 pA/pF, R2 alone, -5.2 ± 1.7 pA/pF, vs. untransfected, -0.6 ± 0.3 pA/pF, $p < 0.05$). Furthermore, expression of $GABA_B$ R1/R2 or R2 alone yielded baclofen-induced GIRK currents (Fig.2-2B-C, Table 2-1, R1/R, -19.8 ± 4.0

FIGURE 2-1: MUSCARINIC ANTAGONIST TREATMENT OR INHIBITION OF ENDOCYTOSIS RESUCES M2 SURFACE EXPRESSION IN PC12 CELLS

(A) NGF- differentiated PC12 cells transfected with m2-CFP cDNA or m2-CFP and Kir3.2c were either untreated or exposed to atropine (100 mM) for 2hr. The same cell was imaged under epifluorescence and TIRF to visualize the expression of m2-CFP in the cytoplasm and membrane surface, respectively. Images adjusted to the same fluorescence intensity scale.
(B) Mean fluorescence measured under TIRF is shown for different combinations, control (n=23), +atropine (n=20) and +Kir3.2c (n=10). Atropine treatment led to a significant increase in m2-CFP expression on the plasma membrane (one-way ANOVA with Dunnett's post hoc, $^{**}p < 0.05$. Mean fluorescence measured under epifluorescence was 8.6 ± 1.9 AU, 15.2 ± 2.3 AU, 7.3 ± 1.9 AU for control, +atropine and +Kir3.2c, respectively.
(C) NGF-differentiated PC12 cells transfected with m2-CFP cDNA were either untreated or exposed to wortmannin (10 mM) for 2hr at 37° C.
(D) Mean fluorescence measured under TIRF in the absence (n=17) or presence (n=14) wortmannin. Wortmannin treatment produced a significant increase in m2-CFP receptor expression on the plasma membrane (Student's t-test, $^{**}p<0.05$).
(E) Summary of muscarinic/GIRK trafficking in PC12 cells. Endogenously released acetylcholine (ACh) acts on m2 muscarinic receptors leading to downregulation of the receptor/channel complex. Surface expression can be rescued by two hour treatment with the competitive muscarinic agonist, atropine, or an inhibitor of endocytosis, wortmannin.

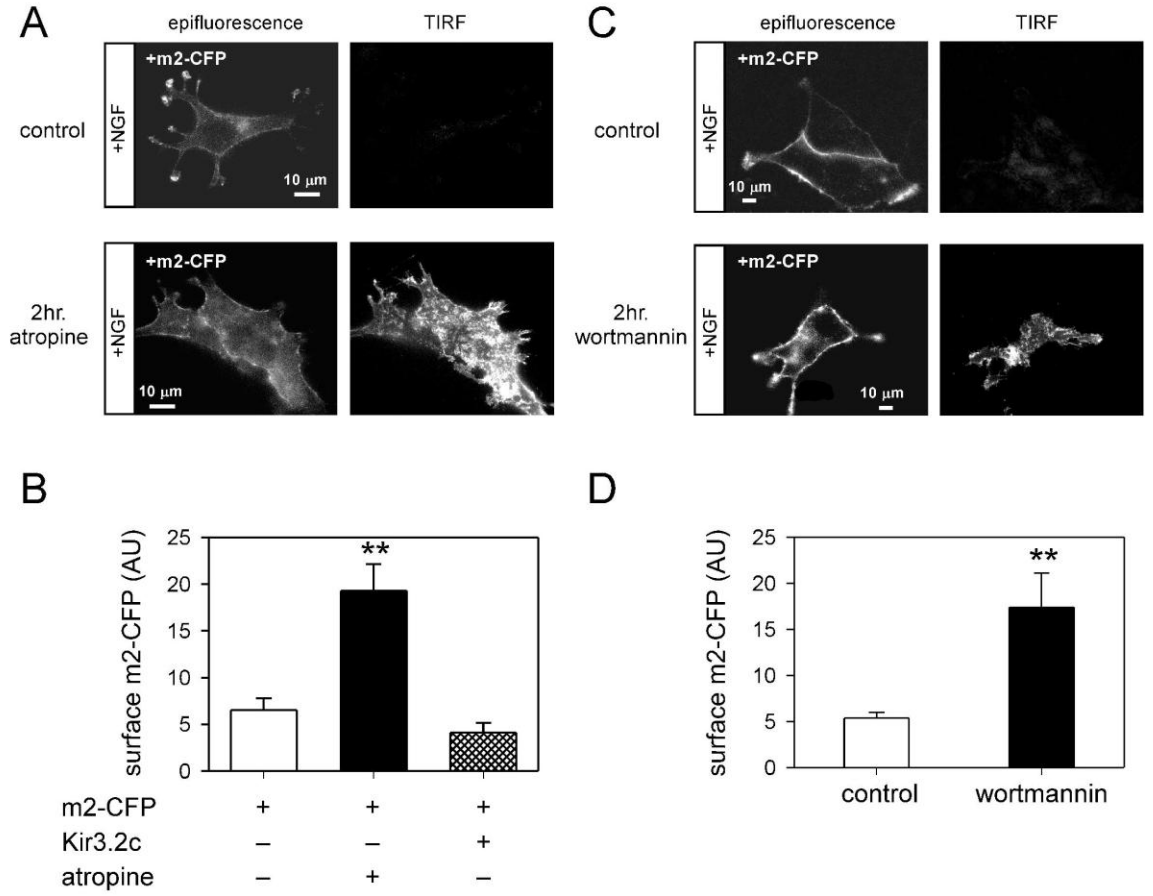
A
epifluorescence
TIRF
control
+NGF
+m2-CFP
10 μm
2hr.
atropine
C
2hr.
wortmannin
B
surface m2-CFP (AU)
**
m2-CFP
Kir3.2c
atropine
D
control
wortmannin
E
ACh
Atropine
m2R
GIRK2c
early
endosome

pa/pF; R2 alone -7.0 ± 4.3 pA/pF, vs. untransfected, -0.2 ± 0.6 pA/pF, $p < 0.05$). In contrast, the $GABA_B$ R1 subunit alone failed to rescue basal or baclofen-induced GIRK currents (Fig.2-2A&D, Table 2-1 basal -1.4 ± 0.9 pA/pF; baclofen-induced, -0.6 ± 0.7, $p > 0.05$ vs. untransfected).

Surprisingly, expression of the $GABA_B$ receptor also rescued muscarinic-mediated GIRK signaling. Significant oxotremorine-induced currents were detected in cells coexpressing $GABA_B$ R1/R2 subunits (Fig. 2-2B-C & D, R1/R2, -6.9 ± 3.7 pA/pF; vs. untransfected, -0.6 ± 0.5 pA/pF, $p < 0.05$). Notably, expression of $GABA_B$ R2 alone was sufficient to rescue muscarinic signaling (-29.0 ± 7.6 pA/pF). Normalizing oxotremorine-induced currents to the Ba^{2+} sensitive basal current revealed a significant increase upon expression of the R2 subunit alone (7.2 ± 1.2, vs. untransfected, 1.4 ± 1.0, $p < 0.05$). Thus, despite the presence of chronic acetylcholine, $GABA_B$ R2 subunit rescued muscarinic signaling, in the absence of the muscarinic atagonist.

$GABA_B$ R2 Expression Rescues Surface Expression of both GIRK2c and m2R

To examine GIRK surface expression directly, we utilized a GIRK2c construct containing a hemagglutinin (HA) tag in the extracellular region (Clancy et al, 2007). Immunostaining with antibodies against HA in nonpermeabilized NGF-treated PC12 cells revealed lack of surface expression of HA-GIRK2c as previously described (not shown). Consistent with the electrophysiology, co-expression of $GABA_B$ R2, but not R1, rescued HA-GIRK2c surface expression (data not shown).

To investigate whether co-expression of $GABA_B$ rescued surface expression of m2Rs, we utilized total internal reflection fluorescence microscopy (TIRF). TIRF allows visualization of fluorophores within 100nm of the plasma membrane, and thus can be used to quantify the level of fluorescently-tagged proteins expressed at the cell surface. When expressed alone, m2-CFP showed very little surface expression and was not significantly greater than CFP alone (not shown; 36.6 ± 5.4 AU vs. 48.3 ± 7.0 AU, $p > 0.05$). Co-expression of the GABA R2 subunit significantly increased m2-CFP TIRF expression (Fig. 2-2E, 84.9 ± 13.2 AU, $p < 0.05$ vs. m2-CFP alone). To determine whether the GABA R2 subunit increased forward trafficking of m2R or

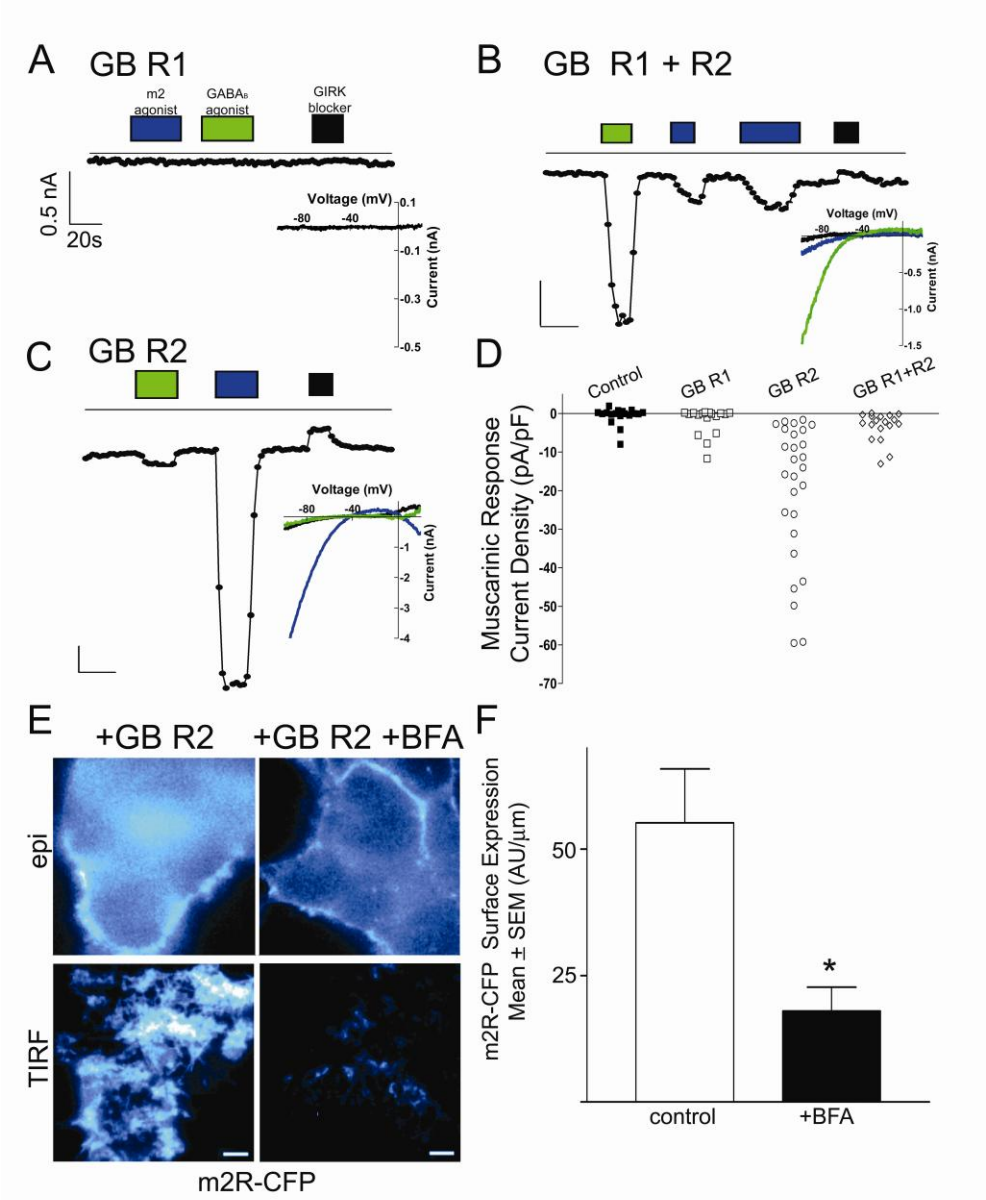

FIGURE 2-2. GABA$_B$ EXPRESSION RESCUES MUSCARINIC-MEDIATED GIRK SIGNALING IN PC12 CELLS.

A-C) Representative current traces from 7 day NGF-treated PC12 cells expressing *A)* GABA$_B$ (GB) R1, *B)* GABA$_B$ R1 + R2, or *C)* GABA$_B$ R2 alone. Blue bars, oxotremorine-M (100nM); green bars, baclofen (100uM); black bars, barium chloride (1mM). Solid lines represent zero current level. Scale bars: 0.5nA and 20s. *Insets*: Current-voltage (I-V) plot of responses. *D)* Scatterplot of responses to oxotremorine-M expressed as current density (pA/pF). Line represents the 75% level for control responses and was used as the cutoff for declaring a response. *E)* Representative images from 7 day NGF-treated PC12 cells expressing m2-CFP and R2-YFP under epifluorescence (top) or TIRF microscopy (bottom). *left*: untreated; *right*: treated with brefeldin-A (BFA;100μM) for 2 hours prior to imaging. Scale bars: 5um. *F)* Quantification of m2R-CFP surface expression as measured under TIRF. *, $p < 0.05$, t-test.

prevented its endocytosis, we applied brefeldin-A (BFA), a fungal metabolite that prevents forward trafficking from the endoplasmic reticulum (Chardin & McCormick, 1999). Two hour treatment with BFA abolished the rescue of m2R surface expression by R2 (Fig. 2-1E&F, 41.5 ± 10.3 AU, $p > 0.05$ vs. m2-CFP alone). Thus, the $GABA_B$ R2 subunit rescues m2R and GIRK2c surface expression in PC12 cells, likely by increasing forward trafficking.

$GABA_B$ R2 Subunits Interact with m2 Muscarinic Receptors at the Plasma Membrane

To assay interactions between receptors at the plasma membrane, we measured potential fluorescence resonance energy transfer (FRET) between GPCRs using TIRF microscopy. FRET efficiency was measured using the acceptor photobleach method (% FRET). When transiently expressed in NGF-treated PC12 cells, we detected significant FRET between the $GABA_B$ R1-CFP and R2-YFP subunits of the $GABA_B$ receptor, as compared to R2-CFP alone (Fig. 2C, 10.5 ± 1.3 vs 0.6 ± 1.2, $p < 0.05$). We also measured significant FRET between m2-CFP and $GABA_B$ R2-YFP (Fig. 2-3A&C, 11.1 ± 1.2, $p < 0.05$ vs. R2-CFP), but not between m2-CFP and R1-YFP (2.9 ± 0.5). Furthermore, we did not measure FRET between $GABA_B$ R2-YFP and the μ opioid receptor (μOR-CFP, 1.4 ±0.7), or the m1 muscarinic receptor (m1-CFP, 1.2 ±0.4), suggesting the interaction between m2R and $GABA_B$ R2 was specific. Thus, $GABA_B$ R2 and m2R show a close association at the plasma membrane of PC12 cells.

$GABA_B$ R2 and m2R Interaction in HEK cells Requires the $GABA_B$ R1 Subunit

To determine if $GABA_B$ R2 and m2R could interact in another mammalian cell line, we co-expressed the GPCRs in HEK-293 cells. Again, we were able to demonstrate significant FRET between the $GABA_B$ R1 and R2 subunits of the $GABA_B$ receptor compared to the R2 subunit expressed alone (Fig. 2-4B, 6.7 ± 0.3 %FRET vs. 0.3 ± 0.6 %FRET, $p < 0.05$). However, the m2 muscarinic receptor failed to show significant FRET with the R2 subunit of the $GABA_B$ receptor when expressed alone (Fig 2-4B, 0.2 ± 0.5 %FRET). We wondered whether expression of both

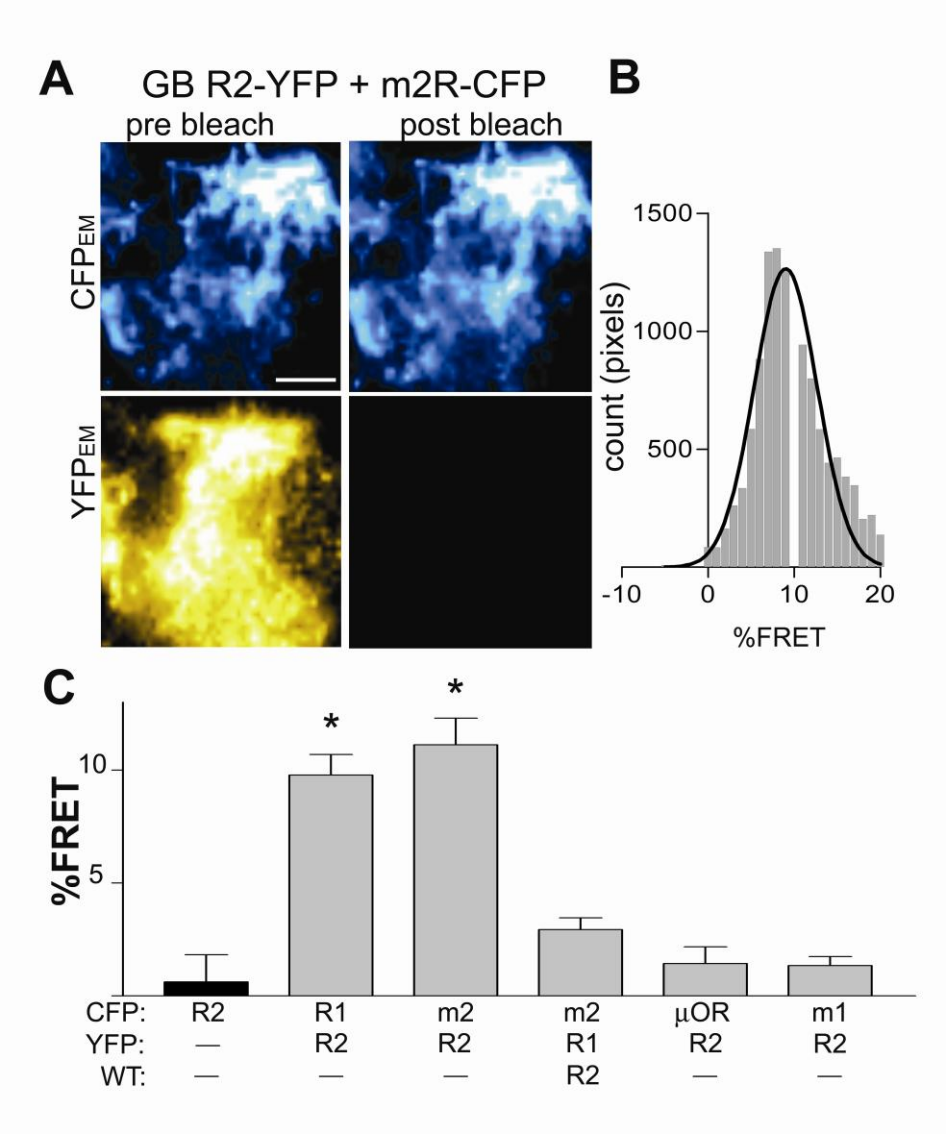

FIGURE 2-3. GABA R2 AND M2R INTERACT AT THE PLASMA MEMBRANE IN PC12S

A) Representative images from PC12 cells expressing $GABA_B$ R2-YFP and m2-CFP. Cells were imaged under TIRF microscopy before (pre bleach) and after (post bleach) 60 second photobleaching with the 514nm laser. Images were collected for the CFP channel (442nm excitation, 475/30nm emission filters, CFP_{EM}) and the YFP channel (514nm excitation, 560/60nm emission filters, YFP_{EM}). *B)* Histogram showing the distribution of pixels showing a given %FRET, measured in ImageJ using the FRETcalc plugin. Images have been scaled to the same intentisy. Scale bars: 10μm. *C)* %FRET by transfection condition. Only the $GABA_B$ R1/R2 and $GABA_B$ R2/m2R pairs showed significant FRET. One-way ANOVA followed by Dunnett's multiple comparison procedure, * $p < 0.05$ vs. $GABA_B$ R2-CFP alone.

subunits of the heterodimer $GABA_B$ receptor might influence oligomerization. Surprisingly, when the m2 muscarinic receptor was co-expressed with the full $GABA_B$ heterodimer, significant FRET was seen between m2R and the R2 subunit, but not the R1 subunit, similar to PC12s (Fig. 2-4A&B, 6.4 ± 1.7 %FRET, $p < 0.05$ vs. R2-C, and 1.8 ± 0.8 %FRET, respectively). Interestingly, m2R does not appear to compete with $GABA_B$ R1 for interaction with R2, as co-expression of m2R does not reduce FRET between $GABA_B$ R1and R2 (Fig. 2-4B, 7.5 ± 0.6 %FRET). Furthermore, neither the μ opioid receptor nor the m1 muscarinic receptor demonstrated significant FRET with $GABA_B$ R2 even in the presence of R1. We also investigated whether the m4 muscarinic receptor, which is similar to m2R, might be able to interact with $GABA_B$ receptors. However we failed to see FRET between m4R and $GABA_B$ R2 even with the R1 subunit present (Fig. 2-4B, 3.0 ± 0.4 %FRET, $p > 0.05$ vs. R2-CFP). Thus, the $GABA_B$ R2 subunit can interact with m2 muscarinic receptors at the plasma membrane in HEK-293 cells if the R1 subunit is also present.

The requirement for $GABA_B$ R1 expression could be due to a conformational change upon $GABA_B$ heterodimerization allowing interaction with m2R or due to a targeting motif within the R1 subunit that changes the cellular distribution of the $GABA_B$ heterodimer. Consistent with the latter hypothesis, co-expression of $GABA_B$ R1 increased co-localization between R2 and m2R (Fig. 2-4C&D, Pearson correlation coefficient (R), R2/m2 alone, 0.3 ± 0.05, vs R2/m2 with R1, 0.7 ± 0.03, $p < 0.05$). This suggests that the $GABA_B$ R1 subunit is responsible for proper targeting of the heterodimer, perhaps through a lipid-binding or other protein-interacting domain.

The m2R C-terminus is Sufficient for Interaction with $GABA_B$ R2

To determine which region of the m2R was responsible for the interaction with $GABA_B$ R2, we created chimeras consisting of C-terminal exchanges between m2R and m1R. Figure 2-5A shows the schematic of the chimeras. Swapping the m1 C-terminal domain into the m2R caused a decrease in FRET with $GABA_B$ R2 compared to wild-type m2R (Fig. 2-5B&D, 2.6 ± 0.4 %FRET vs. 5.3 ± 0.4 %FRET, $p < 0.05$). Conversely, swapping the C-terminal of m2R into m1R

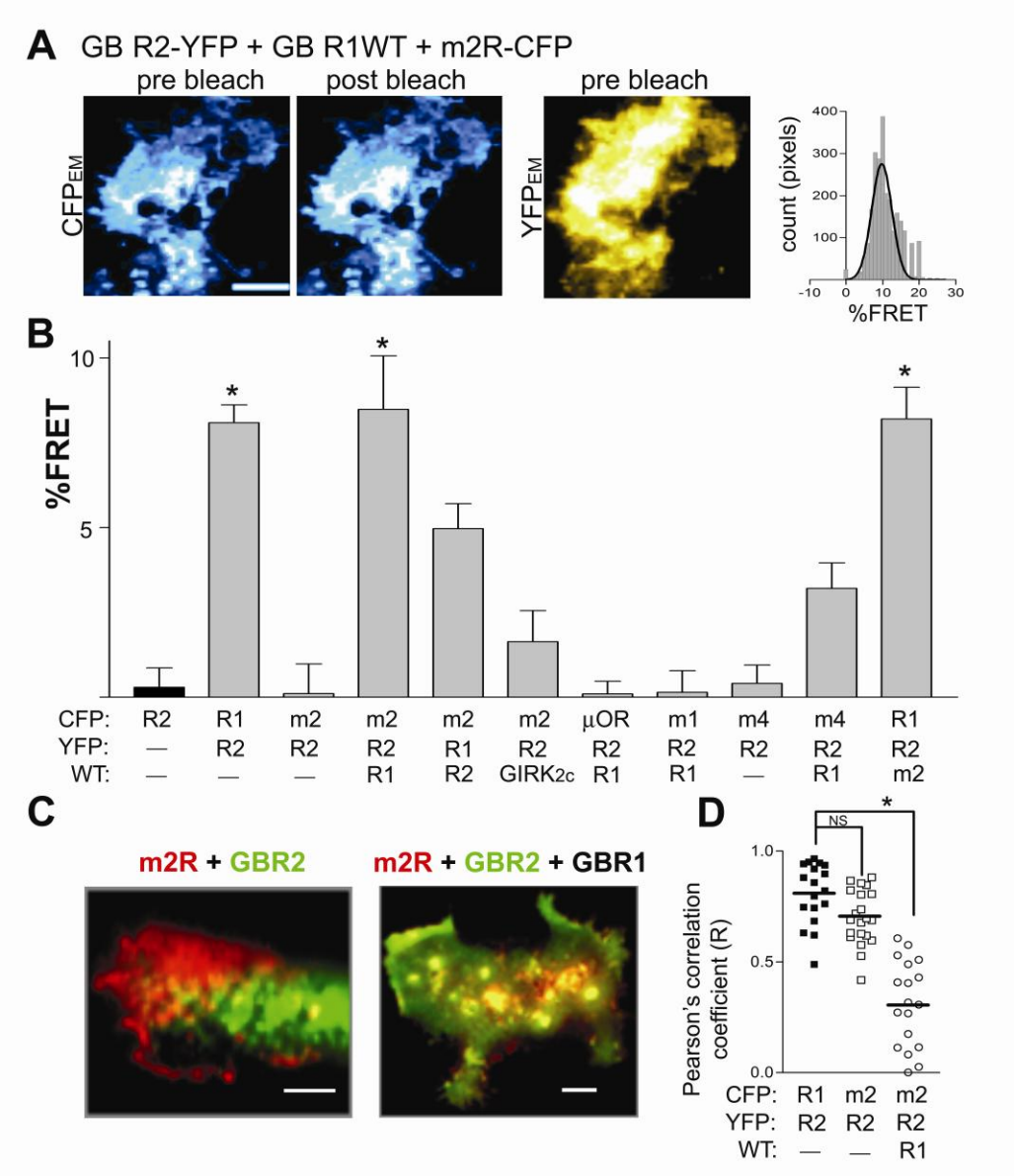

FIGURE 2-4. $GABA_B$ R2 AND M2R INTERACT AT THE PLASMA MEMBRANE IN HEK CELLS IF THE R1 SUBUNIT IS PRESENT.

A) Representative images from HEK cells expressing $GABA_B$ R2-YFP, R1-WT and m2-CFP. Scale bars: 5um. Histograms to the right show the FRET distribution for the cell shown. *B)* %FRET by transfection condition. One-way ANOVA followed by Dunnett's multiple comparison procedure, * $p < 0.05$ vs. R2-CFP alone. *C)* Representative images showing m2R (red), $GABA_B$ R2 (green) and merged (yellow) for cells expressing m2R and $GABA_B$ R2 without (left) or with (right) $GABA_B$ R1. *D)* Pearson correlation coefficient for CFP & YFP images, one-way ANOVA followed by Dunnett's multiple comparison procedure, * $p < 0.05$ vs. $GABA_B$ R1/R2.

was sufficient to gain FRET with R2 (Fig. 2-5C&D, 6.0 ± 0.4 %FRET, $p < 0.05$ vs R2-CFP). These results suggest that the C-terminal domain of m2R mediates interaction with $GABA_B$ R2.

The Proximal C-terminus of $GABA_B$ R2 Mediates Interaction with m2R

We next aimed to determine which regions of the $GABA_B$ R2 subunit mediate the interaction with the m2 receptor. We created a series of truncations in R2, removing the entire C-terminus, the coiled-coil domain or the distal C-terminus downstream of the coiled-coil region. In FRET experiments with the m2R-CFP and $GABA_B$ R1-WT, R2Δ748 and R2Δ776, which lack the coiled-coil domain, failed to FRET with m2R (data not shown, 0.2 ± 0.2 and 1.8 ± 0.5 %FRET, respectively, vs. R2-CFP, -0.4 ± 0.4 %FRET, $p > 0.05$). In contrast, R2Δ820, which retained the coiled-coil domain, retained FRET with m2R (data not shown, 4.4 ± 0.7 %FRET, vs. R2-CFP, $p < 0.05$). The coiled-coil domain has been shown previously to mediate the interaction of $GABA_B$ R1 and R2 (Kammerer et al, 1999). If the $GABA_B$ R1 subunit is necessary for R2 to interact with m2R, these results could be due to loss of the m2R interaction site or loss of interaction with R1.

To distinguish between these possibilities, we created a chimeric receptor containing the N-terminus and transmembrane domains of the $GABA_B$ R1 subunit and the entire C-terminus of the R2 subunit, R1R2C (Fig. 2-6A). Since the $GABA_B$ R1 subunit itself did not show FRET with m2R, if the R2 C-terminus contains the m2R dimerization site this chimera should rescue the interaction. Indeed, the $GABA_B$ R1R2C chimera showed significant FRET with m2R compared the wild type R1 subunit (Fig. 2-6B, 6.0 ± 0.5 vs 1.9 ± 0.6 %FRET, $p < 0.05$). Interestingly, the $GABA_B$ R1R2C and m2R interacted without the need for expression of wild-type $GABA_B$ R1 or R2. This suggests that the $GABA_B$ R1/R2 heterodimer per se is not required for m2R interaction, but instead that some motif in the R1 N-terminus or transmembrane regions may be necessary for localizing the $GABA_B$ receptor to the same subcellular region as m2R. Consistent with this, the $GABA_B$ R1R2C chimera showed a high degree of colocalization with m2R (Pearson's correlation coefficient (R), 0.61 ± 0.02; data not shown). In contrast, $GABA_B$ R2Δ776,

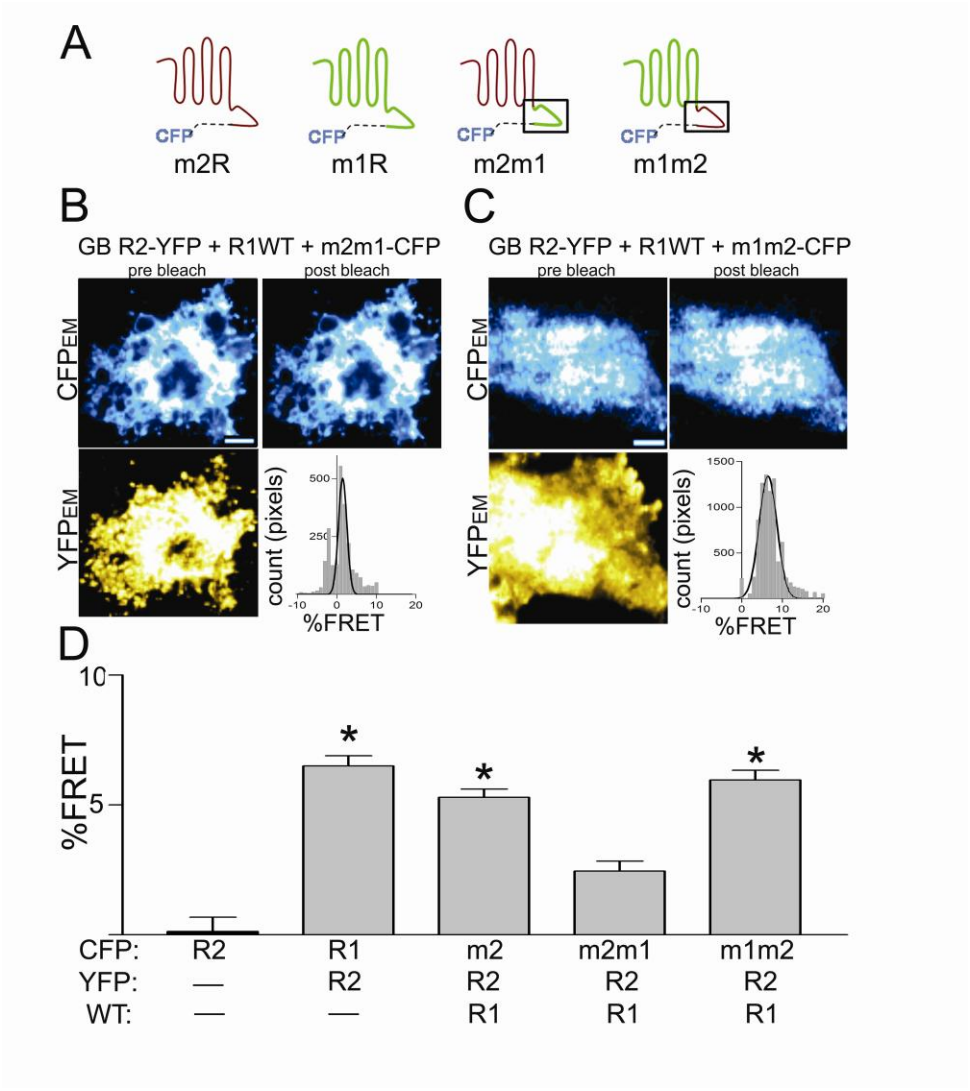

FIGURE 2-5. C-TERMINUS OF M2R MEDIATES INTERACTION WITH $GABA_B$ R2.

A) Schematic showing location of m1/m2 chimeras. *B & C)* Representative images from HEK cells transfected with $GABA_B$ R2-YFP, $GABA_B$ R1-WT and *B)* m2m1-CFP or *C)* m1m2-CFP. Scale bars: 5um. *D)* %FRET by transfection condition, one-way ANOVA followed by Dunnett's multiple comparison procedure, * $p < 0.05$ vs. R2-CFP alone.

which does not contain the coiled-coil domain and likely shows weaker interaction with R1, showed significantly lower colocalization with m2R (0.46 ± 0.04, $p < 0.05$).

To narrow down which region of the $GABA_B$ R2 C-terminus contains the region responsible for interaction with m2R, we made a similar series of C-terminal truncations in the chimeric subunit (Fig. 2-6A). Surprisingly, deletion of the distal C-terminal tail or the coiled-coil domain had no effect on the interaction between the $GABA_B$ R1R2C chimera and m2R (Fig. 2-6C&D, 5.6 ± 0.5 and 5.4 ± 0.6 %FRET, respectively, vs R2-CFP, -0.4 ± 0.5, $p > 0.05$). In fact, $GABA_B$ R1R2CΔ2 showed significant FRET with the muscarinic m1m2C chimera (Fig. 2-6D, 5.0 ± 0.6, $p > 0.05$ vs. R2-CFP). These results suggest that the proximal $GABA_B$ R2 C-terminus is responsible for dimerization with m2R, and that the C-termini of both R2 and m2R are sufficient for interaction.

The C-terminus of $GABA_B$ R2 Directly Binds m2R C-terminus

As an independent assay of $GABA_B$ R2 and m2R interaction, we utilized an *in vitro* binding assay as previously described (Lunn et al, 2007). GST fusion constructs were created to the C-termini of m2R (m2C), m1R (m1C) and $GABA_B$ R1 (R1C) (Fig. 2-7A). These constructs were purified and run on an SDS-PAGE gel at a concentration of 2ug. Proteins were transferred to nitrocellulose membranes and incubated with a histidine fusion construct to the full-length $GABA_B$ R2 C-terminus at 100nM. Consistent with the literature, the $GABA_B$ R2 C-terminus showed very strong binding to the R1 C-terminus, likely due to interactions between the coiled-coiled domains (Fig. 2-7B&C). The $GABA_B$ R2 C-terminus also showed binding to the m2R C-terminus, although not to the m1R C-terminus (Fig. 2-7B). Thus the $GABA_B$ R2 and m2R C-termini can directly bind.

Because the FRET data indicated the proximal $GABA_B$ R2 C-terminus as the site of interaction with m2R, we created a truncated fusion protein, $GABA_B$ R2Δ776. $GABA_B$ R2Δ776

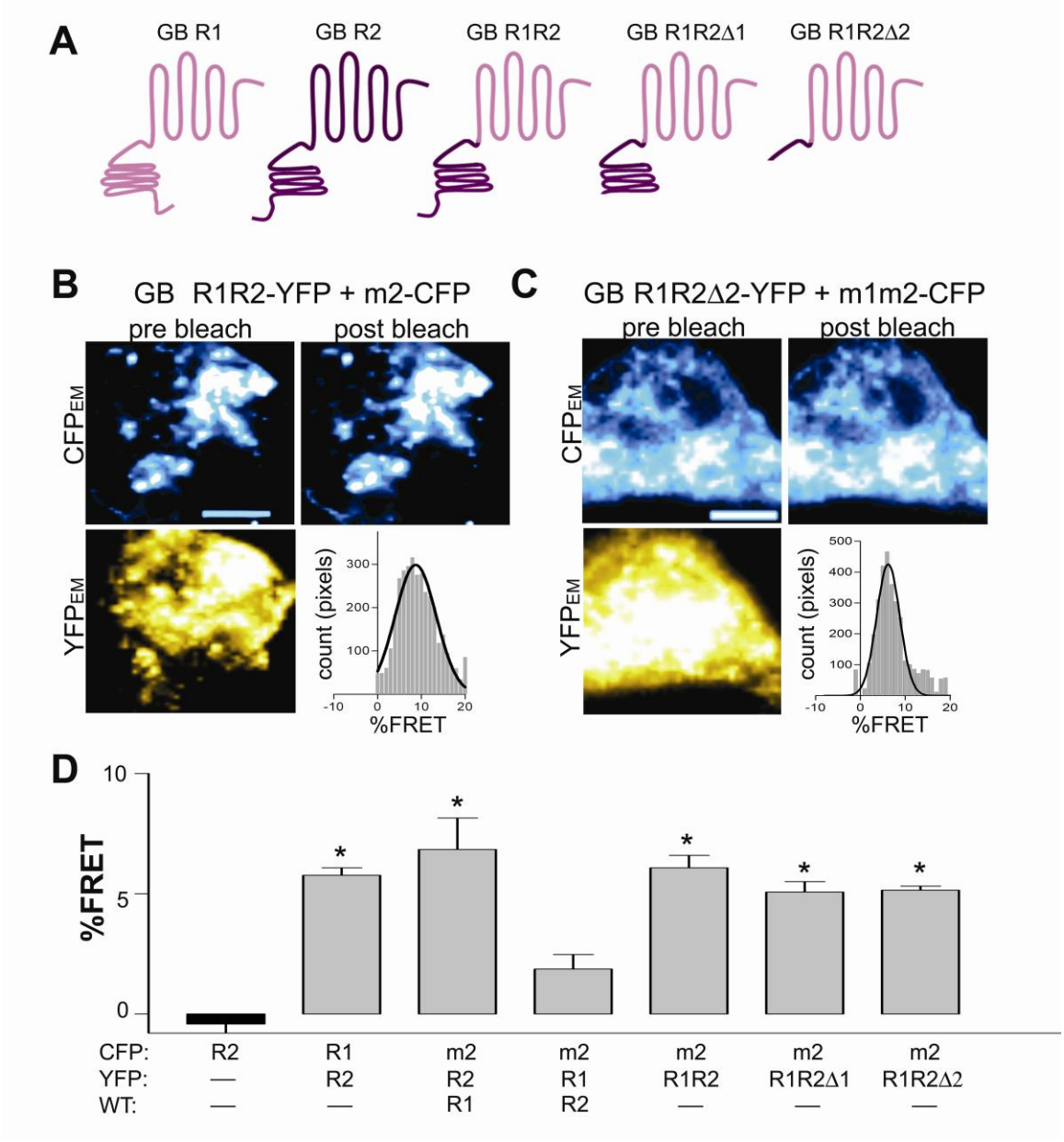

FIGURE 2-6. PROXIMAL $GABA_B$ R2 C-TERMINAL MEDIATES INTERACTION WITH M2R.

A) Schematic showing alignment of truncations and chimeras. *B & C)* Representative images from HEK cells expressing the $GABA_B$ chimera R1R2C and m2-CFP *(B)* or the truncated $GABA_B$ chimera, R1R2CΔ2 and the muscarinic chimera, m1m2C *(C)*. Scale bars: 5um. *D)* Summary of %FRET for the $GABA_B$ R1R2C chimera and truncations. The R1R2Δ776-YFP was able to FRET with m2-CFP and the chimera m1m2-CFP. One-way ANOVA followed by Dunnett's multiple comparison procedure, * $p < 0.05$ vs R2-CFP alone.

showed weak binding to R1C (Fig. 2-7D&E). This truncation lacks the $GABA_B$ R2 coiled-coil domain, suggesting that the proximal R2 C-terminus can only weakly interact with R1C *in vitro*. In contrast, $GABA_B$ R2Δ776 showed significant binding to the m2R C-terminus, but not to m1c (Fig. 2-7D&E). This suggests that the proximal C-terminus of $GABA_B$ R2 is sufficient for the interaction with m2R.

Signaling Through $GABA_B$ is not Required for m2R Rescue

We next wanted to determine the involvement of $GABA_B$ signaling in rescue and signaling of m2R. Hence, we created a $GABA_B$ R2 mutant with a single amino acid substitution at the border of the third transmembrane domain and second intracellular loop (Binet et al, 2007). This mutation, $GABA_B$ $R2_{R575D,}$ rendered the R2 subunit incapable of signaling to G proteins when co-expressed with R1 and GIRK2c channels in HEK cells (-1.1 ± 0.3 pA/pF, compared to -20.8 ± 9.0 pA/pF for wild-type R2, $p < 0.05$, data not shown). This mutation did not affect basal GIRK current levels or $GABA_B$ R2 surface expression as measured by TIRF (data not shown). Thus, $R2_{R575D}$ is a G protein signaling deficient $GABA_B$ R2 mutant.

To determine whether signaling through $GABA_B$ was required for muscarinic trafficking or signaling, we co-expressed R1 and $R2_{R575D}$ in 7 day NGF-treated PC12 cells. Both the wild-type $GABA_B$ R2 and $R2_{R575D}$ were capable of rescuing muscarinic-induced currents to a similar degree (Fig. 2-8A-C & E, -7.1 ± 2.2 and -12.3 ± 2.8 pA/pF, respectively, vs. control, -2.8 ± 1.2 pA/pF, $p < 0.05$). Although basal current levels remained unchanged (data not shown), there was a high degree of variability in basal GIRK responses as measured by barium inhibition. Thus, we normalized Oxo-M responses to basal currents to account for variability in GIRK channel expression (Oxo-M/Basal). While only $GABA_B$ R1/R2 wild-type transfected cells showed baclofen-mediated signaling, both R2 wild-type and $R2_{R575D}$ increased oxotremorine-induced currents compared to control cells (Fig. 2-8F, 1.62 ± 0.3, 2.4 ± 0.4 and 2.4 ± 0.4, respectively, vs. control, 0.65 ± 0.1, $p < 0.05$). Furthermore, the $GABA_B$ R1R2C chimera alone was also able to

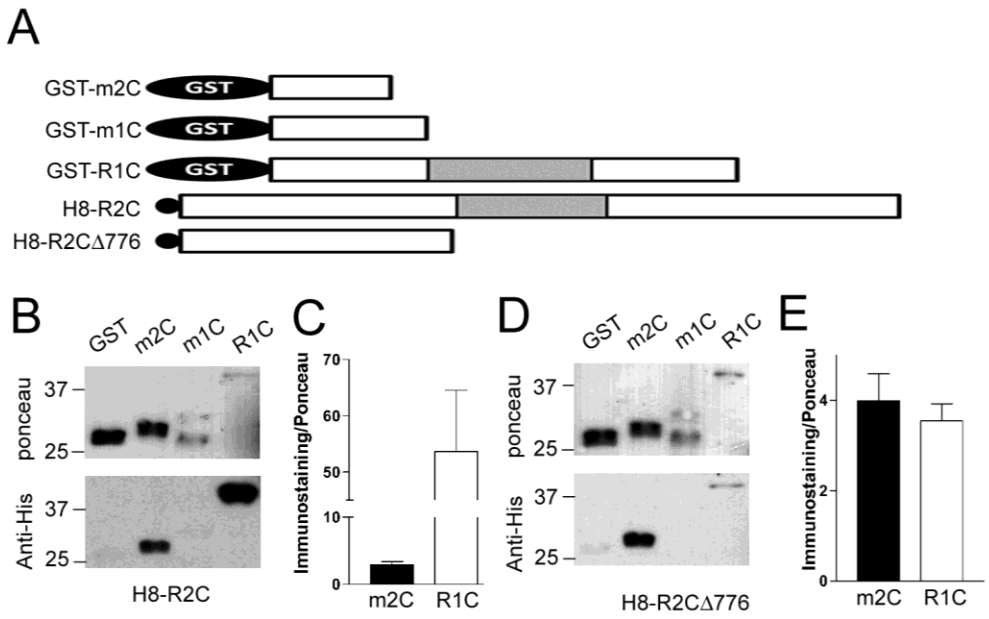

FIGURE 2-7. C-TERMINALS OF GABA R2 AND M2R SHOW BINDING IN VITRO.

A) Schematic showing GST and histidine fusion constructs. *B & D)* Representative blots from *in vitro* binding assay. GST fusion constructs were created for the m C-terminus (m2C), the m1 C-terminus (m1C) or the R1 C-terminus (R1C). 2 ug of GST-tagged protein was loaded onto and SDS PAGE gel and transferred to nitrocellulose. Membranes were incubated with *(B)* a His-tagged full length R2 C-terminus or *(D)* a His-tagged truncated R2, R2Δ776, both at 100nM for 1 hour. Blots were then incubated with an antibody against His and visualized with an ECL solution. (top) Ponceau stained membranes showing size and concentration of GST-tagged fusion proteins. (bottom) Blots probed with Anti-His. *C&E)* Quanification of optical density. Anti-His staining was normalized to total protein as measured by Ponceau staining for m2C and R1C probed with *C)* full length R2 C-terminus (n=4) or *E)* truncated R2CΔ776 (n=3).

rescue muscarinic-induced currents similar to wild-type (Fig. 2-8D-F). The $GABA_B$ R1R2C chimera also failed to show baclofen-mediated currents, consistent with the fact that it lacks the putative G protein signaling site in the R2.

Because a small number of control cells showed small muscarinic-induced currents, we also analyzed the percentage of responders in each condition (Table 2-1). Setting the cut-off for a response at the 75th percentile of control responses revealed that 3/16 (18.75%) control cells showed measurable oxotremorine induced currents above background noise. In contrast, 9/22 (40.9%) of $GABA_B$ R1/R2 wild-type transfected cells showed oxotremorine responses. Similarly, 16/19 (84.2%) of $GABA_B$ $R1/R2_{R575D}$ transfected cells and 9/13 (69.2%) of $GABA_B$ R1R2C transfected cells showed responses. Each of the $GABA_B$ transfected conditions differed significantly from the control distribution in a binomial test ($p < 0.05$). This suggests that m2R does not signal through the $GABA_B$ receptor, nor is $GABA_B$ signaling required for rescue of m2R surface expression.

DISCUSSION

In this study, we provide novel evidence that direct association of $GABA_B$ receptors with m2 muscarinic receptors functionally rescues cholinergic signaling in neuronal PC12 cells. The rescue of m2R surface expression and functional signaling occurs despite the presence of chronic stimulation with cholinergic agonist. In contrast to heterologous desensitization, we suggest the $GABA_B$ receptor is directly involved in heterologous re-sensitization. Importantly, $GABA_B$ receptors did not appear to associate closely with other muscarinic receptors, including m1 and m4, or with other $G\alpha i/o$ coupled receptors, such as the μ opioid receptor, suggesting a specific association between $GABA_B$ R2 and m2R. Consistent with this, we provide biochemical data that the C-terminal domain of $GABA_B$ R2 and m2R bind directly to each other. Interestingly, G protein signaling of the $GABA_B$ R2 subunit is not required for functional rescue of the m2R. We

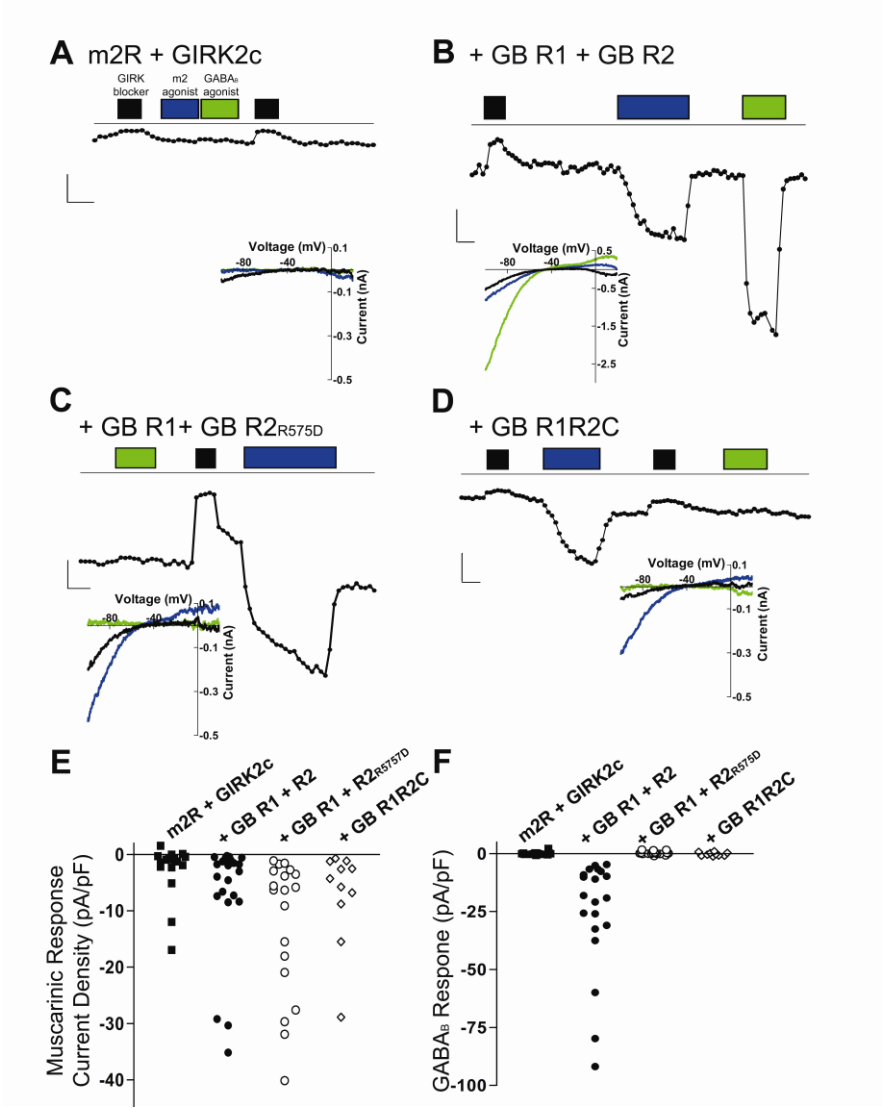

FIGURE 2-8. SIGNALING THROUGH $GABA_B$ IS NOT REQUIRED FOR RESCUE OF MUSCARINIC-MEDIATED CURRENTS.

A-D) Representative current traces from PC12 cells expressing *A)* m2R, GIRK2c alone or co-expressed with *B)* $GABA_B$ R1 and R2 wild-type (WT), *C)* $GABA_B$ R1 WT and $GABA_B$ $R2_{R575D,}$ or *D)* $GABA_B$ R1R2C. Currents were recorded in whole-cell patch clamp mode by applying voltage ramps from -120 to +50 mV, from a holding potential of -40mV. Traces shown represent current levels at -120mV over time and during application of barium (1 mM, black boxes), oxotremorine-M (10μM, white boxes) or baclofen (100_mM, shaded boxes). Scale bars: 200pA, 10s. *Insets:* Current-voltage (I-V) plots of responses to baclofen or oxotremorine. Currents reverse around -40mV, which is E_k and consistent with currents being mediate by GIRK channels. *E)* Scatterplot of responses to oxotremorine-M expressed as current density (pA/pF). Line represents the 75% level for control responses and was used as the cutoff for declaring a response. *F)* Scatterplot of baclofen responses expressed as current density. Line represents the 75% level for control responses. Only $GABA_B$ WT showed a baclofen-mediated response.

TABLE 2-1: GIRK RESPONSES BY TRANSFECTION CONDITION

PC12 Transfection Condition	Barium Inhibition (pA/pF) ± SEM	Oxotremorine Response (pA/pF) ± SEM	Baclofen Response (pA/pF) ± SEM	# of cells with oxotremorine response/total # of cells
Untransfected	-0.65 ± 0.3	-0.60 ± 0.5	-0.16 ± 0.6	3/18
$GABA_B$ R1	-1.4 ± 0.9	-1.8 ± 0.9	-0.6 ± 0.7	5/17
$GABA_B$ R2	-5.2 ± 1.7*	-29.4 ± 7.6*	-7.0 ± 4.3*	28/28
$GABA_B$ R1+R2	-5.3 ± 1.1*	-6.9 ± 3.7*	-19.8 ± 4.0*	13/19
m2R, GIRK2c	-5.4 ± 2.0	-2.8 ± 1.2	-0.1 ± .16	3/16
+$GABA_B$ R1+R2	-6.3 ± 2.1	-7.1 ± 2.2*	-37.4 ± 9.6*	9/22
+$GABA_B$ R1+$R2_{R575D}$	-7.5 ± 1.8	-12.3 ± 2.8*	-0.3 ± 0.2	16/19
+$GABA_B$ R1RC	-4.7 ± 1.7	-7.1 ± 2.5*	-0.2 ± 0.2	9/13

Mean current densities (pA/pF) ± SEM for barium-inhibited, oxotremorine-induced and baclofen-induced currents by transfection condition in 7 day NGF-treated PC12 cells. Far right column shows the number of cells with an oxotremorine-induced response over the total number of cells. The 75th percentile of control responses was used as the cut-off for declaring an oxotremorine response. Asterisks represent significance at $p < 0.05$ in a one-way ANOVA followed by Dunnett's multiple comparison procedure compared to untransfected cells (top four rows) or cells expressing m2 and GIRK2c alone (bottom four rows).

discuss the findings in the context of a model where a macromolecular signaling complex contains different types of GPCRs and GIRK channel at the plasma membrane

$GABA_B$ R2 and m2R Associate Through Their C-terminal Domains

An emerging concept with GPCRs is the dimerization of different receptors, which can then alter function or generate new signaling properties (Franco et al, 2007). Dimerization can involve interactions among transmembrane domain and/or between C-terminal domains. For example, truncation of the C-terminal domains reduces dimerization of μ and δ opioid receptors (Fan et al, 2005). Similarly, the $GABA_B$ R1 and R2 subunits dimerize through coiled-coil domains in their C-terminal domains (Kammerer et al, 1999; Margeta-Mitrovic et al, 2000). We found the association of $GABA_B$ R2 and m2R involves the C-terminal domains of both receptors, but does not require the coiled-coil domain of $GABA_B$ R2. Instead, both FRET experiments and protein-protein binding assays indicated the proximal C-terminal domain of R2 (between amino acid 740 and 776) is sufficient for interacting with m2R. While the putative binding sequence is only 23 amino acids for m2R and 36 amino acids for $GABA_B$ R2, relatively short sequences of amino acids have been shown previously to be involved in GPCR dimerization. For example, deleting the last 15 amino acids of the C-terminal domain disrupts dimerization of δ opioid receptors (Cvejic & Devi, 1997). The strong interaction mediated by the coiled-coil domains in the $GABA_B$ R1 and R2 C-terminal domains and the association of m2R and R2 via the proximal R2 C-terminal domain raises the possibility that m2R could associate with the $GABA_B$ R1/R2 dimer.

$GABA_B$ Rescues m2R Surface Expression

The functional consequences of GPCR dimerization varies widely. In some cases heterodimerization has a direct effect on signaling. For example, activation of Gαi by the serotonin 5-HT_{2A} receptor is greatly enhanced by dimerization with the metabotropic glutamate mGluR-2 receptor (Gonzalez-Maeso et al, 2008). In other cases heterodimerization leads to the development of novel functional properties, as in the case of μ and δ opioid receptor, both of

which couple to pertussis toxin (PTX) sensitive G proteins but signal through a PTX-insensitive pathway as a heterodimer (George et al, 2000). In PC12 cells, the association of $GABA_B$ R2 and m2R, however, dramatically alters receptor trafficking in a way that promotes signaling (i.e. re-sensitization). Previous studies have also reported changes in agonist-induced internalization upon heterodimerization. For example, heterodimerization of dopamine D1 and D3 receptors reduces D1 internalization upon stimulation with a D1-specific agonist but promotes heterodimer internalization with co-application of D1 and D3 specific agonists (Fiorentini et al, 2008). Also, β2 adrenergic receptors have been shown to interact with both κ and δ opioid receptors (Jordan et al, 2001). Interestingly, β2 interaction with δ opioid receptors promotes δ internalization in response to adrenergic stimulation but β2 interaction with κ opioid receptors prevents β2 internalization in response to adrenergic stimulation (Jordan et al, 2001). The latter functional response is similar to that of $GABA_B$ R and m2R, promoting 're-sensitization'.

Brefeldin-A treatment, which disrupts forward trafficking (Chardin & McCormick, 1999), prevents the rescue of m2R surface expression by $GABA_B$ R1/R2 subunits. This finding suggests the rescue by $GABA_B$ R2 involves forward trafficking of the receptor complex, perhaps in the ER or endosomal compartments, though we cannot rule out a change in endocytosis as well. Previous studies have shown that $GABA_B$ R2 promotes forward trafficking of R1 in the $GABA_B$ heterodimer (Margeta-Mitrovic et al, 2000). Additionally, both $GABA_B$ R1/R2 subunits have recently been shown to interact with an extracellular calcium sensing receptor (ECaR), a member of the same Class C GPCR family. Chang et al (2007) have found that the R1 subunit reduces surface expression while the R2 increases surface expression of ECaR. Furthermore, the interaction between the $GABA_B$ R1/R2 subunits and ECaR is competitive (Chang et al, 2007). By contrast, m2R and $GABA_B$ R1 bind to different regions of $GABA_B$ R2, suggesting a non-competitive interaction among these two GPCRs.

In contrast to our PC12 experiment, we found that $GABA_B$ R1 enhances the interaction between $GABA_B$ R2 and m2R in HEK293 cells. Part of this enhancement could be due to a membrane targeting domain in the R1; $GABA_B$ R1 co-expression appears to increase

colocalization between R2 and m2R in HEK293 cells. The $GABA_B$ R1 subunit has two sushi domain repeats in the N-terminal domain. The function of these domains remains largely unknown, but have recently been shown to bind an extracellular matrix protein (Blein et al, 2004). In our study, a chimeric $GABA_B$ R1R2C, which does not couple to G proteins on its own, clearly associates with m2R. In PC12 cells, we did observe small baclofen-induced currents with ectopic expression of only the $GABA_B$ R2 subunit. These baclofen-activated currents could be due to low levels of endogenous $GABA_B$ R1 subunit expression or, alternatively, the presence of a chaperone or adaptor protein that promotes $GABA_B$ R2-m2R interaction in the absence of $GABA_B$ R1.

$GABA_B$ R and m2R Colocalization

While few studies have looked at the cellular distribution of both $GABA_B$ and muscarinic m2 receptors, both receptors are clearly expressed in the same brain regions and likely co-expressed in subpopulations of cells. Postsynaptically, $GABA_B$ receptors and m2Rs signal to GIRK channels, leading to inhibition. While m2R is well-characterized for its ability to activate GIRK channels in cardiac cells (Yamada et al, 1998), there are several examples of m2R-GIRK coupling in central nervous system neurons as well. m2R signaling to GIRKs has been documented in several populations of interneurons, such as those in the striatum, neocortex and hippocampus (Calabresi et al, 1998; Xiang et al, 1998; McQuiston & Madison, 1999). Given that GABAergic interneurons are known to have extensive networks of recurrent inhibition, and that $GABA_B$ receptors have been documented postsynaptically on several interneuron types as well (Ng & Yung, 2001; Lacey et al, 2005; Price et al, 2005), it seems reasonable that $GABA_B$ and m2R would overlap in their distribution. Furthermore, m2R has been shown to activate GIRK conductances in excitatory cells as well including thalamic reticular neurons (McCormick & Prince, 1986) and CA1 pyramidal neurons (Seeger & Alzheimer, 2001). $GABA_B$ receptors have also been shown to signal to GIRK channels in CA1 pyramidal cells (Sloviter et al, 1999; Leung et al, 2006; Sohn et al, 2007). Thus, it is plausible that $GABA_B$ could regulate m2R signaling postsynaptically in some neurons.

Presynaptically, $GABA_B$ receptors and m2Rs signal to G proteins that inhibit voltage-gated calcium channels and reduce transmitter release. In the hippocampus, m2R is found predominantly presynaptically on a subset of GABAergic neurons (Rouse et al, 2000; Miyashita et al, 2007; Gonzalez et al, 2008) where $GABA_B$ receptors are likely expressed as autoreceptors (Ariwodola & Weiner, 2004; Cobb et al, 1999). In support of this, GABAergic inhibition can be attenuated by presynaptic signaling of m2Rs (Koos & Tepper, 2002; Apergis-Schoute et al, 2007). Conversely, $GABA_B$ and m2Rs are likely both present on presynaptic afferents in the spinal cord, thus poised to co-ordinate glutamate release and mediate spinal analgesia (Li et al, 2002; Ataka et al, 2000; Iyadomi et al, 2000; Zhang et al, 2007). It is conceivable that $GABA_B$ receptor could partially re-sensitize m2 muscarinic signaling despite high levels of acetylcholine.

LITERATURE CITED

Apergis-Schoute J, Pinto A, Pare D (2007) Muscarinic control of long-range GABAergic inhibition within the rhinal cortices. J Neurosci 27:4061-4071.

Ariwodola OJ, Weiner JL (2004) Ethanol potentiation of GABAergic synaptic transmission may be self-limiting: role of presynaptic GABA(B) receptors. J Neurosci 24:10679-10686.

Ataka T, Kumamoto E, Shimoji K, Yoshimura M (2000) Baclofen inhibits more effectively C-afferent than Adelta-afferent glutamatergic transmission in substantia gelatinosa neurons of adult rat spinal cord slices. Pain 86:273-282.

Balasubramanian S, Teissere JA, Raju DV, Hall RA (2004) Hetero-oligomerization between GABAA and GABAB receptors regulates GABAB receptor trafficking. J Biol Chem 279:18840-18850.

Bernard V, Brana C, Liste I, Lockridge O, Bloch B (2003) Dramatic depletion of cell surface m2 muscarinic receptor due to limited delivery from intracytoplasmic stores in neurons of acetylcholinesterase-deficient mice. Mol Cell Neurosci 23:121-133.

Bettler B, Kaupmann K, Mosbacher J, Gassmann M (2004) Molecular structure and physiological functions of GABA(B) receptors. Physiol Rev 84:835-867.

Binet V, Duthey B, Lecaillon J, Vol C, Quoyer J, Labesse G, Pin JP, Prezeau L (2007) Common structural requirements for heptahelical domain function in class A and class C G protein-coupled receptors. J Biol Chem 282:12154-12163.

Blein S, Ginham R, Uhrin D, Smith BO, Soares DC, Veltel S, McIlhinney RA, White JH, Barlow PN (2004) Structural analysis of the complement control protein (CCP) modules of GABA(B) receptor 1a: only one of the two CCP modules is compactly folded. J Biol Chem 279:48292-48306.

Calabresi P, Centonze D, Pisani A, Sancesario G, North RA, Bernardi G (1998) Muscarinic IPSPs in rat striatal cholinergic interneurones. J Physiol 510 (Pt 2):421-427.

Chardin P, McCormick F (1999) Brefeldin A: the advantage of being uncompetitive. Cell 97:153-155.

Chang W, Tu C, Cheng Z, Rodriguez L, Chen TH, Gassmann M, Bettler B, Margeta M, Jan LY, Shoback D (2007) Complex formation with the Type B gamma-aminobutyric acid receptor affects the expression and signal transduction of the extracellular calcium-sensing receptor. Studies with HEK-293 cells and neurons. J Biol Chem 282:25030-25040.

Clancy SM, Boyer SB, Slesinger PA (2007) Coregulation of natively expressed pertussis toxin-sensitive muscarinic receptors with G protein-activated potassium channels. J Neurosci 27:6388-6399.

Cobb SR, Manuel NA, Morton RA, Gill CH, Collingridge GL, Davies CH (1999) Regulation of depolarizing GABA(A) receptor-mediated synaptic potentials by synaptic activation of GABA(B) autoreceptors in the rat hippocampus. Neuropharmacology 38:1723-1732.

Cvejic S, Devi LA (1997) Dimerization of the delta opioid receptor: implication for a role in receptor internalization. J Biol Chem 272:26959-26964.

Dichter MA, Tischler AS, Greene LA (1977) Nerve growth factor-induced increase in electrical excitability and acetylcholine sensitivity of a rat pheochromocytoma cell line. Nature 268:501-504.

Fan T, Varghese G, Nguyen T, Tse R, O'Dowd BF, George SR (2005) A role for the distal carboxyl tails in generating the novel pharmacology and G protein activation profile of mu and delta opioid receptor hetero-oligomers. J Biol Chem 280:38478-38488.

Fowler CE, Aryal P, Suen KF, Slesinger PA (2007) Evidence for association of GABA(B) receptors with Kir3 channels and regulators of G protein signalling (RGS4) proteins. J Physiol 580:51-65.

George SR, Fan T, Xie Z, Tse R, Tam V, Varghese G, O'Dowd BF (2000) Oligomerization of mu- and delta-opioid receptors. Generation of novel functional properties. J Biol Chem 275:26128-26135.

Gonzalez-Maeso J, Ang RL, Yuen T, Chan P, Weisstaub NV, Lopez-Gimenez JF, Zhou M, Okawa Y, Callado LF, Milligan G, Gingrich JA, Filizola M, Meana JJ, Sealfon SC (2008) Identification of a serotonin/glutamate receptor complex implicated in psychosis. Nature 452:93-97.

Gonzalez I, Arevalo-Serrano J, Perez JL, Gonzalo P, Gonzalo-Ruiz A (2008) Effects of beta-amyloid peptide on the density of M2 muscarinic acetylcholine receptor protein in the hippocampus of the rat: relationship with GABA-, calcium-binding protein and somatostatin-containing cells. Neuropathol Appl Neurobiol.

Iyadomi M, Iyadomi I, Kumamoto E, Tomokuni K, Yoshimura M (2000) Presynaptic inhibition by baclofen of miniature EPSCs and IPSCs in substantia gelatinosa neurons of the adult rat spinal dorsal horn. Pain 85:385-393.

Jordan BA, Trapaidze N, Gomes I, Nivarthi R, Devi LA (2001) Oligomerization of opioid receptors with beta 2-adrenergic receptors: a role in trafficking and mitogen-activated protein kinase activation. Proc Natl Acad Sci U S A 98:343-348.

Kammerer RA, Frank S, Schulthess T, Landwehr R, Lustig A, Engel J (1999) Heterodimerization of a functional GABAB receptor is mediated by parallel coiled-coil alpha-helices. Biochemistry 38:13263-13269.

Koos T, Tepper JM (2002) Dual cholinergic control of fast-spiking interneurons in the neostriatum. J Neurosci 22:529-535.

Lacey CJ, Boyes J, Gerlach O, Chen L, Magill PJ, Bolam JP (2005) GABA(B) receptors at glutamatergic synapses in the rat striatum. Neuroscience 136:1083-1095.

Leung LS, Peloquin P (2006) GABA(B) receptors inhibit backpropagating dendritic spikes in hippocampal CA1 pyramidal cells in vivo. Hippocampus 16:388-407.

Li DP, Chen SR, Pan YZ, Levey AI, Pan HL (2002) Role of presynaptic muscarinic and GABA(B) receptors in spinal glutamate release and cholinergic analgesia in rats. J Physiol 543:807-818.

Lunn ML, Nassirpour R, Arrabit C, Tan J, McLeod I, Arias CM, Sawchenko PE, Yates JR, 3rd, Slesinger PA (2007) A unique sorting nexin regulates trafficking of potassium channels via a PDZ domain interaction. Nat Neurosci 10:1249-1259.

Margeta-Mitrovic M, Jan YN, Jan LY (2000) A trafficking checkpoint controls GABA(B) receptor heterodimerization. Neuron 27:97-106.

McCormick DA, Prince DA (1986) Acetylcholine induces burst firing in thalamic reticular neurones by activating a potassium conductance. Nature 319:402-405.

McQuiston AR, Madison DV (1999) Muscarinic receptor activity has multiple effects on the resting membrane potentials of CA1 hippocampal interneurons. J Neurosci 19:5693-5702.

Miyashita T, Rockland KS (2007) GABAergic projections from the hippocampus to the retrosplenial cortex in the rat. Eur J Neurosci 26:1193-1204.

Ng TK, Yung KK (2001) Differential expression of GABA(B)R1 and GABA(B)R2 receptor immunoreactivity in neurochemically identified neurons of the rat neostriatum. J Comp Neurol 433:458-470.

Pan HL, Wu ZZ, Zhou HY, Chen SR, Zhang HM, Li DP (2008) Modulation of pain transmission by G protein-coupled receptors. Pharmacol Ther 117:141-161.

Price CJ, Cauli B, Kovacs ER, Kulik A, Lambolez B, Shigemoto R, Capogna M (2005) Neurogliaform neurons form a novel inhibitory network in the hippocampal CA1 area. J Neurosci 25:6775-6786.

Robbins MJ, Calver AR, Filippov AK, Hirst WD, Russell RB, Wood MD, Nasir S, Couve A, Brown DA, Moss SJ, Pangalos MN (2001) GABA(B2) is essential for G protein coupling of the GABA(B) receptor heterodimer. J Neurosci 21:8043-8052.

Rouse ST, Edmunds SM, Yi H, Gilmor ML, Levey AI (2000) Localization of M(2) muscarinic acetylcholine receptor protein in cholinergic and non-cholinergic terminals in rat hippocampus. Neurosci Lett 284:182-186.

Seeger T, Alzheimer C (2001) Muscarinic activation of inwardly rectifying K(+) conductance reduces EPSPs in rat hippocampal CA1 pyramidal cells. J Physiol 535:383-396.

Sohn JW, Lim A, Lee SH, Ho WK (2007) Decrease in PIP(2) channel interactions is the final common mechanism involved in PKC- and arachidonic acid-mediated inhibitions of GABA(B)-activated K+ current. J Physiol 582:1037-1046.

Sloviter RS, Ali-Akbarian L, Elliott RC, Bowery BJ, Bowery NG (1999) Localization of GABA(B) (R1) receptors in the rat hippocampus by immunocytochemistry and high resolution autoradiography, with specific reference to its localization in identified hippocampal interneuron subpopulations. Neuropharmacology 38:1707-1721.

White JH, Wise A, Main MJ, Green A, Fraser NJ, Disney GH, Barnes AA, Emson P, Foord SM, Marshall FH (1998) Heterodimerization is required for the formation of a functional GABA(B) receptor. Nature 396:679-682.

Xiang Z, Huguenard JR, Prince DA (1998) Cholinergic switching within neocortical inhibitory networks. Science 281:985-988.

Zhang HM, Zhou HY, Chen SR, Gautam D, Wess J, Pan HL (2007) Control of glycinergic input to spinal dorsal horn neurons by distinct muscarinic receptor subtypes revealed using knockout mice. J Pharmacol Exp Ther 323:963-971.

A portion of Chapter 2 has been published in Clancy SM, Boyer SB, and Slesinger PA (2007) Coregulation of natively expressed pertussis toxin-sensitive muscarinic receptors with G-protein-activated potassium channels. JNeurosci 27:6388-99. The data presented in Chapter 2 represent work for which the thesis author was primarily responsible and are used by permission of the co-authors. Other parts of Chapter 2 are in preparation for publication of the material as it may appear in the Journal of Neuroscience, 2008, Boyer SB, Clancy SM, Thomas SM, and PA Slesinger. The dissertation author was the primary investigator and author of this paper.

CONCLUDING REMARKS

Ion channels directly influence the electrical excitability of both cardiac and neuronal cells. Inwardly rectifying potassium channels in particular play a key role in setting the membrane potential and mediating inhibition. Thus proper membrane targeting of these channels is crucial to their function. This work has addressed mechanisms of trafficking of two different classes of inward rectifiers, Kir2 and Kir3. The results suggest that inwardly rectifying potassium channel trafficking is more complex than previously thought.

Because they are constitutively active inward rectifiers, trafficking of Kir2 channels provides a necessary means for functional regulation. The finding that the small GTPase Rac1 can affect Kir2.1 trafficking provides a novel mechanism of regulation. Interestingly, this effect was specific for Rac1. As RhoA activation has been shown to inhibit Kir2 channels (Jones SV, 2003), the balance of different GTPase activation may provide another level of regulation for Kir2 currents. RhoGTPases play crucial roles in the central nervous system. As key regulators of the actin cytoskeleton they play a role in extension of axons and dendrites, establishment of neuronal polarity, axon guidance and synaptogenesis, to name a few (de Curtis I, 2008). The role of Kir2 channel modulation in neurons remains unclear, but small changes in Kir2 expression can lead to significant changes in membrane excitability.

Direct consequences of Kir2 regulation are more readily seen in cardiac myocytes. Overexpression or downregulation of Kir2.1 can lead to cardiac dysfunction and potentially fatal arrhythmias. Several mutations associated with Andersens Syndorme have been discovered in Kir2.1, and at least some of these result in reduced surface expression (Bendahhou et al, 2003; Ballester et al, 2006). Although our results suggest that Rac1 may inhibit endocytosis, we cannot rule out changes in forward trafficking as well. Futhermore, Kir2 family members are capable of forming heteromeric channels, and some studies suggest that heteromerization may have implications for Andersons Syndrome (Preisig-Muller et al, 2002). As Rac1 affected only Kir2.1 and not Kir2.2-2.3, subunits this raises the issue of GTPase effects on heteromeric channels. The effect of Rac1 on heteromeric Kir2 channels remains to be seen. Kir2.1 could play a

dominant role in trafficking other Kir2 subunits. Alternately, some balance of trafficking motifs could lead to increased complexity of regulation for native, heteromeric channels.

Kir3 channels are also crucial regulators of cardiac and neuronal signaling, and mediate G-protein coupled receptor induced inhibition. Here we have shown that two different GPCRs, m2 muscarinic recptors and $GABA_B$ receptors, are capable of trafficking Kir3 channels. Thus despite a variety of trafficking motifs contained within individual Kir3 subunits (Ma et al, 2002), further regulation can be accomplished by the formation of multi-protein complexes. It seems unlikely that m2 and $GABA_B$ receptors represent the only GPCRs capable of trafficking Kir3 channels. Conceivably, it is a common feature of GPCR-ion channel interactions to form complexes and traffic as units. The question then becomes what determines how such complexes are formed; i.e. can Kir3 channels form a complex with any GPCR or is there active regulation of complex formation? This question becomes more important when one considers that GPCR regulation can determine Kir3 channel trafficking. We have shown that downregulation of m2 receptors due to chronic agonist exposure also leads to loss of Kir3 surface expression. If Kir3 channels are passive passengers of GPCRs, why do they contain trafficking motifs at all? It seems likely that either active processes direct proper complex formation or at least regulate subcellular localization to such an extent as to regulate complex formation.

The finding that $GABA_B$ can directly interact with and traffic m2 receptors directly was also surprising. These receptors represent two different classes of GPCRs with little apparent structural or sequence similarity. The discovery that small amino acid sequences mediate this interaction suggests some as yet unidentified motif within these regions allowing binding. This also provides further evidence for the promiscuity of $GABA_B$ receptors. Interestingly, it is the $GABA_B$ R2 subunit which binds m2 receptors. The $GABA_B$ R2 subunit is responsible for forward trafficking of the R1/R2 heterodimer and may play the same role with m2. Furthermore, interaction with $GABA_B$ R2 can increase surface expression of an extracellular calcium sensing receptor (Chang et al, 2007). This could represent then a more general role for $GABA_B$ R2 as a chaperone protein.

The requirement for $GABA_B$ R1 to allow R2-m2 interactions was unexpected. It remains unclear whether this requirement extends beyond HEK cells. On one hand, expression of the $GABA_B$ R2 subunit alone in PC12 cells yielded small baclofen-induced currents, suggesting the presence of endogenous R1. On the other hand, the C-terminal domains of $GABA_B$ R2 and m2 were capable of binding *in vitro*, suggesting that the R1 is not necessary for interaction per se. Our results suggest that the $GABA_B$ R1 subunit may be necessary for localization between R2 and m2. The $GABA_B$ R1 subunit contains a pair of sushi domain repeats in the N-terminus whose function remains largely unknown (Blein et al, 2004) and it is tempting to speculate that this region may be responsible for membrane localization. However, it is also conceivable that another protein in PC12s may subserve the same role. If the $GABA_B$ R1 subunit is in fact necessary this would represent the first example of a GPCR hetero-trimer.

The interaction between $GABA_B$ R2 and m2 provides a novel mechanism to regulate surface expression during chronic agonist exposure. Our results suggest that $GABA_B$ R2 increases forward trafficking of m2, although it is unclear whether endocytosis of m2 is still occurring. If so, this may explain why functional rescue is only seen in approximately half of $GABA_B$ R1/R2 expressing cells. Alternately, there could be competition for G-protein binding and/or activation. The fact that m2 responses were consistently smaller than $GABA_B$ mediated responses suggests less surface expression of m2 or a decrease in m2 ligand-binding or G-protein coupling. Further studies may in fact show a shift in sensitivity upon interaction. Nonetheless, $GABA_B$ co-expression clearly increases m2 muscarinic signaling despite elevated levels of acetylcholine, with implications for muscarinic signaling throughout the central nervous system.

This work provides evidence for novel mechanisms of regulating surface expression of inwardly rectifying potassium channels. We propose that trafficking of these channels is a complex process that depends upon co-localization with effector proteins and formation of macromolecular complexes. This work will aid us in understanding the role of inwardly rectifying potassium channels in both cardiac and neuronal function.

LITERATURE CITED

Ballester Ly BDWWBLIHMKDVCGGAL, Jr. (2006) Trafficking-competent and trafficking-defective KCNJ2 mutations in Andersen syndrome. Human Mutation 27:388-388.

Bendahhou S DMRPNMT-FMFYHPLJ (2003) Defective potassium channel Kir2.1 trafficking underlies Andersen-Tawil syndrome. Journal of Biological Chemistry 278:51779-51785.

Blein S, Ginham R, Uhrin D, Smith BO, Soares DC, Veltel S, McIlhinney RA, White JH, Barlow PN (2004) Structural analysis of the complement control protein (CCP) modules of GABA(B) receptor 1a: only one of the two CCP modules is compactly folded. J Biol Chem 279:48292-48306.

Chang W, Tu C, Cheng Z, Rodriguez L, Chen TH, Gassmann M, Bettler B, Margeta M, Jan LY, Shoback D (2007) Complex formation with the Type B gamma-aminobutyric acid receptor affects the expression and signal transduction of the extracellular calcium-sensing receptor. Studies with HEK-293 cells and neurons. J Biol Chem 282:25030-25040.

de Curtis I (2008) Functions of Rac GTPases during neuronal development. Dev Neurosci 30:47-58.

Franco R, Casado V, Cortes A, Ferrada C, Mallol J, Woods A, Lluis C, Canela EI, Ferre S (2007) Basic concepts in G-protein-coupled receptor homo- and heterodimerization. ScientificWorldJournal 7:48-57.

Jones SV (2003) Role of the small GTPase Rho in modulation of the inwardly rectifying potassium channel Kir2.1. Mol Pharmacol 64:987-993.

Ma D, Zerangue N, Raab-Graham K, Fried SR, Jan YN, Jan LY (2002) Diverse trafficking patterns due to multiple traffic motifs in G protein-activated inwardly rectifying potassium channels from brain and heart. Neuron 33:715-729.

Preisig-Muller R, Schlichthorl G, Goerge T, Heinen S, Bruggemann A, Rajan S, Derst C, Veh RW, Daut J (2002) Heteromerization of Kir2.x potassium channels contributes to the phenotype of Andersen's syndrome. Proc Natl Acad Sci U S A 99:7774-7779.